AD-A041 163 SHAKER RESEARCH CORP BALLSTON LAKE N Y F/G 13/9
FUNDAMENTALS OF GAS LUBRICATION.(U)
MAY 77 C H PAN N00014-74-C-0278
UNCLASSIFIED SRC-76-TR-22 NL

1 OF 2
ADA
041163

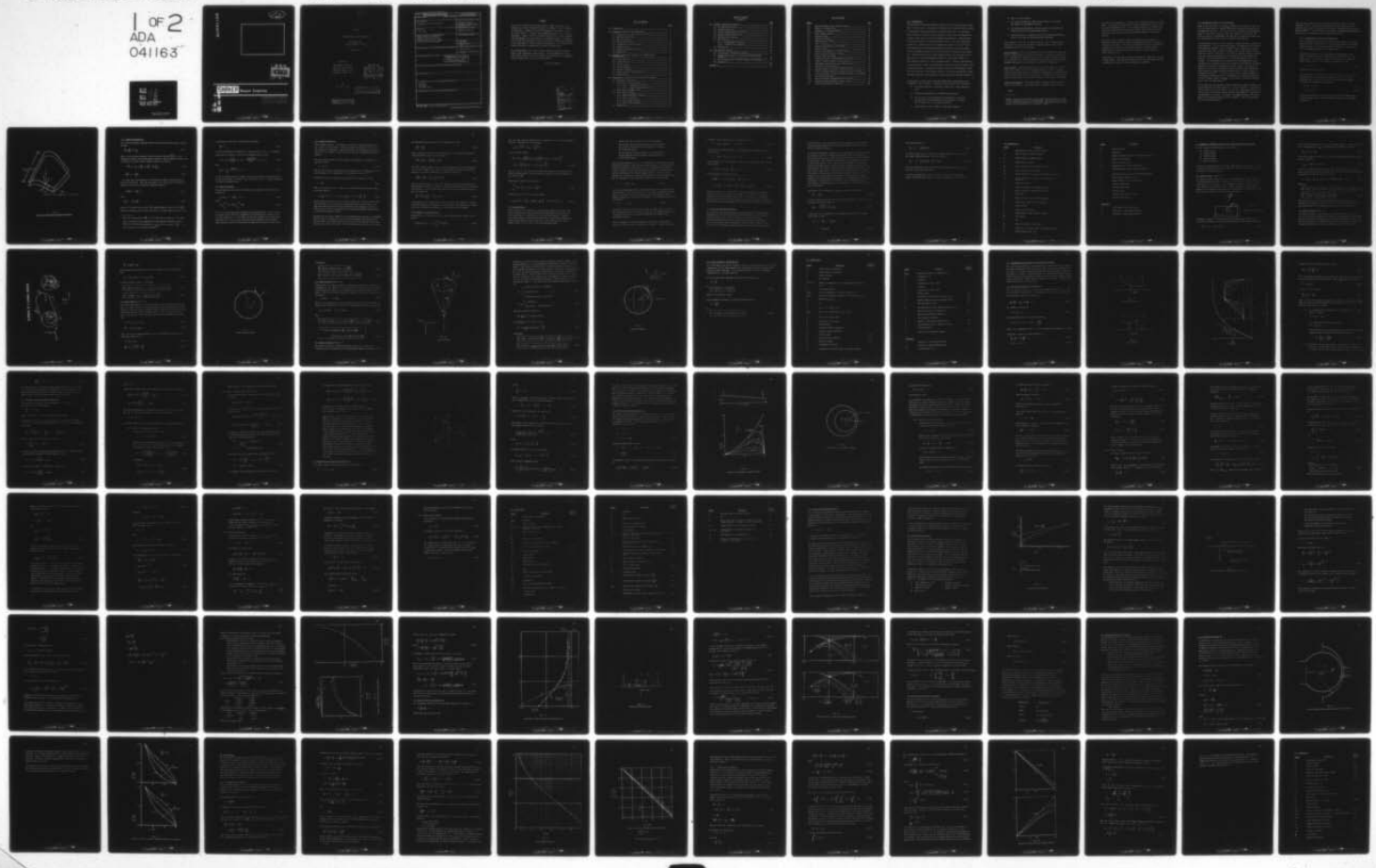

(12)

SHAKER Research Corporation

(12)

76-TR-22

FUNDAMENTALS OF GAS LUBRICATION

Prepared Under

Contract N00014-74-C-0278

NR062-490 code 438

May 13, 1977

Prepared For

Department of the Navy
Office of Naval Research
800 North Quincy Street
Arlington, Virginia 22217

By

Dr. C. H. T. Pan

SHAKER RESEARCH CORPORATION
Northway 10 Executive Park
Ballston Lake, N.Y. 12019

SECURITY CLASSIFICATION OF THIS PAGE (When Data Entered)

REPORT DOCUMENTATION PAGE

READ INSTRUCTIONS BEFORE COMPLETING FORM

1. REPORT NUMBER	2. GOVT ACCESSION NO. / 3. RECIPIENT'S CATALOG NUMBER
4. TITLE (and Subtitle): Fundamentals of Gas Lubrication	5. TYPE OF REPORT & PERIOD COVERED: Technical Report
	6. PERFORMING ORG. REPORT NUMBER: -76-TR-22
7. AUTHOR(s): C.H.T. Pan	8. CONTRACT OR GRANT NUMBER(s): N00014-74-C-0278
9. PERFORMING ORGANIZATION NAME AND ADDRESS: Shaker Research Corporation, Northway 10 Executive Park, Ballston Lake, New York 12019	10. PROGRAM ELEMENT, PROJECT, TASK AREA & WORK UNIT NUMBERS
11. CONTROLLING OFFICE NAME AND ADDRESS	12. REPORT DATE: May 1977
	13. NUMBER OF PAGES: 108
14. MONITORING AGENCY NAME & ADDRESS (if different from Controlling Office)	15. SECURITY CLASS. (of this report): Unclassified
	15a. DECLASSIFICATION/DOWNGRADING SCHEDULE

16. DISTRIBUTION STATEMENT (of this Report)

DISTRIBUTION STATEMENT A
Approved for public release;
Distribution Unlimited

17. DISTRIBUTION STATEMENT (of the abstract entered in Block 20, if different from Report)

18. SUPPLEMENTARY NOTES

19. KEY WORDS (Continue on reverse side if necessary and identify by block number)

Tribology
Bearings
Gas Lubrication

20. ABSTRACT (Continue on reverse side if necessary and identify by block number)

DD FORM 1 JAN 73 1473 EDITION OF 1 NOV 65 IS OBSOLETE

SECURITY CLASSIFICATION OF THIS PAGE (When Data Entered)

PREFACE

In the fall of 1976 the author was invited to render a lecture on Gas Bearings in a course entitled "Principles of Tribology" at the University of Pittsburgh. A number of texts on the subject are available (36, 37, 38, 39, 40, and 41). Together, these publications cover the field quite thoroughly. However, being the products during an era of rapid technological developments, their perspectives are somewhat diffused. Therefore, this writing was undertaken in order to project the theoretical foundation of gas lubrication as a mature technical discipline. It is offered as an overview reference, supplementing the texts previously cited.

The encouragement by the Office of Naval Research to make this writing reach a wider readership is most welcome. This distribution as a contract report allows the writer to express his gratitude for the continuing research support given to him by ONR since 1961.

--C.H.T.P., May 1977

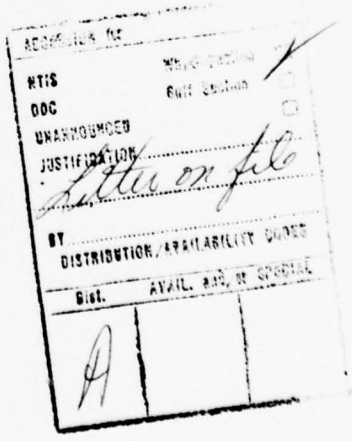

TABLE OF CONTENTS

Table of Contents

(Continued)

LIST OF FIGURES

1.0 INTRODUCTION

Men have derived beneficial mechanical effects from air and other gases in many ways. In most cases, a moving body is involved, and the relative kinetic energy is converted to create levitation or to perform useful work. Viscous shear would contribute to parasitic losses directly or would cause the generation of turbulent flows which in turn would precipitate dissipation. Compressibility of the gaseous medium is often an essential feature of the useful mechanical process; e.g. expansion work in heat engines and propulsion nozzles. Fluid film lubrication is an exceptional mechanical process in that viscous shear stress contributes directly to the useful function of developing a load capacity. Although viscosity also causes bearing friction, the equivalent lift-to-drag ratio of a typical "hydrodynamic wedge" is in the order of 1000 to 1, which compares favorably to a high performance wing. Lubricant compressibility is the distinctive feature of gas bearings in contrast to the more common liquid lubricated bearings. Although basic concepts such as the "hydrodynamic wedge" are still applicable to gas bearings despite of lubricant compressibility, many additional features in gas bearings are unique and require separate attention.

The potentials for large scale industrial application of gas bearings were recognized in the late 1950's. Advocates of gas lubrication have emphasized

- The gaseous lubricant is chemically stable over a wide temperature range.
- Atmospheric contamination is avoided by gas bearings.
- The viscosity of a gas increases with temperature so that the heating effect in overloading a gas bearing tends to increase the restoring force to overcome the overload.
- A gas bearing is more suitable for high speed operation.

- There is no fire hazard.
- Use of gas bearings can reduce thermal gradient in the rotor and enhance its mechanical integrity.
- For high-speed applications, the gas bearing is inherently more noise free than the rolling-element bearing.
- System simplicity is enhanced by use of self-acting gas bearings which do not require cooling/circulation equipment.

These optimistic views must be tempered with more subtle engineering considerations before one can confidently substitute gas bearings for more conventional oil-lubricated bearings.

Surface Chemistry - Modern lubricating oils contain additives of long chain molecular species which form low friction surface coatings on bearing surfaces. Consequently, sliding friction in oil bearings is minimal even when full separation of the bearing surfaces by the fluid film is not realized. Boundary lubrication of gas bearings is essentially not possible*.

Lift-off Speed - Viscosity of gases is less than 10^{-3} times that of lubricating oils. Thus, for a self-acting gas bearing, the lift-off speed is proportionally higher than its oil-lubricated counterpart. Friction heating at the sliding contact prior to lift-off is accordingly more intense and is therefore more likely to cause material damage in self-acting gas bearings.

Chemical Deterioration - The gaseous medium is chemically quite stable at ordinary environments. Lubricating oils, in contrast, would decompose at

---

* Boundary lubrication is sometimes used in gas bearing gyroscope to ensure minimal starting friction for prolonged usage. The friction coefficient of such surfaces is typically > 0.30[1] while that of conventional bearing surfaces in the presence of oil is usually < 0.10[2].

a relatively low temperature. For most oils, coking would take place below 300°C. In the event of inadvertent malfunction, sliding friction can cause considerable temperature rise. If the coking temperature is reached, the endothermic chemical process would function as a sink to moderate further temperature rise and thus would prevent material damage of the bearing surfaces.

These three factors combine to make gas bearings more susceptible to mechanical damage and thus preclude widespread application of gas bearings in heavy duty equipment. The same considerations also exert a dominating influence in the choice of satisfactory materials for gas bearings. Beneficial use of gas bearings must be predicated on the avoidance of these limiting factors.

Nomenclature for mathematical symbols are separately summarized at the end of each chapter. Where different definitions for the same symbol are used in different sections, the section numbers are indicated.

2.0 MATHEMATICAL THEORY OF GAS LUBRICATION

Theory of gas lubrication is generally regarded as an extension of the fluid film lubrication theory of Reynolds,[3] which was originally formulated for an incompressible lubricant. The crucial issue is concerned with an appropriate account of the density variation within the lubricant film such that the basic principles of thermodynamics are satisfied to a degree consistent with the approximations already invoked in momentum considerations.

In certain ways, analysis of a gas bearing is simpler than that required for liquid bearings. As to be demonstrated below, the temperature in a gas bearing film may be regarded to be a constant[4], even though viscous heating necessarily cause some temperature rise above that of the bearing surfaces. Since the viscosity coefficient of most gases is dependent solely on temperature, an isoviscous approximation is quite satisfactory for studying gas bearings. In a liquid bearing film, the isoviscous approximation is less reliable. The gas bearing film is inherently a single phase constituent. Irrespective of the local pressure level relative to the ambient, the gaseous lubricating film remains a homogeneous medium. However, in a liquid film bearing, it has been an established empirical knowledge that a homogeneous liquid state is assured only when the local pressure is near or above the atmospheric pressure[5]. Where the pressure tends to become subambient in a self-acting liquid bearing film, a two-phase flow structure is prevalent. In fact a totally rigorous treatment of this aspect of the liquid lubricant film is yet to be demonstrated.[6]

On the other hand, the kinematic boundary condition at bearing surfaces need more attention in gas bearing analysis. It is not unusual for a gas bearing film thickness to be in the order of 1 μm or less. Under such a condition, a velocity slip at the bearing surface may not be negligible[7], especially if the atmosphere is rarefied. Furthermore, the common assumption of impermeability of the bearing surface may not be valid[8]. This is particularly true for sintered materials.

Still one other complication in gas lubrication theory arises at cryogenic temperature levels. The local Mach number may be quite large, such that phenomena akin to those in high-speed gas dynamics involving fluid inertia may become evident[9]. In the following, the classical isothermal gas lubrication theory will be developed with the continuum point of view.

2.1 Scaling Rules in Thin Film Viscous Flow

The fluid dynamic point of view of gas lubrication concerns a film-like domain which may be described by a small distance measure from a smooth reference surface. The fluid in question is physically characterized by the thermodynamic properties of gaseous media.

The geometrical properties of the domain are characterized by two scales. The small scale, C, is the measure of the bearing gap. The large scale, R, is the global measure of the surface, including its overall extent as well as its radius of curvature. The ratio

$$\varepsilon = C/R \ll 1 \tag{2.1}$$

indicates thinness of the film.

Let V be the scale of the velocity field in concern. If $\vec{n}$ is a local unit normal vector of the reference surface, and if $\vec{V}$ is a local velocity vector of the flow field, then lubrication fluid dynamics is further characterized by the condition.

$$|\vec{V} \cdot \vec{n}| = O\{\varepsilon V\} \tag{2.2}$$

$$\vec{U} = \vec{V} - \vec{V} \cdot \vec{n} \tag{2.3}$$

is then the projection of the velocity vector onto the tangent plane of the reference surface. These geometrical concepts are illustrated in Figure 2.1.

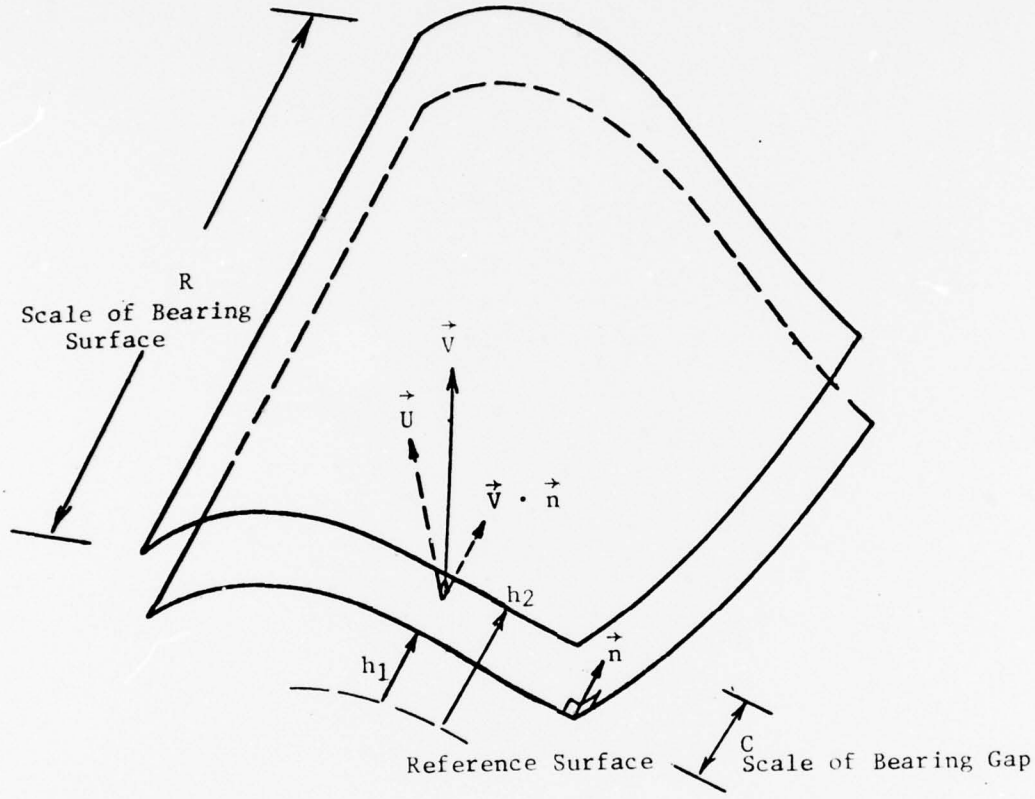

Fig. 2.1

Thin Film Between Nearly Parallel Surfaces

2.2 Momentum Conservation

If a local curvalinear coordinate system is used such that the gradient operator becomes

$$\vec{\nabla} = \vec{\nabla_2} + \vec{n}\,\frac{\partial}{\partial y} \tag{2.4}$$

where y is the distance measured from the reference surface; $\vec{\nabla_2}$ is the two-dimensional surface constrained gradient operator; then the momentum equilitorium conditions for either liquid or gaseous lubrication flows are

$$-\vec{\nabla_2}\, p + \frac{\partial}{\partial y}\left(\mu \frac{\partial \vec{U}}{\partial y}\right) = 0 \quad \{\frac{\rho V^2}{R};\ \frac{\rho V}{\tau};\ \frac{\mu V}{R^2}\} \tag{2.5}$$

$$\left|\frac{\partial p}{\partial y}\right| = 0 \quad \{\frac{\mu V}{\varepsilon R}\} \tag{2.6}$$

τ is a time scale representative of the duration in which fluctuations of the flow field take place. The right hand side of e.q. (2.5) may be discarded provided *one* is willing to neglect the numerical values of

$$\varepsilon^2\left(\frac{\rho VR}{\mu}\right)^{*};\quad \varepsilon^2\left(\frac{\rho R^2}{\mu\tau}\right);\quad \varepsilon^2 \tag{2.7}$$

then

$$\vec{\nabla_2}\, p = \frac{\partial}{\partial y}\left(\mu \frac{\partial \vec{U}}{\partial y}\right) \tag{2.8}$$

Now eq. (2.6) shows p may vary by $O\{\frac{\mu V}{R}\}$ along $\vec{n}$ whereas it may vary by $O\{\frac{\mu V}{\varepsilon^2 R}\}$ along the reference surface, then, since $O\{\varepsilon^2\}$ is already omitted from eq. (2.5)

---

* Note that one may allow $\varepsilon\,\frac{\rho VR}{\mu} = O\{\varepsilon^{-\alpha}\}$ with $0<\alpha<1$ so long as $\varepsilon^{1-\alpha}$ is small. This is the basis for the usefulness of the turbulent lubrication theory [10,11]. An auxilliary requirement for eq.(2.8) to be valid is $|\frac{\rho V^2}{p}| << 1$; this is peculiar to a gaseous lubricant[9].

in writing eq. (2.8), one is also entitled to assert

$$\frac{\partial p}{\partial y} = 0 \tag{2.9}$$

If the film thickness is bounded by $y = (h_1, h_2)$ and $(\vec{U}_1, \vec{U}_2)$ are the boundary conditions of $\vec{U}$, then eq. (2.8) can be integrated twice to yield

$$\vec{U}(y) = \vec{U}_1 + \frac{I_1(y)}{I_1(h_2)}\{\vec{U}_2 - \vec{U}_1\} - \{\frac{I_1(y)I_2(h_2)}{I_1(h_2)} - I_2(y)\}\vec{\nabla} p \tag{2.10}$$

where

$$I_m(y) = \int_{h_1}^{y} \frac{\eta^{(m-1)} d\eta}{\mu}; \quad m = 1, 2 \tag{2.11}$$

η being the dummy coordinate along $\vec{n}$. Thus far the question of compressibility has not been brought up. Therefore eqs. (2.10) and (2.11) are equally applicable to liquid and gaseous fluids.

2.3 Mass Conservation

The continuum mass conservation condition can be expressed over the full film thickness as

$$\frac{\partial}{\partial t}(\overline{\rho h}) + \vec{\nabla} \cdot (\overline{\rho \vec{U} h}) + \Sigma\Phi = 0 \tag{2.12}$$

where

$$\overline{\rho h} = \int_{h_1}^{h_2} \rho dy; \quad \overline{\rho \vec{U} h} = \int_{h_1}^{h_2} \rho \vec{U} dy \tag{2.13}$$

and $\Sigma\Phi$ is the total mass efflux through both bearing surfaces. Eq. (2.12) may be formally derived by direct integration of the differential continuity equation with respect to y. In so doing, one must pay attention to the functional dependence of (h_1, h_2) on both t and the surface coordinates and accordingly impose Leibnitz's rule for differentiating integrals which have variable limits.

2.4 Energy Conservation

With a liquid lubricant, ρ is constant, and since it appears homogeneously in eq. (2.12), it can be dropped. Whereupon further integration of eq. (2.11) with respect to y (assuming a constant viscosity) and subsequent substitution into eq. (2.12), without ρ, would yield the classical incompressible Reynolds equation.

For a gas, density depends on both pressure and temperation according to the equation of state:

$$\rho = f(p, T) \tag{2.14}$$

The thin film condition has justified the approximation of y-independence of p, thus the question of y-dependency of ρ is reduced to that of T [4].

For most lubrication problems, the perfect gas law is suitable, so that

$$\rho = \frac{p}{\mathcal{R}T} \tag{2.15}$$

where $\mathcal{R}$ is the gas constant. Temperature in the lubrication film must satisfy the energy equation:

$$\rho C_v \left(\frac{\partial}{\partial t} + \vec{V} \cdot \vec{\nabla}\right)T - \vec{\nabla} \cdot (\kappa \vec{\nabla} T) = \frac{p}{\rho}\left(\frac{\partial}{\partial t} + \vec{V} \cdot \vec{\nabla}\right)\rho + \mu \frac{\partial \vec{U}}{\partial y} \cdot \frac{\partial \vec{U}}{\partial y} \tag{2.16}$$

The two terms on the left of eq. (2.16) are respectively convective (and transient) and conduction cooling effects respectively, while the two terms on the right hand side are respectively flow work and viscous dissipation effects. (Note that the thin film approximation has allowed considerable simplification of the viscous dissipation term).

Assuming that the thermal gradient in the bearing-journal structure is negligible, then the extent of temperature variation in the lubricant film depends on the balance between the cooling terms on one side and the flow work and viscous dissipation terms on the other side. The flow work term is seen to be of the order,

upon estimating pressure variation according to eq. (2.10)

$$\frac{\mu V}{\varepsilon^2 R\tau}, \quad \frac{\mu V^2}{\varepsilon^2 R^2} \tag{2.17}$$

which is similar to that of the dissipation term. The relative impotance of transient thermal capacity to conduction is

$$\left(\frac{\rho C_v}{\tau}\right)\left(\frac{\varepsilon^2 R^2}{\kappa}\right) = \left(\frac{\mu C_p}{\kappa}\right)\left(\frac{C_v}{C_p}\right)\left(\frac{\varepsilon^2 \rho R^2}{\mu\tau}\right) \tag{2.18}$$

Since $\frac{\mu C_p}{\kappa}$ (Prandtl number) and C_v/C_p of most gases are $0\{1\}$ then recalling eq. (2.7), one can thus justify neglecting the transient thermal capacity term. Similarly, the relative importance of convective cooling is

$$\left(\frac{\rho C_v V}{R}\right)\left(\frac{\varepsilon^2 R^2}{\kappa}\right) = \left(\frac{\mu C_p}{\kappa}\right)\left(\frac{C_v}{C_p}\right)\left(\frac{\varepsilon^2 \rho V R}{\mu}\right) \tag{2.19}$$

which is again negligible. Thus, the temperature field in the lubricant film is determined by conduction cooling of the heat arising from viscous dissipation and flow work. The fractional temperature rise within the lubricant film can thus be estimated as

$$\frac{\mu V^2}{\kappa T} = \left(\frac{\mu C_p}{\kappa}\right)\left(\frac{V^2}{C_p T}\right) = \left(\frac{\mu C_p}{\kappa}\right)(\gamma-1)M^2 \tag{2.20}$$

Consequently, if the "bearing Mach number" is small, then temperature variation across the lubricant film thickness can be neglected. Accordingly, one commonly accepts the isothermal approximation in the analysis of gas bearings.

2.5 Isothermal Gas Bearing Theory

Substituting eq. (2.15) into eq. (2.12) and dividing out the constant RT, one obtains

$$\frac{\partial}{\partial t}\left[p(h_2-h_1)\right] + \vec{\nabla}_2 \cdot \left[p\int_{h_1}^{h_2} \vec{U}\,dy\right] \frac{\Sigma\Phi}{\partial T} = 0 \tag{2.21}$$

Now, since gas viscosity depends only on temperature, it can also be regarded as constant. Therefore eq. (2.11) becomes

$$I_1(y) = \frac{(y-h_1)}{\mu}; \quad I_2(y) = \frac{(y^2-h_1^2)}{2\mu}$$

then eq. (2.10) becomes

$$\vec{U}(y) = \vec{U}_1 + (\frac{y-h_1}{h_2-h_1})(\vec{U}_2-\vec{U}_1)-[(\frac{y-h_1}{h_2-h_1})(h_2^2-h_1^2) - (y^2-h_1^2)]\frac{\vec{\nabla} p}{2\mu}$$

$$= \{\vec{U}_1 + (\frac{y-h_1}{h})(\vec{U}_2-\vec{U}_1)\} - \{(y-h_1)(h_2-y)\frac{\vec{\nabla} p}{2\mu}\} \qquad (2.22)$$

where $h = h_2 - h_1$. The two groups enclosed by brackets are respectively the Couette (linear profile) and the Poiseuille (parabolic profile) components of the velocity field.

Integrating across the film thickness:

$$\int_{h_1}^{h_2} \vec{U}dy = \frac{1}{2}(\vec{U}_1 + \vec{U}_2)(h) - \frac{\vec{\nabla} p}{12\mu} h^3 \qquad (2.23)$$

substitute into eq. (2.21) one finally finds

$$\frac{\partial}{\partial t}(ph) + \vec{\nabla} \cdot [\frac{1}{2}(\vec{U}_1 + \vec{U}_2)ph] - \frac{1}{12\mu}\vec{\nabla} \cdot (h^3 p \vec{\nabla} p) + \frac{\Sigma\Phi}{\rho T} = 0 \qquad (2.24)$$

2.6 Coupling Effects

While Equation (2.24), together with appropriate boundary and initial conditions, completely describes the mathematical conditions to be satisfied by the film pressure in a gas bearing, it is often not possible to complete its solution without considering coupling effects which require simultaneous solution with another system of equations. These coupling effects most commonly appear in one or more of the following three forms:

- Surface flux, Φ, is a function of the film pressure.
- The bearing film thickness depends on the film pressure due to either flexibility (foil bearings) or compliance of the bearing surface.
- The bearing film thickness depends on the kinematics of bearing components which depends on the global effects of the film pressure.

The nonlinear appearance of (p, h, ϕ) in Equation (2.24) makes the overall mathematical problem of the total system quite unwieldy. Fortunately, the "external" problem is usually linear. It is often possible to find the "Green's function" of the external problem so that such a coupling effect can thus be expressed as a linear integral equation. Thus, for a gas bearing with a porous wall, the Green's function for the isothermal viscous gas flow through a porous medium can be found so that one can write

$$\Phi = \iint \frac{1}{2} p^2 G_\phi \, dA \qquad (2.25)$$

G_ϕ is the corresponding Green's function and dA is an area element of the porous surface. Similarly, in the case of a flexible or compliant bearing surface, a suitable elasticity equation can be first solved to yield a Green's function; then the elastic deformation of the compliant surface can be written as

$$\Delta h = \iint p \, G_h \, dA \qquad (2.26)$$

The Green's function problem in either case is a major topic by itself, for the present purpose it suffices to indicate that either Equation (2.25) or Equation (2.26) would be solved together with the isothermal gas lubrication equation.

When the kinematics of bearing components is involved, time dependence becomes an inherent feature in addition to coupling. In many cases, time

dependence may be treated by a perturbation of h; i.e.

$$h = h_o(\vec{r}) + \delta h(\vec{r}, t); \quad |\delta h| << |h_o| \tag{2.27}$$

$\vec{r}$ being the local position vector. Accordingly, the film pressure can be assumed to be

$$p = p_o(\vec{r}) + \delta p(\vec{r}, t); \quad |\delta p| << |p_o| \tag{2.28}$$

Then Equation (2.24) for impermeable surfaces can be separated into a steady-state problem:

$$\vec{\nabla}_2 \cdot \{\frac{1}{2}(\vec{U}_1 + \vec{U}_2)p_o h_o - \frac{h_o^3}{12\mu} p_o \vec{\nabla}_2 p_o\} = 0 \tag{2.29}$$

and a dynamically perturbed problem:

$$h_o \frac{\partial \delta p}{\partial t} + \vec{\nabla}_2 \cdot \{\frac{1}{2}(\vec{U}_1 + \vec{U}_2)h_o \delta p - \frac{h_o^3}{12\mu} \vec{\nabla}_2 (p_o \delta p)\}$$

$$= - p_o \frac{\partial \delta h}{\partial t} - \vec{\nabla}_2 \cdot \{[\frac{1}{2}(\vec{U}_1 + \vec{U}_2)p_o - \frac{h_o^2}{4\mu} p_o \vec{\nabla}_2 p_o]\delta h\} \tag{2.30}$$

Equation (2.29) must be solved first; its nonlinear character requires an iterative process in the numerical procedure. Equation (2.30) is linear with respect to the dependent variable δp. δh is treated as the driving function, while the steady-state solution p_o appears in various coefficients. The dynamically perturbed problem will be treated more thoroughly in Section 6.

2.7 Global Bearing Characteristics

In performing a gas bearing analysis, one is ultimately concerned with the computation of flow rate as well as the force and moment vectors exerted by the bearing film. The flow rate is mainly a concern of externally-pressurized bearings in order to establish the flow supply requirement. The flow calculation requires knowledge of the film inlet pressure, which is obtained by establishing continuity between the supply restrictor and the

film inlet flux. Force and moment vectors are required not only for the nominal operating condition but also for perturbation effects to ensure static and dynamic stability.

At the nominal operating condition, static equilibrium is maintained between the external load and the integrated film force; and, in the case of a self-acting bearing, also between the drive torque and the viscous friction in the bearing. Both requires consideration of the hydrodynamic stresses at the bearing surface. Due to the thin film character of lubrication problems, the shear stress is several orders of magnitude smaller than the film pressure; the scale for the shear stress being $\mu V/C$ while that for the film pressure being $\mu VR/C^2$. Therefore, in the computation of the bearing force vector, the shear stress is commonly neglected. However, in the computation of the bearing moment vector--e.g., bearing friction torque--sometimes the film pressure is inherently of no consequence; therefore, the contribution from shear must be retained. Thus, a distinction must be made between a pressure-moment (e.g., pitch-moment of a tilting-pad bearing) and a shear-torque.

The pressure force acting on an element of bearing surface dA is

$$d\vec{F}_p = \vec{n}p\,dA \tag{2.31}$$

$\vec{n}$ is the outward normal unit vector of the surface element. The shear force acting on the surface element is

$$d\vec{F}_s = \left\{\frac{\mu(\vec{U}_2-\vec{U}_1)}{h} - \frac{h}{2}\vec{\nabla}p\right\}dA \tag{2.32}$$

To allow for the contribution of the ambient back pressure, the bearing force vector is thus

$$\vec{F} = \iint d\vec{F}_p - \iint \vec{n}p_a\,dA$$

$$= \iint \vec{n}(p-p_a)\,dA \tag{2.33}$$

The pressure-moment is

$$\vec{M}_p = \iint \vec{r}\times\vec{n}(p-p_a)dA \tag{2.34}$$

$\vec{r}$ is the position vector of the surface element measured from the origin of the chosen coordinate system. The shear torque is

$$\vec{T}_s = \iint \{\frac{\mu}{h}\vec{r}\times(\vec{U}_2-\vec{U}_1) - \frac{h}{2}\vec{r}\times\vec{\nabla}_2 p\}dA \tag{2.35}$$

If one is interested in the static equilibrium condition, then p_o would be used for p in the above equations.

To calculate perturbation effects on the force vector and the pressure moment, δp would be used instead of $(p-p_a)$ in Equations (2.33) and (2.34).

2.8 Nomenclature

Symbol	Definition
C	Representative scale for film thickness
C_p	Specific heat at constant pressure
C_v	Specific heat at constant volume
$\vec{F}$	Fluid film force vector
$\vec{F}_p$	Force vector due to fluid film pressure
$\vec{F}_s$	Force vector due to wall shear
G_h	Green's function for surface deformation, Eq. (2.26)
G_Φ	Green's function for surface flux at porous wall, Eq. (2.25)
h	Bearing gap, h_2-h_1
Δh	Elastic deformation of compliant surface
I_m	Normal coordinate integrals, Eq. (2.11)
M	Mach number
$\vec{M}_p$	Moment vector due to fluid film pressure
$\vec{n}$	Outward unit normal vector of bearing
p	Fluid pressure
$\vec{r}$	Surface position vector
R	Representative linear extent of bearing
$\mathfrak{R}$	Gas constant
t	Time
$\vec{T}_s$	Torque vector due to wall shear
$\vec{U}$	Projection of velocity vector on reference surface
V	Representative scale of $\vec{V}$

Symbol	Definition
$\vec{V}$	Velocity Vector
x	Coordinate
y	Normal coordinate measured from reference surface
α	Numerical coefficient
γ	Ratio of specific heats
$\delta(\ )$	Perturbation of ( ) from steady state
$\vec{\nabla}$	Three-dimensional spatial gradient operator
$\vec{\nabla}_2$	Two-dimensional surface spatial gradient operator
ε	Film thickness parameter, C/R
η	Dummy variable of y for integration
κ	Thermal conductivity
μ	Viscosity coefficient
ρ	Density of gas
τ	Representative scale for time
Φ	Bearing wall mass flux

Subscripts

0	Pertaining to the steady state
1	Referring to lower bearing surface
2	Referring to upper bearing surface

3.0 GOVERNING DIFFERENTIAL EQUATIONS FOR COMMON BEARING CONFIGURATIONS

The most common bearing geometries include those of

- slider bearing
- journal bearing
- thrust bearing
- conical bearing
- spherical bearing

For each of these geometries, the operator $\vec{\nabla}$ assumes a special form. In the following, the terms associated with $\vec{\nabla}^2$ in eq. (2.24) are developed for each of these five bearing geometries.

3.1 Slider Bearing (Figure 3.1)

The simplest slider bearing is one with a rectangular plan form and riding on a flat moving surface which has a uniform rectilinear velocity which is directed along one side of the slider. A very important application of the gas lubricated slider is the read/write head of a disc or drum type computer memory. The geometry of a rectangular head riding on a rotating disc is more general, this will be used as the model in the following derivation.

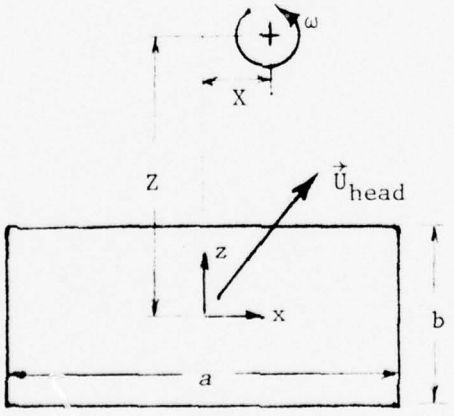

Fig. 3.1

Slider on a Rotating Disc

As shown in Figure 3.1, one may describe the present geometry with a set of Cartesian coordinates (x, z) such that the plan form of the slider is given by

$$-\frac{a}{2} \leq x \leq \frac{a}{2} \; ; \quad -\frac{b}{2} \leq z \leq \frac{b}{2} \tag{3.1}$$

Let $(\vec{i}, \vec{k})$ be the unit vectors of this coordinate system. The head itself may have a sliding velocity $\vec{U}_{head}$ corresponding to an actuation operation:

$$\vec{U}_{head} = \vec{i}\, u_2 + \vec{k} w_2 \tag{3.2}$$

Let the disc center be located at (X, Z) in the chosen coordinate system, then the disc velocity is

$$\vec{U}_{disc} = \vec{i}\omega(Z-z) + \vec{k}\omega(x-X) \tag{3.3}$$

Since the coordinate system is fixed to the center of the plan form of the slider, then considering the upper and lower surfaces of the bearing film to be respectively the head and the disc, one has

$$\vec{U}_1 = \vec{U}_{disc} - \vec{U}_{head} = \vec{i}[\omega(Z-z)-u_2] + \vec{k}[\omega(x-X)-w_2]; \quad \vec{U}_2 = 0 \tag{3.4}$$

Therefore,

$$\boxed{\vec{\nabla} \cdot [\tfrac{1}{2}(\vec{U}_1 + \vec{U}_2)ph] = \frac{1}{2}\{[\omega(Z-z) - u_2]\frac{\partial}{\partial x} + [\omega(x-X) - w_2\frac{\partial}{\partial z}]\}(ph)} \tag{3.5}$$

$$\boxed{\vec{\nabla} \cdot (h^3 p \vec{\nabla} p) = \frac{\partial}{\partial x}(h^3 p \frac{\partial p}{\partial x}) + \frac{\partial}{\partial z}(h^3 p \frac{\partial p}{\partial z})} \tag{3.6}$$

When the head is at a large distance from the disc center, (x,z) may be neglected in comparison to (X, Z) in eq. (3.5). That is, the disc velocity may be approximated by the tangential disc velocity at the head center.

3.2 Journal Bearing (Figure 3.2)

The journal bearing is characterized by a cylindrical surface. The curvature of the surface has significance mainly in the film shape of the eccentric gap and in projecting the pressure field to form the resultant bearing force. From the standpoint of the differential equation, the cylindrical surface can be simply described by a Cartesian coordinate system (θ, z) such that

SCHEMATIC OF A JOURNAL BEARING

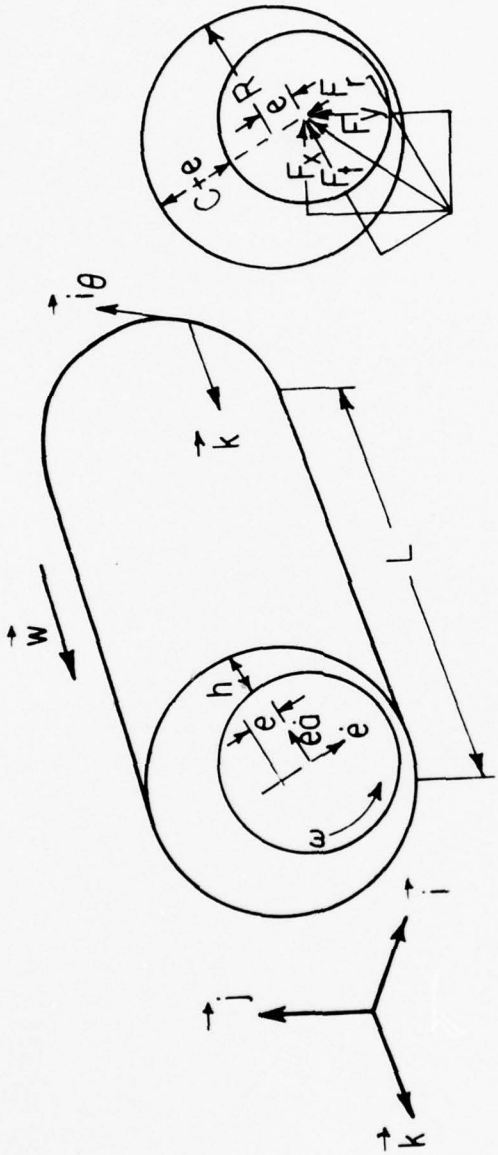

$$\epsilon = Ce$$
$$H = \frac{h}{C}$$
$$= 1 - \epsilon \cos\theta$$

$$\vec{\nabla} = \vec{i}_\theta \frac{\partial}{R\partial\theta} + \vec{k} \frac{\partial}{\partial z} \tag{3.7}$$

Each surface may rotate about, as well as translate along, the journal axis. Thus

$$\vec{U}_1 = \vec{i}_\theta \omega_1 R + \vec{k} w_1; \quad \vec{U}_2 = \vec{i}_\theta \omega_2 R + \vec{k} w_2 \tag{3.8}$$

R being the journal radius. Accordingly

$$\boxed{\vec{\nabla} \cdot [\frac{1}{2}(\vec{U}_1 + \vec{U}_2)ph] = \frac{1}{2} \left[(\omega_1 + \omega_2)\frac{\partial}{\partial\theta} + (w_1 + w_2)\frac{\partial}{\partial z} \right] (ph)} \tag{3.9}$$

$$\boxed{\vec{\nabla} \cdot (h^3 p \vec{\nabla} p) = \frac{\partial}{R\partial\theta} (h^3 p \frac{\partial p}{R\partial\theta}) + \frac{\partial}{\partial z} (h^3 p \frac{\partial p}{\partial z})} \tag{3.10}$$

3.3 Thrust Bearing (Figure 3.3)

The overall configuration of the thrust bearing is in the most part similar to that of a slider. However, the plan form may be either an annulus or a sector thereof, so that the natural coordinate system is that of the cylindrical polar coordinates, with the origin coincident with the axis of rotation. Writing $(\vec{i}_r, \vec{i}_\theta)$ for the unit vectors along the radial and circumferential directions, then

$$\vec{U}_1 = \vec{i}_\theta r\omega_1; \quad \vec{U}_2 = \vec{i}_\theta r\omega_2 \tag{3.11}$$

$$\vec{\nabla} = \vec{i}_r \frac{\partial}{\partial r} + \vec{i}_\theta \frac{\partial}{r\partial\theta} \tag{3.12}$$

then r is the local radial coordinate. Due to the inherent curvature of the coordinate system, for any

$$\vec{f} = \vec{i}_r f_r + \vec{i}_\theta f_\theta \tag{3.13}$$

$$\vec{\nabla} \cdot \vec{f} = \frac{1}{r} \left\{ \frac{\partial(rf_r)}{\partial r} + \frac{\partial f_\theta}{\partial\theta} \right\} \tag{3.14}$$

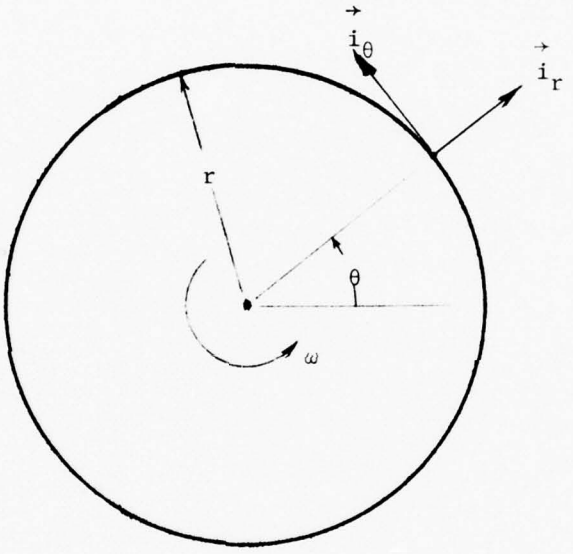

Fig. 3.3
Thrust Bearing Geometry

Consequently,

$$\vec{\nabla}_2 \cdot \left[\frac{1}{2}\,(\vec{U}_1 + \vec{U}_2)ph\right] = \frac{1}{2}(\omega_1 + \omega_2)\,\frac{\partial(ph)}{\partial\theta} \tag{3.15}$$

$$\vec{\nabla}_2 \cdot (h^3 p \vec{\nabla}_2 p) = \frac{1}{r^2}\left[\frac{\partial}{\partial r}\,(rh^3 p\,\frac{\partial p}{\partial r}) + \frac{\partial}{\partial\theta}\,(h^3 p\,\frac{\partial p}{\partial\theta})\right] \tag{3.16}$$

3.4 Conical Bearing (Figure 3.4)

Geometrically, the conical bearing is naturally described by the conical polar coordinates (R, ϕ). However, for a description of the sliding speed, as well as overall mechanical effects, the cylindrical polar coordinates (r,θ) are more useful. These two coordinate systems are related to each other through the half apex angle γ:

$$r = R\sin\gamma; \qquad \phi = \theta\sin\gamma \tag{3.17}$$

Except for the expression of $(\vec{U}_1, \vec{U}_2)$, equations (3.15) and 3.16) would be applicable upon replacing (r, θ) by (R, ϕ). The sliding velocities are, however

$$\vec{U}_1 = \vec{i}_\phi\, R\sin\gamma\omega_1; \qquad \vec{U}_2 = \vec{i}_\phi\, R\sin\gamma\omega_2 \tag{3.18}$$

Thus

$$\vec{\nabla}_2 \cdot \left[\frac{1}{2}(\vec{U}_1 + \vec{U}_2)ph\right] = \frac{1}{2}\,(\omega_1 + \omega_2)\sin\gamma\,\frac{\partial(ph)}{\partial\theta} = \frac{1}{2}\,(\omega_1 + \omega_2)\,\frac{\partial(ph)}{\partial\theta} \tag{3.19}$$

$$\begin{aligned}\vec{\nabla}_2 \cdot (h^3 p \vec{\nabla}_2 p) &= \frac{1}{R}\left[\frac{\partial}{\partial R}\,(Rh^3 p\,\frac{\partial p}{\partial R}) + \frac{\partial}{\partial\phi}\,(h^3 p\,\frac{\partial p}{R\partial\theta})\right] \\ &= \frac{1}{r^2}\left[\sin^2\gamma r\,\frac{\partial}{\partial r}\,(rh^3 p\,\frac{\partial p}{\partial r}) + \frac{\partial}{\partial\theta}\,(h^3 p\,\frac{\partial p}{\partial\theta})\right]\end{aligned} \tag{3.20}$$

3.5 Spherical Bearing (Figure 3.5)

The spherical surface is commonly described in terms of (ϕ, θ) which are respectively the co-latitudinal and the longitudinal angular coordinates. The

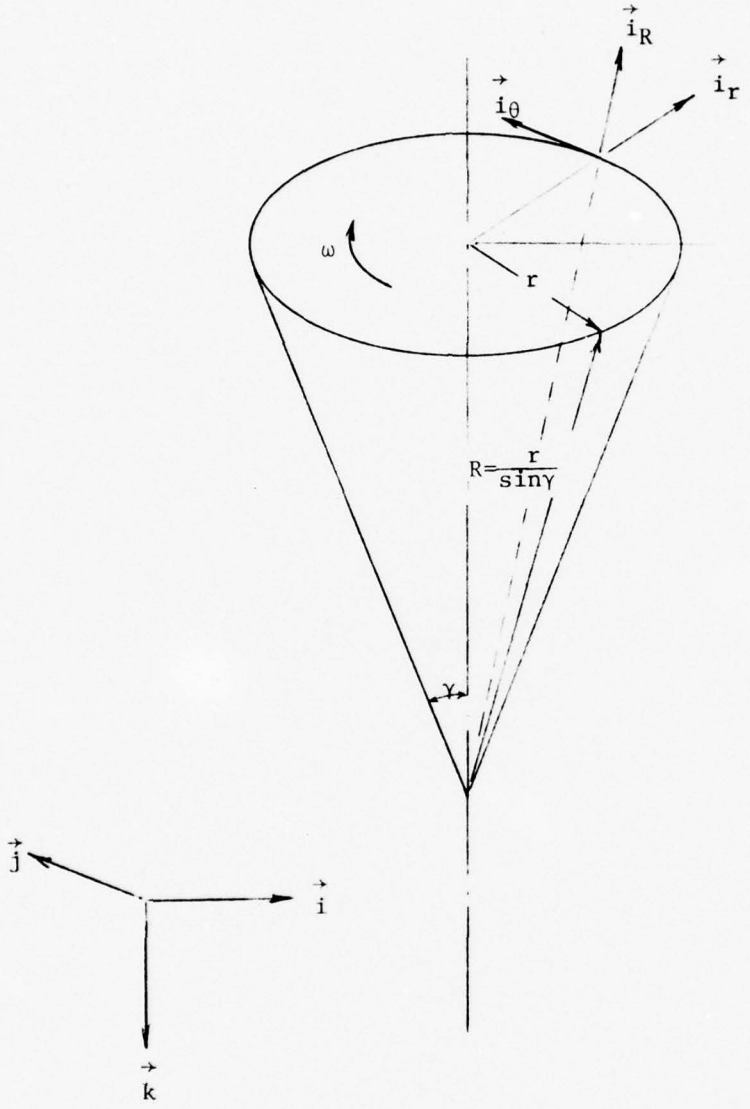

Fig. 3.4

Conical Bearing

direction of the polar axis, $\vec{k}$, would be oriented to preserve symmetry in the bearing geometry; i.e., a bearing border is described by a small circle (ϕ = const.). The triad of unit vectors of the chosen coordinate system, ($\vec{i}_\phi$, $\vec{i}_\theta$, $\vec{n}$), is defined in terms of (ϕ, θ) with respect to the reference Cartesian triad ($\vec{i}$, $\vec{j}$, $\vec{k}$). The spherical bearing is often used to allow "free orientation" of the "spin vector". Thus the spin vector, $\vec{\omega}$, may not coincide with the polar axis, $\vec{k}$. In general, the orientation of $\vec{\omega}$ is given by the angular parameters (α, β) with respect to the Cartesian reference. These relationships are illustrated in Figure 3.5. The spin vector, and the associated surface velocity are

$$\vec{\omega} = \omega \left\{ \begin{array}{l} \vec{i}_\phi \left[\sin\alpha\cos\phi\cos(\beta-\theta) - \cos\alpha\sin\phi\right] \\ + \vec{i}_\theta \sin\alpha\sin(\beta-\theta) \\ + \vec{n} \left[\sin\alpha\sin\phi\cos(\beta-\theta) + \cos\alpha\cos\phi\right] \end{array} \right\} \tag{3.21}$$

$$\vec{U} = \omega R \left\{ \begin{array}{l} \vec{i}_\phi \sin\alpha\sin(\beta-\theta) \\ + \vec{i}_\theta \left[\cos\alpha\sin\phi - \sin\alpha\cos\phi\cos(\beta-\theta)\right] \end{array} \right\} \tag{3.22}$$

The surface gradient operator is

$$\vec{\nabla} = \frac{1}{R\sin\phi} \left\{ \vec{i}_\phi \sin\phi \frac{\partial}{\partial\phi} + \vec{i}_\theta \frac{\partial}{\partial\theta} \right\} \tag{3.23}$$

and divergence of $\vec{f} = \vec{i}_\phi f_\phi + \vec{i}_\theta f_\theta$ is

$$\vec{\nabla} \cdot \vec{f} = \frac{1}{R\sin\phi} \frac{\partial}{\partial\phi} (\sin\phi f_\phi) + \frac{\partial f_\theta}{\partial\theta} \tag{3.24}$$

Accordingly

$$\boxed{\vec{\nabla} \cdot (\vec{U}ph) = \omega \left[\sin\alpha\sin(\beta-\theta) \frac{\partial ph}{\partial\phi} + \cos\alpha \frac{\partial}{\partial\theta} \left\{ \left[1 - \frac{\tan\alpha}{\tan\phi} \cos(\beta-\theta)\right] ph \right\} \right]} \tag{3.25}$$

$$\boxed{\vec{\nabla} \cdot (h^3 p \vec{\nabla} p) = \frac{1}{R^2\sin^2\phi} \left\{ \sin\phi \frac{\partial}{\partial\phi} (\sin\phi h^3 p \frac{\partial p}{\partial\phi}) + \frac{\partial}{\partial\theta} (h^3 p \frac{\partial p}{\partial\theta}) \right\}} \tag{3.26}$$

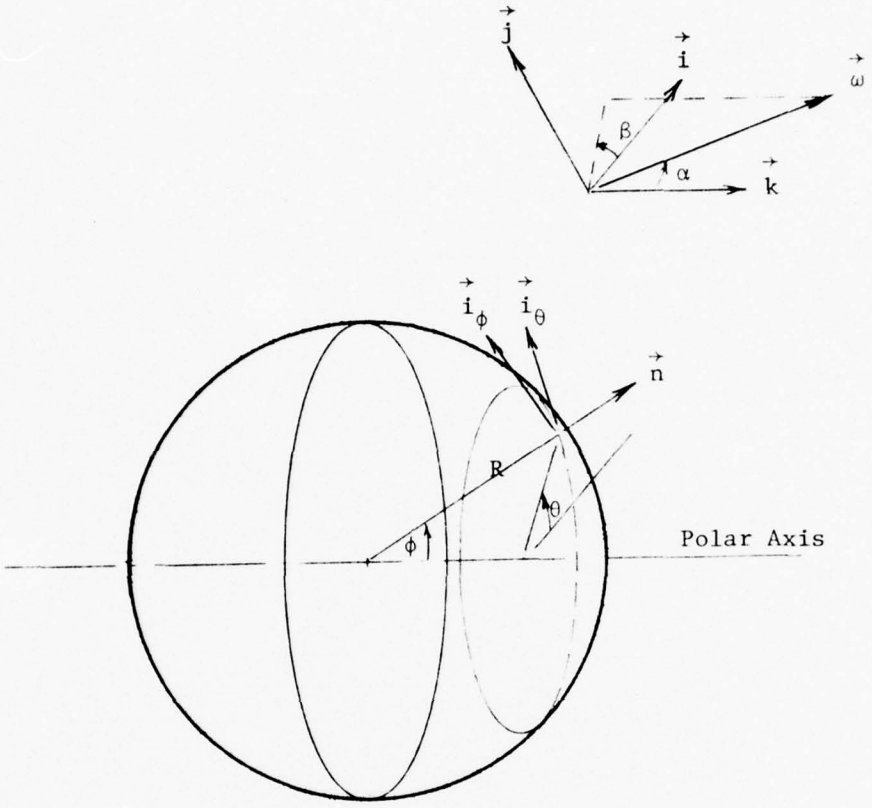

Fig. 3.5

Spherical Bearing

3.6 Useful Coordinate Transformations

It is seen above, that due to coordinate curvature, the expressions of $\vec{\nabla}_\zeta \cdot (h^3 \vec{\nabla}_\zeta p)$ respectively for the thrust bearing, the conical bearing, and the spherical bearing become quite cumbersome. It is sometimes useful to perform a coordinate transformation to facilitate analysis.

For thrust and conical bearings, the required transformation is

$$d\zeta = \frac{dr}{r}$$

Or,

$$\boxed{\zeta = \ln(r/r_o); \quad r = r_o \exp\{\zeta\}} \tag{3.27}$$

where r_o is a reference radius.

For the spherical bearing, the required transformation is

$$d\zeta = \frac{d\phi}{\sin\phi}$$

Or,

$$\boxed{\zeta = \ln \tan \frac{\phi}{2}; \quad \sin\phi = \operatorname{sech}\zeta; \quad \cos\phi \approx -\tan\zeta} \tag{3.28}$$

3.7 Nomenclature

Symbol	Definition	Chapter/ Section
a	Slider width in x-direction	
b	Slider width in z-direction	
C	Radial clearance	
e	Eccentricity	
f_r, f_θ, f_ϕ	Radial, circumferential, and colattitudinal components of $\vec{f}$	
$\vec{f}$	An arbitrary vector	
F_x, F_y	x- and y-components of journal bearing force	
F_r, F_t	Radial and tangential components of journal bearing force	
h	Bearing gap, h_2-h_1	
H	h/C	
$\vec{i}$	Unit vector along x-axis	
$\vec{i}_r, \vec{i}_\theta$	Radial and circumferential unit vectors	
$\vec{j}$	Unit vector along y-axis	
$\vec{k}$	Unit vector along z-axis	
p	Fluid pressure	
r	Cylindrical radial coordinate	
r_o	Reference radial coordinate	
R	Journal radius	3.2
R	Conical radial coordinate	3.4
R	Spherical radius	3.5
u	x-component of velocity	
$\vec{U}$	Projection of velocity vector on reference surface	

Symbol	Definition	Chapter/ Section
$\vec{U}_{head}$	Traversing velocity of read/write head	
w	z-component of $\vec{U}$	
x	Coordinate	
X	x-coordinate of disk center	
z	Coordinate	
Z	z-coordinate of disk center	
α	Attitude angle	3.2
α	Inclination of spin vector from polar axis	3.5
β	Dihedral angle of planes containing $\vec{\omega}$ and $\vec{k}$	3.5
γ	Half apex angle of cone	3.4
$\vec{\nabla}_2$	Two-dimensional surface spatial gradient operator	
ε	Eccentricity ratio of journal, e/C	3.2
ζ	Transformed meridianal coordinate	
θ	Polar angular coordinate	
ϕ	Angular coordinate on conical surface	3.4
ϕ	Colattitudinal angle of spherical bearing	3.5
ω	Rotational speed	
$\vec{\omega}$	Spin vector of spherical bearing	3.5

Subscripts

1	Referring to lower bearing surface
2	Referring to upper bearing surface
$(\dot{})$	Time-derivative of ( )

4.0 REPRESENTATIVE SOLUTIONS OF SELF-ACTING GAS BEARINGS

In a self-acting gas bearing, compressibility is manifested mainly in terms of the relative magnitude between the viscous wedge action and the ambient pressure level. At a highly compressible condition, the film pressure tends to be so adjusted to preserve a Couette character in the velocity profile at all interior points with the exception of sliding exit edges, where through a sharp pressure gradient the ambient boundary condition is satisfied. Examples illustrating this feature are given below.

4.1 Infinitely Long Sliders (Figure 4.1)

This is a special case of 3.1. (x, z, X) are neglected relative to Z. $U = \omega Z$ is the constant sliding speed. Also assumed to vanish are $(u_2, w_2, \Phi, \frac{\partial}{\partial z}, \frac{\partial}{\partial t})$. The differential equation is reduced to

$$\frac{d}{dx}\left(\frac{Uph}{2} - \frac{1}{12\mu} h^3 p \frac{dp}{dx}\right) = 0 \tag{4.1}$$

The boundary conditions are

$$p\ (x = 0, a) = p_a \tag{4.2}$$

Non-dimensionalization is achieved by defining

$$\bar{x} = x/a; \quad \bar{h} = h/C; \quad \bar{p} = p/p_a; \quad \Lambda = \frac{6\mu U a}{p_a C^2}$$

where C is a representative gap. Λ is the compressibility number for a slider.

Equations 4.1 and 4.2 are then rewritten as

$$\frac{d}{dx}\left(\Lambda \bar{p}\bar{h} - \bar{h}^3 \bar{p} \frac{d\bar{p}}{d\bar{x}}\right) = o \tag{4.3}$$

$$\bar{p}\ (\bar{x} = 0, 1) = 1 \tag{4.4}$$

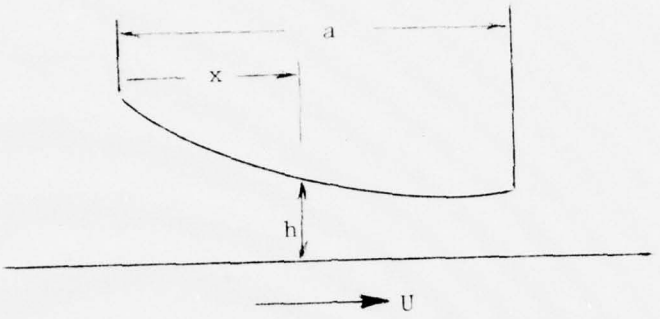

Fig. 4.1
Infinitely Long Slider

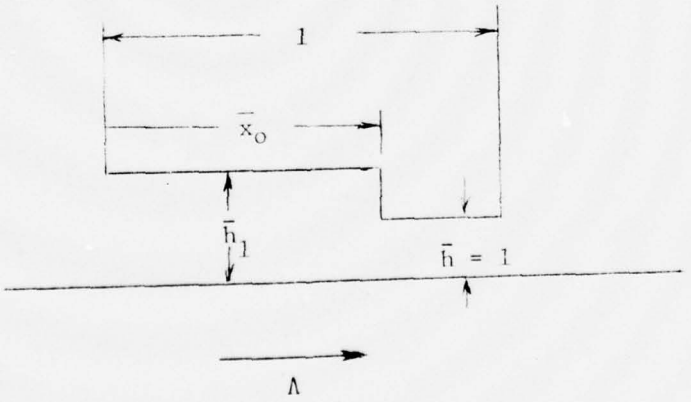

Fig. 4.2
Step - Slider

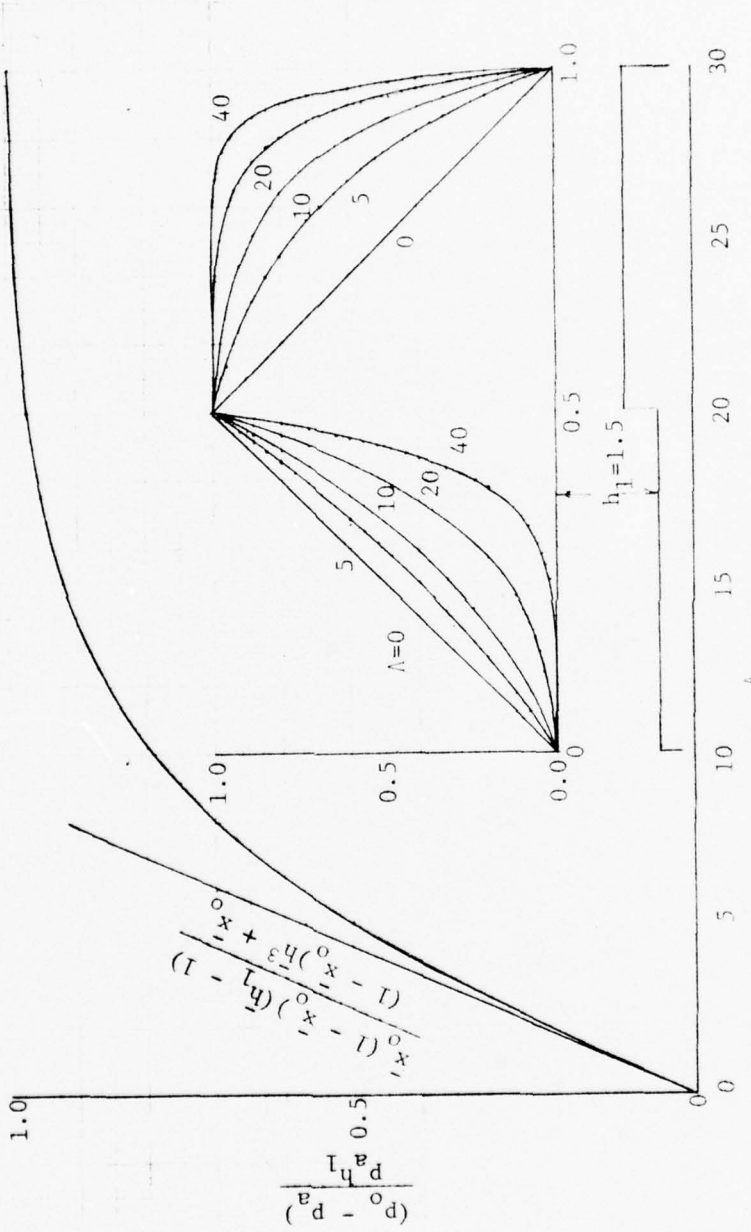

Fig. 4.3

Pressure Distributions in Step Slider

Equation (4.3) can be integrated once to yield

$$\bar{p}\bar{h}\left(1 - \frac{\bar{h}^2}{\Lambda}\frac{d\bar{p}}{d\bar{x}}\right) = \bar{h}^* \tag{4.5}$$

$\bar{h}^*$ is an integration constant; it represents the equivalent gap if the velocity profile were purely of the couette type. Suppose $\frac{d\bar{p}}{dx}$ vanishes at $\bar{x}^*$, then

$$\bar{h}^* = (\bar{p}\bar{h})\Big|_{\bar{x}^*} \tag{4.6}$$

At $(\bar{x} = 0, 1)$, $\bar{p} = 1$, then

$$\frac{d\bar{p}}{d\bar{x}} = \frac{\Lambda}{\bar{h}^3}\left(\bar{h} - \frac{\bar{h}^*}{\bar{p}}\right) \tag{4.7}$$

Thus, if Λ is to be recognized as positive by convention, then at either ambient edge, the sign of the pressure gradient is determined only by $(\bar{h} - \bar{h}^*)$. The following observations can be made.

4.1.1 $\bar{h}$ converges from the leading edge. An extremum of $\bar{p} = \bar{p}^*$ would exist at $\bar{x}^*$ where

$$\bar{h}^* = \bar{h}\,(\bar{x}^*) < \bar{h}\,(0)$$

This condition can only be satisfied by

$$\bar{h}^* < \bar{h}\,(0);\ \bar{p}^* > 1$$

Thus pressure near a converging leading edge is elevated from the ambient and must satisfy the constraint on its maxima:

$$1 < \bar{p}^* = \frac{\bar{h}^*}{\bar{h}(\bar{x}^*)} < \frac{\bar{h}(0)}{\bar{h}(\bar{x}^*)} \tag{4.8}$$

4.1.2 $\bar{h}$ diverges from the leading edge. Using similar reasoning as above, one concludes that pressure near a diverging leading edge is reduced from the ambient and its minima is bracketed in the range

$$\frac{\bar{h}\ (0)}{\bar{h}(\bar{x}^*)} < \bar{p}^* < 1 \tag{4.9}$$

The above results are affected by compressibility mainly in the constraints of pressure extrema according to (4.8) and (4.9). Further progress would depend on specific details of $\bar{h}$. Of special interest is the step slider, shown in Figure 4.2, which can be solved in close form [12].

4.2 Infinitely Long Step Sliders (Figure 4.2)

$\bar{h}$ is sectionally constant in the two regions ($0 < \bar{x} < \bar{x}_o$, $\bar{x}_o < \bar{x} < 1$). Equation (4.5) can be rewritten as

$$\frac{d\bar{p}}{d\bar{x}} = \lambda\left(1 - \frac{\gamma}{\bar{p}}\right) \tag{4.10}$$

where $\gamma = \bar{h}^*/\bar{h}$ and $\lambda = \Lambda/\bar{h}^2$ are constants in each region.

From Equation (4.10), one reasons that $\bar{p}$ must be monotonic in the range $0 < \bar{x} < \bar{x}_o$. If one further imposes Equation (4.5) as a matching condition at the step,

$$\bar{h}_1\left\{1 - \frac{\bar{h}_1^2}{\Lambda}\frac{d\bar{p}}{d\bar{x}}\ (\bar{x}_o^-)\right\} = \frac{\bar{h}^*}{\bar{p}(\bar{x}_o)} = 1 - \frac{1}{\Lambda^2}\frac{d\bar{p}}{d\bar{x}}\ (\bar{x}_o^+) \tag{4.11}$$

then one would reach the conclusions, for $\bar{h}_1 > 1$

$$1 < \frac{\bar{h}^*}{\bar{p}(\bar{x}_o)} < \bar{h}_1; \qquad \bar{p}(\bar{x}_o) > 1 \tag{4.12}$$

in order to satisfy the boundary conditions at ($\bar{x} = 0,1$). Equation (4.10) can be formally integrated for either region to yield:

$$\bar{p} - 1 + \gamma_1\ \ell n\ \left(\frac{\bar{p}-\gamma_1}{1-\gamma_1}\right) = \lambda_1\bar{x} \tag{4.13}$$

for $0 \le \bar{x} \le x_o$, where $\gamma_1 = \bar{h}^*/\bar{h}_1$ and $\lambda_1 = \Lambda/\bar{h}_1^2$; and

$$\bar{p} - 1 + \bar{h}^*\ \ell n\ \left(\frac{\bar{h}^*-\bar{p}}{\bar{h}^*-1}\right) = \Lambda(\bar{x}-1) \tag{4.14}$$

for $\bar{x}_o \le \bar{x} \le 1$.

These equations must result in the same $\bar{p}(\bar{x}_o) = \bar{p}_o$, therefore one obtains

$$\bar{h}_1(\bar{p}_o - 1) + \bar{h}^* \ln\left(\frac{\bar{p}_o\bar{h}_1 - \bar{h}^*}{\bar{h}_1 - \bar{h}^*}\right) = \frac{\Lambda}{\bar{h}_1}\bar{x}_o \tag{4.15}$$

$$\bar{p}_o - 1 + \bar{h}^* \ln\left(\frac{\bar{h}^* - \bar{p}_o}{\bar{h}^* - 1}\right) = \Lambda(\bar{x}_o - 1) \tag{4.16}$$

They define simultaneously the numerical constants $(\bar{p}_o, \bar{h}^*)$ for each set of $(\bar{h}_1, \bar{x}_o; \Lambda)$. The correct solution can be found in the range

$$1 < \bar{p}_o < \bar{h}^* < \bar{h}_1 \tag{4.17}$$

At extreme values of Λ, the limiting behaviors can be examined analytically.

4.2.1 Small Λ (Incompressible Case)

One may seek the solution in the form

$$\bar{p}_o = 1 + \Lambda\pi_o + O\{\Lambda^2\} \tag{4.18}$$

Substituting into Equations (4.15) and (4.16), collecting terms in the first power of Λ, one finds two simple linear algebraic equations which can be readily solved to yield

$$\bar{h}^* = \left[\frac{(1-\bar{x}_o)\bar{h}_1^2 + \bar{x}_o}{(1-\bar{x}_o)\bar{h}_1^3 + \bar{x}_o}\right]\bar{h}_1; \qquad \pi_o = \frac{\bar{x}_o(1-\bar{x}_o)(\bar{h}_1 - 1)}{(1-\bar{x}_o)\bar{h}_1^3 + x_o} \tag{4.19}$$

Accordingly,

$$\begin{aligned} \bar{p}(0 \le \bar{x} \le \bar{x}_o) &= 1 + \Lambda\,\pi_o\,\frac{\bar{x}}{\bar{x}_o} \\ \bar{p}(\bar{x}_o \le \bar{x} \le 1) &= 1 + \Lambda\,\pi_o\left(\frac{1-\bar{x}}{1-\bar{x}_o}\right) \end{aligned} \tag{4.20}$$

These seem to be the incompressible step-bearing solutions.

4.2.2 Large Λ (Highly Compressible Case)

The limiting behaviors of Equations (4.15) and (4.16) for large Λ require

$$\lim_{\Lambda\to\infty} (\bar{p}_o, \bar{h}^*) = (\bar{h}_1, \bar{h}_1)$$

Writing $\delta\bar{h} = \bar{h}_1 - \bar{h}^*$ and $\delta\bar{p} = \bar{h}_1 - \bar{p}_o$; then Equations (4.15) and (4.16) become:

$$\bar{h}_1(\bar{h}_1-1-\delta\bar{p}) + (\bar{h}_1-\delta\bar{h})\ \ell n\left[\frac{\bar{h}_1(\bar{h}_1-1)+\delta\bar{h}-\bar{h}_1\delta\bar{p}}{\delta\bar{h}}\right] = \frac{\Lambda\bar{x}_o}{\bar{h}_1} \qquad (4.21)$$

$$\bar{h}_1-1-\delta\bar{p} + (\bar{h}_1-\delta\bar{h})\ \ell n\left[\frac{\delta\bar{p}-\delta\bar{h}}{(\bar{h}_1-1)-\delta\bar{h}}\right] = -\Lambda(1-\bar{x}_o) \qquad (4.22)$$

For large Λ, dominating terms for the respective lefthand sides of the above equations are those containing $\ell n\delta\bar{h}$ and $\ell n(\delta\bar{p}-\delta\bar{h})$. Thus, for a first approximation,

$$\begin{bmatrix} \delta\bar{h} \\ \delta\bar{p} \end{bmatrix} = \frac{(\bar{h}_1-1)}{1+E_o}\begin{bmatrix} h_1E_1(1-E_2) \\ h_1E_1(1-E_2)+E_2(1-E_1) \end{bmatrix} \qquad (4.23)$$

where (E_o, E_1, E_2) are exponentially vanishing functions:

$$E_1 = \exp\left(-\frac{\Lambda\bar{x}_o}{\bar{h}_1^2}\right); \qquad E_2 = \exp\left(-\frac{\Lambda(1-\bar{x}_o)}{\bar{h}_1}\right)$$

$$E_o = E_1\{(\bar{h}_1-1) - \bar{h}_1E_2\} \qquad (4.24)$$

Accordingly, upon substituting $\delta\bar{h}$ into Equation (4.13) and

retaining only terms with commeasurate accuracy, one finds

$$\bar{p}(0 \le \bar{x} \le \bar{x}_o) = 1 + \frac{(\bar{h}_1-1)(1-E_2)}{1+E_o}\left[\exp\left(-\frac{\Lambda(\bar{x}_o-\bar{x})}{\bar{h}_1^{\,2}}\right) - E_1\right]$$

$$\bar{p}(\bar{x}_o \le \bar{x} \le 1) = 1 + \frac{(\bar{h}_1-1)(1-E_1)}{1+E_o}\left[1-\exp\left(-\frac{\Lambda(1-\bar{x})}{\bar{h}_1^{\,2}}\right)\right] \qquad (4.25)$$

In essence, $\bar{p}$ has become almost sectionally uniform; $\bar{p}(0 \le \bar{x} < \bar{x}_o) = 1$ and $\bar{p}(\bar{x}_o \le \bar{x} < 1) = \bar{h}_1$, except for boundary layer behaviors as $\bar{x} \to (\bar{x}_o^{\,-}, 1^-)$.

Sample results for ($\bar{h}_1 = 1.5$, $\bar{x}_o = 0.50$) are shown for a full range of Λ in Figure 4.3. The primary effects of compressibility are related to the pressure peak (which occurs at the step junction) and the pressure profiles on its two sides. For small values of Λ, the amount of peak pressure elevation above the ambient is essentially proportional to the product of the sliding speed and the fluid viscosity and is insensitive to the ambient pressure level. At large compressibility numbers, the peak pressure asymptotically approaches a constant multiple of the ambient pressure; this asymptotic multiple is numerically equal to the gap ratio $\bar{h}_1$. The pressure profile is approximately triangular at a small compressibility number, which causes concavity in the inlet portion and convexity in the exit portion of the pressure profile. As Λ becomes asymptotically large, the pressure profile approaches two horizontal lines with a rapid increase at the step and a rapid decrease at the exit edge.

4.3 Infinitely Long Taper Slider (Figure 4.4)

For a taper slider, the film thickness may be described as

$$\bar{h} = 1 + (1 - \bar{x})\,\Delta\bar{h} \qquad (4.26)$$

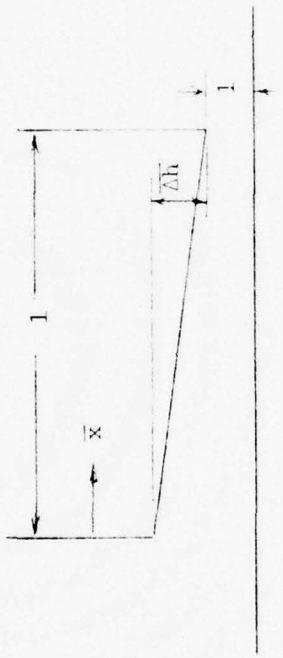

Fig. 4.4

Tapered Slider

so that

$$\frac{d\bar{h}}{d\bar{x}} = -\Delta\bar{h} \tag{4.27}$$

which is a constant. This fact allows one to reduce Equation (4.5) into an exact integral with the aid of the transformation

$$\psi = \bar{p}\bar{h}; \qquad d\xi = -\frac{\Delta\bar{h}}{\bar{h}}\,d\bar{x}; \qquad \xi = \ell n\bar{h} \tag{4.28}$$

Equation (4.5) accordingly can be rewritten as

$$\psi\{1 + \frac{1}{\lambda}\,(\frac{d\psi}{d\xi} - \psi)\} = \bar{h}^*; \qquad \lambda = \frac{\Lambda}{\Delta\bar{h}} \tag{4.29}$$

This equation can be integrated in closed form; whereupon substitution of the original variable $\bar{h}$ for $\ell n\xi$ yields

$$\frac{(\psi-\beta_1)(\psi-\beta_2)}{(1-\beta_1)(1-\beta_2)}\left[\frac{1-\beta_2}{1-\beta_1}\,\frac{\psi-\beta_1}{\psi-\beta_2}\right]^{\frac{\lambda}{(\beta_1-\beta_2)}} = \bar{h}^2 \tag{4.30}$$

where

$$(\beta_1, \beta_2) = \frac{\lambda}{2} \pm \sqrt{\frac{\lambda^2}{4} - \lambda\bar{h}^*} \tag{4.31}$$

For small values of λ, (β_1, β_2) are complex:

$$(\beta_1, \beta_2) = \frac{\lambda}{2} \pm i\gamma; \qquad \gamma = \sqrt{\lambda\bar{h}^* - \frac{\lambda^2}{4}} \tag{4.32}$$

Then, instead of Equation (4.30)

$$\left[\frac{(\psi - \frac{\lambda}{2})^2 + \gamma^2}{(1 - \frac{\lambda}{2})^2 + \gamma^2}\right] \exp\left[\frac{\lambda}{\gamma}\tan^{-1}\frac{\gamma(\psi-1)}{(1 - \frac{\lambda}{2})(\psi - \frac{\lambda}{2}) + \gamma^2}\right] = \bar{h}^2 \tag{4.33}$$

For each λ, $\bar{h}^*$ is found by satisfying the inlet boundary condition ($\psi = 1 + \Delta\bar{h}$ when $\bar{h} = 1 + \Delta\bar{h}$) in either Equation (4.30) or (4.33), depending on whether (β_1, β_2) are real or complex. This complicates the computation process somewhat; the general numerical features are as shown in Figure 4.5. At small Λ, $\bar{p}$ is directly proportional to Λ so that the actual film pressure is independent of the ambient pressure. As Λ becomes increasingly larger, however, $\bar{p}$ does increase indefinitely, but becomes ultimately bounded by the asymptotic limit $\bar{p}\bar{h} = 1 + \Delta\bar{h}$ whereupon at the trailing edge $\bar{p}$ drops abruptly to meet the ambient condition.

4.4 Plain Journal Bearing (Figure 4.6)

The simplest journal bearing is a rotating journal with its axis displaced from, but remaining parallel to the axis of the stationary bushing. Both the journal and the bushing surfaces are purely cylindrical. Axial motion is assumed to be absent. The following conditions thus prevail for Equations (3.9) and (3.10)

$$\omega_1 = \omega; \quad \omega_2 = 0$$

$$w_1 = w_2 = 0$$

$$h = C(1 - \varepsilon\cos\theta) \tag{4.34}$$

Using the dimensionless variables

$$\bar{z} = z/R; \quad \bar{p} = p/p_a; \quad \bar{h} = h/C = 1 - \varepsilon\cos\theta$$

$$\Lambda = \frac{6\mu\omega R^2}{p_a C^2} \tag{4.35}$$

then Equation (2.24), for impermeable walls and at steady state, is reduced to

$$\frac{\partial}{\partial\theta}\left(\bar{h}^3\bar{p}\,\frac{\partial\bar{p}}{\partial\theta}\right) + \frac{\partial}{\partial\bar{z}}\left(\bar{h}^3\bar{p}\,\frac{\partial\bar{p}}{\partial\bar{z}}\right) = \Lambda\,\frac{\partial}{\partial\theta}\left(\bar{p}\bar{h}\right) \tag{4.36}$$

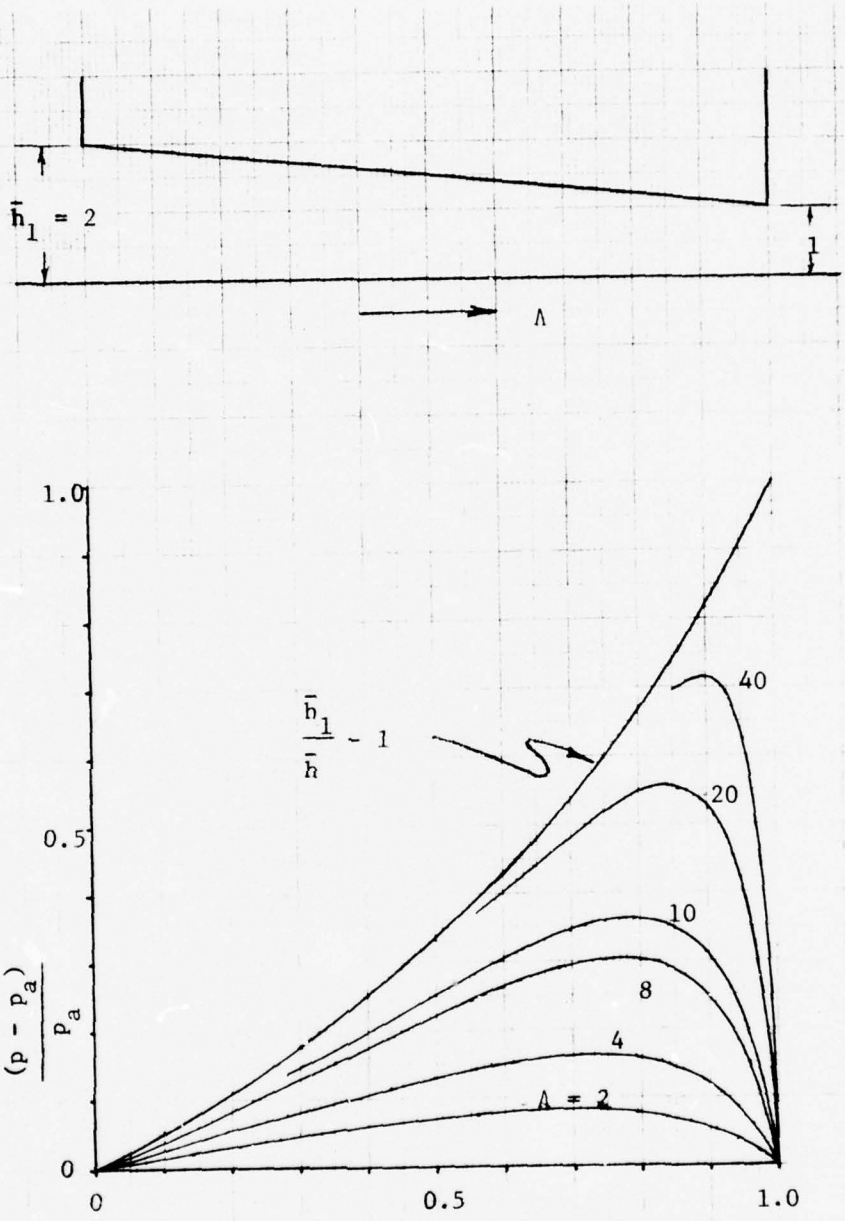

Fig. 4.5

Pressure Distributions in Tapered Slider

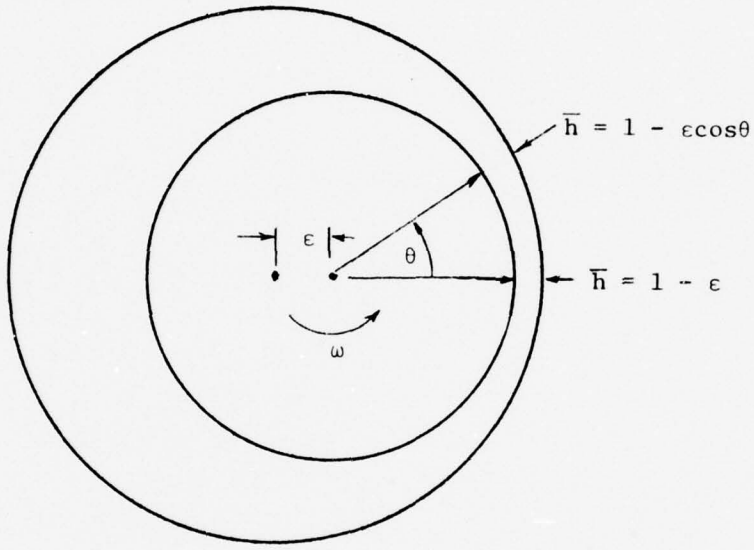

Fig. 4.6

Cross Section of Eccentric Journal

The boundary conditions are

$$\bar{p}(\bar{z} = \pm L/D) = 1 \tag{4.37}$$

and periodicity in θ.

In its complete form, Equation (4.36) is not amenable to a rigorous closed form solution. Results obtained by numerical computation have been quite thoroughly compiled for engineering analysis [13,14]. Asymptotic approximations have in some instances rendered closed form solutions, while in other cases simplified the numerical formulation considerably. These are reviewed in the following to bring out the relevant physical features which are substantially valid irrespective of the asymptotic approximations.

4.4.1 Small Eccentricity Solution

Presuming analytical continuity in the limiting condition $\varepsilon \to 0$, a power series solution may be postulated:

$$\bar{p} = 1 + \varepsilon p_\varepsilon \tag{4.38}$$

Substituting into Equation (4.36) and collecting terms associated with the first power of ε, one obtains

$$\frac{\partial}{\partial\theta}\left\{\left(\frac{\partial}{\partial\theta} - \Lambda\right)\bar{p}_\varepsilon\right\} + \frac{\partial^2 p_\varepsilon}{\partial \bar{z}^2} = \Lambda\sin\theta \tag{4.39}$$

and the corresponding boundary conditions are

$$\bar{p}_\varepsilon(\bar{z} = \pm L/D) = 0 \tag{4.40}$$

This formulation is known as the "Linearized P" solution [15,16] and is valid for all (Λ, L/D) provided $o(\varepsilon^2)$ is sufficiently small.

An analogous formulation can be carried out with the expansion

$$\psi = \bar{p}\bar{h} = 1 + \varepsilon\psi_\varepsilon \tag{4.41}$$

Accordingly, Equation (4.36) is reduced to

$$\frac{\partial}{\partial\theta}\{(\frac{\partial}{\partial\theta} - \Lambda)\psi_\varepsilon\} + \frac{\partial^2\psi_\varepsilon}{\partial z^2} = \cos\theta \tag{4.42}$$

with the boundary conditions

$$\psi_\varepsilon(\bar{z} = \pm L/D) = -\cos\theta \tag{4.43}$$

This latter formulation is known as the "Linearized PH" solution [17].

It is almost self evident that $\bar{p}_\varepsilon$ and ψ_ε are related to each other by

$$\psi_\varepsilon = \bar{p}_\varepsilon - \cos\theta \tag{4.44}$$

The advantage of treating ψ instead of $\bar{\bar{p}}\bar{\bar{h}}$ as the unknown is due to the asymptotic condition

$$\lim_{\Lambda\to\infty} \psi = \text{constant} \tag{4.45}$$

for all ε, even though the constant itself is somewhat dependent on ε. This interesting result will be further elaborated in Section 4.4.2. For any finite Λ, however, ψ_ε does not have any advantage over $\bar{p}_\varepsilon$. In the present section, no further attention will be given to ψ_ε.

The harmonic dependence on θ in the nonhomogeneous term of Equation (4.39) and the inherent θ-periodicity of $\bar{p}_\varepsilon$ suggest the solution to be of the form

$$\bar{p}_\varepsilon = \mathrm{Re}\{qe^{i\theta}\} \tag{4.46}$$

Accordingly, Equation (4.39) is reduced to

$$\{\frac{d^2}{d\bar{z}^2} - (1 + i\Lambda)\}q = -i\Lambda \tag{4.47}$$

A closed form solution satisfying the boundary condition

$$q(\bar{z} = \pm L/D) = 0 \tag{4.48}$$

is

$$q = \left(\frac{i\Lambda}{1+i\Lambda}\right)\left[1 - \frac{\cosh\sqrt{1+i\Lambda}\ \bar{z}}{\cosh\sqrt{1+i\Lambda}\ \left(\frac{L}{D}\right)}\right] \tag{4.49}$$

Since $\bar{p}$ as given by Equation (4.46) is a sinusoidal function of θ, real and imaginary portions of q represent respectively a component in phase with the minimum gap region and a quadrative component shifted a quadrant toward the convergent side of the bearing gap.

$$\lim_{\Lambda\to 0} q = i\Lambda\left\{1 - \frac{\cosh\bar{z}}{\cosh\left(\frac{L}{D}\right)}\right\} \tag{4.50}$$

$$\lim_{\Lambda\to\infty} q = 1 - \frac{\cosh\sqrt{i\Lambda}\ \bar{z}}{\cosh\sqrt{i\Lambda}\ \left(\frac{L}{D}\right)} \tag{4.51}$$

Thus, at small Λ, q is proportional to Λ and is a purely quadrature component. At large Λ, except for the end regions $\sqrt{i\Lambda}\,(L/D-|\bar{z}|) = 0\{1\}$, q is essentially uniform with respect to $\bar{z}$ and is inphase with the minimum gap.

4.4.2 Large Λ Solution

For large Λ, Equation (4.36) may be rewritten as

$$\frac{\partial(\psi)}{\partial\theta} = \frac{1}{\Lambda}\left\{\frac{\partial}{\partial\theta}\left(\bar{h}^3\bar{p}\,\frac{\partial\bar{p}}{\partial\theta}\right) + \frac{\partial}{\partial\bar{z}}\left(\bar{h}^3\bar{p}\,\frac{\partial\bar{p}}{\partial\bar{z}}\right)\right\} \tag{4.52}$$

where $\psi = \bar{p}\bar{h}$. If one <u>presumes</u> the terms enclosed in the brackets to be bounded, then as $\Lambda \to \infty$, Equation (4.52) would indicate

$$\lim_{\Lambda\to\infty} \frac{\partial(\psi)}{\partial\theta} = 0 \tag{4.53}$$

This condition is a bit unusual in two aspects. Firstly, Equation (4.53) is in direct contradiction with the boundary condition

$$\frac{\partial(\psi)}{\partial\theta}\Big|_{\bar{z}=\pm L/D} = \frac{\partial\bar{h}}{\partial\theta} = \varepsilon\sin\theta \tag{4.54}$$

Secondly, Equation (4.53) has a totally different structure as compared with Equation (4.36) from the standpoint of the theory of partial differential equations.

To remove the above two objections, one must reformulate the present problem in terms of a "matched asymptotic expansion" [18]. With such an approach, Equation (4.53) is to be imposed only in the open domain

$$|\bar{z}| < \frac{L}{D} \tag{4.55}$$

as an "outer solution." Whereas, in order that the boundary conditions may be reconciled, an edge region bordering each end would be recognized such that

$$\frac{\partial\bar{p}}{\partial\bar{z}} = O\{\sqrt{\Lambda}\} \quad \text{for } 0 \leq \frac{L}{D} - |\bar{z}| = O\{\Lambda^{-1/2}\} \tag{4.56}$$

Accordingly, a rescaling of the axial coordinate is in order; namely, for the edge regions, one can define

$$\zeta = \sqrt{\Lambda}\,(\frac{L}{D} - |\bar{z}|) \tag{4.57}$$

so that instead of Equation (4.52), one has the edge equation

$$\bar{h}\,\frac{\partial^2}{\partial\zeta^2}\,(\frac{\psi_e^2}{2}) - \frac{\partial\psi_e}{\partial\theta} = -\frac{1}{\Lambda}\,\frac{\partial}{\partial\theta}\,\{\bar{h}\,\frac{\partial}{\partial\theta}\,(\frac{\psi_e^2}{2}) - (\frac{\psi_e^2}{2})\varepsilon\sin\theta\} \tag{4.58}$$

where $\psi_e = (\bar{p}\bar{h})_{edge}$. Neglecting the righthand side of Equation

(4.58) no longer causes the two objections previously raised with respect to Equation (4.53). The boundary condition at $\zeta = 0$ can be directly identified with Equation (4.54).

The procedure to connect the "outer solution" with the boundary layer solution remains to be developed. The key is contained in the "mass content rule" for self-acting gas bearings [4] which is to be derived in the following.

Because $\bar{h}$ does not depend on $\bar{z}$, Equation (4.36) can be rewritten as

$$\frac{\partial^2}{\partial \bar{z}^2}\left(\frac{\bar{h}^3\bar{p}^2}{2}\right) = \frac{\partial}{\partial\theta}\left\{\Lambda(\bar{p}\bar{h}) - \bar{h}^3\bar{p}\,\frac{\partial \bar{p}}{\partial\theta}\right\} \tag{4.59}$$

Integrating both sides over the full circumference, as $\bar{p}$ and $\bar{h}$ are both periodic, the righthand side would vanish; so that

$$\frac{d^2}{d\bar{z}^2}\int_0^{2\pi}(\bar{h}^3\bar{p}^2)\,d\theta = 0 \tag{4.60}$$

or,

$$\int_0^{2\pi}(\bar{h}^3\bar{p}^2)\,d\theta = C_0 + C_1\bar{z} \tag{4.61}$$

Since $\bar{p}(\bar{z} = \pm L/D) = 1$, one obtains

$$C_1 = 0$$

$$C_0 = \int_0^{2\pi}\bar{h}^3 d\theta = 2\pi\left(1 + \frac{3}{2}\varepsilon^2\right)$$

Therefore

$$\boxed{\frac{1}{2\pi}\int_0^{2\pi}(\bar{h}^3\bar{p}^2)\,d\theta = 1 + \frac{3}{2}\varepsilon^2} \tag{4.62}$$

This is the celebrated "Mass Content Rule."

Equation (4.62) is valid for all $\bar{z}$. If one applies it to the outer solution, then

$$\lim_{\Lambda\to\infty} \psi^2 \frac{1}{2\pi} \int_0^{2\pi} \bar{h} d\theta$$

$$= \lim_{\Lambda\to\infty} \psi^2 = 1 + \frac{3}{2}\varepsilon^2$$

Or,

$$\lim_{\Lambda\to\infty} \psi = \sqrt{1 + \frac{3}{2}\varepsilon^2}$$

$$\lim_{\Lambda\to\infty} \bar{p} = \frac{\sqrt{1 + \frac{3}{2}\varepsilon^2}}{1 - \varepsilon\cos\theta} \tag{4.63}$$

As the "edge solution" must blend into the "outer solution" smoothly, this also becomes the second boundary condition for Equation (4.58):

$$\bar{p}_{edge}(\zeta\to\infty,\theta) = \frac{\sqrt{1 + \frac{3}{2}\varepsilon^2}}{1 - \varepsilon\cos\theta} \tag{4.64}$$

It is clear now that $\psi = \bar{p}\bar{h} \to$ constant is a condition prevailing at large Λ for all ε. The asymptotic value of ψ, however, is an explicit function of ε according to Equation (4.63). The global inaccuracy of this approximation is $O\{1/\sqrt{\Lambda}\}$ which corresponds to the axial fraction of the edge region. Thus the "linearized PH" solution actually does not accomplish any improvement beyond ψ = constant in the central region. The term given by Equation (4.44) furnishes a portion of the next improvement, which is of $O\{1/\sqrt{\Lambda}\}$ in the global sense.

To extend the accuracy in the large Λ region, the outer solution may be found by solving Equation (4.52) with the expansion

$$\psi = \sqrt{1 + \frac{3}{2}\varepsilon^2} + \Lambda^{-1}\psi_1 + \ldots \tag{4.65}$$

obtaining

$$\psi_1 = \psi_{10} - \frac{3}{2}\varepsilon\sqrt{1 + \frac{3}{2}\varepsilon^2}\sin\theta$$

ψ_{10} is an additional constant to be determined by Equation (4.62) and turns out to be

$$\psi_{10} = 0$$

Thus,

$$\psi_1 = -\frac{3}{2}\varepsilon\sqrt{1 + \frac{3}{2}\varepsilon^2}\sin\theta \tag{4.66}$$

The "edge solution" should be similarly expanded as

$$\psi_e = \psi_{e0} + \Lambda^{-1}\psi_{e1} + \ldots \tag{4.67}$$

The leading terms are to satisfy the following conditions:

$$\frac{\partial\psi_{e0}}{\partial\theta} - \bar{h}\frac{\partial}{\partial\zeta}\left(\psi_{e0}\frac{\partial\psi_{e0}}{\partial\zeta}\right) = 0$$

$$\psi_{e0}(\zeta=0,\theta) = \bar{h} \tag{4.68}$$

$$\psi_{e0}(\zeta\to\infty,\theta) = \sqrt{1 + \frac{3}{2}\varepsilon^2}$$

$$\frac{\partial\psi_{e1}}{\partial\theta} - \bar{h}\frac{\partial}{\partial\zeta}\left(\psi_{e0}\frac{\partial\psi_{e1}}{\partial\zeta} + \psi_{e1}\frac{\partial\psi_{e0}}{\partial\zeta}\right)$$

$$= \bar{h}\frac{\partial}{\partial\theta}\left(\psi_{e0}\frac{\partial\psi_{e0}}{\partial\theta}\right) - \frac{\psi_{e0}^2}{2}\varepsilon\cos\theta \tag{4.69}$$

$$\psi_{e1}(\zeta=0,\theta) = 0$$

$$\psi_{e1}(\zeta\to\infty,\theta) = -\frac{3}{2}\varepsilon\sqrt{1+\frac{3}{2}\varepsilon^2}\,\sin\theta$$

Since further correction would be of $O\{\Lambda^{-2}\}$ for both the "outer" and the "edge" solutions, local accuracy up to $O\{\Lambda^{-1}\}$ is achieved by $(\psi_0, \psi_1, \psi_{e0}, \psi_{01})$ everywhere. Global accuracy, however, is of $O\{\Lambda^{-3/2}\}$.

4.4.3 Long Journal Bearing

If L/D is very large, (L/2) instead of R is a more appropriate scale for the axial coordinate. If one defines

$$\eta = 2z/L = \left(\frac{D}{L}\right)\bar{z} \tag{4.70}$$

then Equation (4.36) becomes

$$\frac{\partial}{\partial\theta}\left(\bar{h}^3\bar{p}\,\frac{\partial\bar{p}}{\partial\theta} - \Lambda\bar{\bar{p}}\bar{h}\right) = -\left(\frac{D}{L}\right)^2\frac{\partial}{\partial\eta}\left(\bar{h}^3\bar{p}\,\frac{\partial\bar{p}}{\partial\eta}\right) \tag{4.71}$$

Clearly, if one lets the righthand side vanish, one again obtains an "outer solution" which is not valid for $1-|\eta| = O\{D/L\}$. The outer solution is governed by

$$\frac{d}{d\theta}\left(\bar{h}^3\bar{p}\,\frac{d\bar{p}}{d\theta} - \Lambda\bar{\bar{p}}\bar{h}\right) = 0$$

Or, integrating once,

$$\bar{h}^3\bar{p}\,\frac{d\bar{p}}{d\theta} = \Lambda(\bar{\bar{p}}\bar{h} - \psi^*) \tag{4.72}$$

ψ^* is a constant of integration. The value $\bar{p}_0 = \bar{p}(\theta=0)$ may be regarded as the second constant of integration, thus

$$\bar{p}(\theta) = \bar{p}_0 + \Lambda\int_0^\theta d\theta'\left(\frac{1}{\bar{h}^2} - \frac{\psi^*}{\bar{h}^3\bar{p}}\right) \tag{4.73}$$

For every ψ^*, the correct value of $\bar{p}_0$ is found by the condition

$$\bar{p}(\pm 2n\pi) = \bar{p}(0) \tag{4.74}$$

A suitable continuous iteration procedure is to increment n repeatedly to find $\bar{p}(0)$:

$$\bar{p}_0 = \bar{p}_0' + \Lambda \int_0^{-2n\pi} d\theta \left(\frac{1}{\bar{h}^2} - \frac{\psi^*}{\bar{h}^3 \bar{p}}\right) \tag{4.75}$$

Integration in the negative θ direction assures numerical stability. Convergence is reached when further increment of n cease to yield significant change. Whereupon the "mass content rule" would be checked to verify the correctness of ψ^*.

The ambient boundary condition is satisfied by the construction of an edge solution. The axial coordinate for the edge solution is to be rescaled in order to retain the righthand side of Equation (4.71). Thus defining

$$\zeta = \left(\frac{L}{D}\right)(1 - |\eta|) \tag{4.76}$$

at either end, the edge problem is expressed as

$$\frac{\partial}{\partial\theta}\left(\bar{h}^3 \bar{p}_e \frac{\partial \bar{p}_e}{\partial\theta} - \Lambda \bar{p}_e \bar{h}\right) + \frac{\partial}{\partial\zeta}\left(\bar{h}^3 \bar{p}_e \frac{\partial \bar{p}_e}{\partial\zeta}\right) = 0 \tag{4.77}$$

The required boundary conditions include

$$\bar{p}_e(\theta+2\pi, \zeta) = \bar{p}_e(\theta, \zeta); \qquad \left.\frac{\partial \bar{p}_e}{\partial\theta}\right|_{\theta+2\pi,\zeta} = \left.\frac{\partial \bar{p}_e}{\partial\theta}\right|_{\theta,\zeta}$$

$$\bar{p}_e(\theta, \zeta=0) = 1$$

$$\bar{p}_e(\theta, \zeta\to\infty) = \bar{p}(\theta) \tag{4.78}$$

The last expressions ensure smooth blending of $\bar{p}_e$ into the "outer solution."

4.4.4 Short Journal Bearing

If L/D is small, the compressibility number would have to be rescaled as

$$\Lambda_{sh} = (\frac{L}{D})^2 \Lambda \tag{4.79}$$

Accordingly, Equation (4.71) can be rewritten as

$$\frac{\partial}{\partial \eta} (\bar{h}^3 \bar{p} \frac{\partial \bar{p}}{\partial \eta}) - \Lambda_{sh} \frac{\partial}{\partial \theta} (\bar{p}\bar{h}) = - (\frac{L}{D})^2 \frac{\partial}{\partial \theta} (\bar{h}^3 \bar{p} \frac{\partial \bar{p}}{\partial \theta}) \tag{4.80}$$

The righthand side is dropped when $(\frac{L}{D}) \to 0$. If η is replaced by $\zeta/\sqrt{\Lambda_{sh}}$, Equation (4.80) becomes identical as Equation (4.58), which is concerned with the edge problem with a large compressibility number. The axial boundary conditions are, however, different. Here, one has

$$\bar{p}(\eta = \pm 1, \theta) = 1 \tag{4.81}$$

4.5 Nomenclature

Symbol	Definition	Chapter/ Section
a	Slider width in x-direction	
C_0, C_1	Constants	
D	Journal diameter	
E_0, E_1, E_2	Expoential functions in compressible step slider solution, eq. (4.24)	4.2
h	bearing gap, $h_2 - h_1$	
$\bar{h}$	h/C	
$\bar{h}_1$	Inlet to exit gap ratio	
$\bar{h}^*$	Constant of integration in slider solution	
$\delta\bar{h}$	$\bar{h}_1 - \bar{h}^*$ for step slider at large Λ	4.2
$\Delta\bar{h}$	$\bar{h}_1 - 1$ of taper slider	4.3
L	Journal length	
p	Fluid pressure	
p_a	Ambient pressure	
p_e	Perturbation of $\bar{p}$ with respect to ε	
$\bar{p}$	p/p_a	
$\bar{p}_\varepsilon$	Edge solution of $\bar{p}$ for long journal	
$\bar{p}_o$	$\bar{p}$ at $\bar{x}_o$ of step slider	
$\bar{p}^*$	Extremum of $\bar{p}$	
$\delta\bar{p}$	$\bar{h}_1 - \bar{p}_o$ of step bearing for large Λ	
q	Function in solution of p_ε for journal, eq. (4.46)	
R	Journal radius	
U	Sliding speed	

Symbol	Definition	Chapter/ Section
x	Coordinate	
$\bar{x}$	x/a	
$\bar{x}_o$	Width fraction of step	
$\bar{x}^*$	Value of $\bar{x}$ at pressure peak	
z	Axial coordinate of journal	
$\bar{z}$	z/R of journal	
β_1, β_2	Numerical parameters in taper slider solution, eq. (4.31) and (4.32)	4.3
γ	$\bar{h}^*/\bar{h}$ for step slider	4.2
γ	Numerical parameter in taper-slider solution, eq. (4.32)	4.3
ϵ	Eccentricity ratio of journal, e/C	4.4
ζ	Dimensionless axial edge coordinate for long journal	4.4.3
η	Dimensionless axial coordinate of long journal, $2z/L$	4.4.3
θ	Polar angular coordinate	
θ'	Dummy variable of integration for θ	
λ	$\Lambda/\bar{h}^2$ for step slider	4.2
λ	$\Lambda/\Delta\bar{h}$ for taper slider	4.3
ω	Rotational speed	
Λ	Compressibility number for slider, $\frac{6\mu U a}{p_a C^2}$	4.1
Λ	Compressibility number for journal, $\frac{6\mu\omega R^2}{p_a C^2}$	4.4
Λ_{sh}	Short journal compressibility number, $(\frac{L}{D})^2 \Lambda$	4.4
μ	Viscosity coefficient	
ξ	Independent variable of taper slider solution $\ell n\bar{h}$	4.3

Symbol	Definition	Chapter/ Section
Π_o	Incompressible step slider solution	4.2
ψ	$\frac{\bar{p}\bar{h}}{}$	
ψ_1	First order term in reciprocal expansion for the "outer solution" of journal at large Λ, eq. (4.66)	4.4
ψ_e	"Edge solution" of ψ for journal at large Λ	4.4
ψ_{eo}, ψ_{el}	Leading terms in reciprocal expansion for ψ_e eq. (4.67)	4.1
ψ_ε	Perturbation of ψ with respect to ε	4.4
ψ^*	Constant of integration in solution for an infinitely long journal	4.4

5.0 EXTERNALLY-PRESSURIZED BEARINGS

In an externally-pressurized gas bearing the pressurization level (relative to the ambient) set the range of film pressure. Due to compressibility, the supply-to-ambient pressure ratio, instead of the pressure difference, is the governing parameter in the operating characteristics of the bearing. The steady-state governing equation for the most general externally-pressurized bearing is

$$\vec{\nabla} \cdot (h^3 p \vec{\nabla} p) = \frac{12\mu}{T} \Sigma\Phi \tag{5.1}$$

$\Sigma\Phi$ accounts for effluxes through both bearing surfaces. For externally pressurized porous gas bearings, $\Sigma\Phi$ would normally be negative.

In comparison to the self-acting gas bearing, mathematics required to solve the externally pressurized gas bearing is relatively straight forward. The unknown of Equation (5.1) may be considered to be $\frac{1}{2} p^2$ and the equation is in fact linear. In many instances, when the gap is uniform and the surfaces are impermeable, closed form exact solutions are available. However, to analyze an externally-pressurized bearing, most of the time, one cannot treat Equation (5.1) as an isolated problem because the bearing film is often only a portion of the overall pneumatic network between the pressurized source and the ambient. This is because an externally-pressurized bearing generally would require some kind of upstream restriction to realize a stiffness. It is when the restriction system is included that the overall analysis can become substantially more complicated.

In a porous bearing, restriction takes place in a distributed manner. Its complete analysis involves solving the pressure-flow field problem together with Equation (5.1) with appropriate pressure and flow continuity conditions at the interface between the porous material and the bearing film. The porous bearing surface itself introduces some additional complication since the non-slip condition on the velocity profile would have to be revised. Some of these questions are topics of current research.

For bearings with impermeable walls, there are three major discrete

restrictor types; namely, the capillary restrictor, the orifice restrictor, and the inherent restrictor. The most commonly used restrictor type is the last one--the capillary restriction seldomly can be achieved with a practical configuration, the orifice type restrictor is vulnerable to "pneumatic hammer" instability.

In the following sections, general features of the inherent restrictor will first be discussed; then representative solutions of Equation (5.1) for impermeable walls will be presented with allowance for the use of inherent upstream restriction.

5.1 The Inherent Restrictor

When gas enters into the bearing gap from an essentially stagnant state in the supply reservoir, its pressure undergoes an abrupt drop due to the formation of the velocity head. Subsequently, under the action of wall shear stresses, the velocity profile gradually develops into a parabolic distribution whereby its pressure undergoes an additional drop. The flow length required for the velocity profile development process to complete is proportional to the flow Reynolds number. Due to these phenomena, the effective film inlet pressure is lower than the supply stagnation pressure by an amount which is proportional to the velocity head at film inlet. Thus, if the supply hole is properly sized, to make this pressure drop significant, there is an "inherent inlet restriction."

A theoretical model for the behavior of the inherent restrictor is the entrance of an incompressible viscous flow into a parallel channel [19,20]. According to this calculation, the static pressure distribution at the channel entrance can be described in a universal manner as shown in Figure 5.1. The symbols used in labeling the graph are:

p_o	static pressure at entry	x	distance from entry
p	local static pressure	ν	kinematic viscosity of liquid
ρ	density of liquid	h	channel height
U_m	mean velocity		

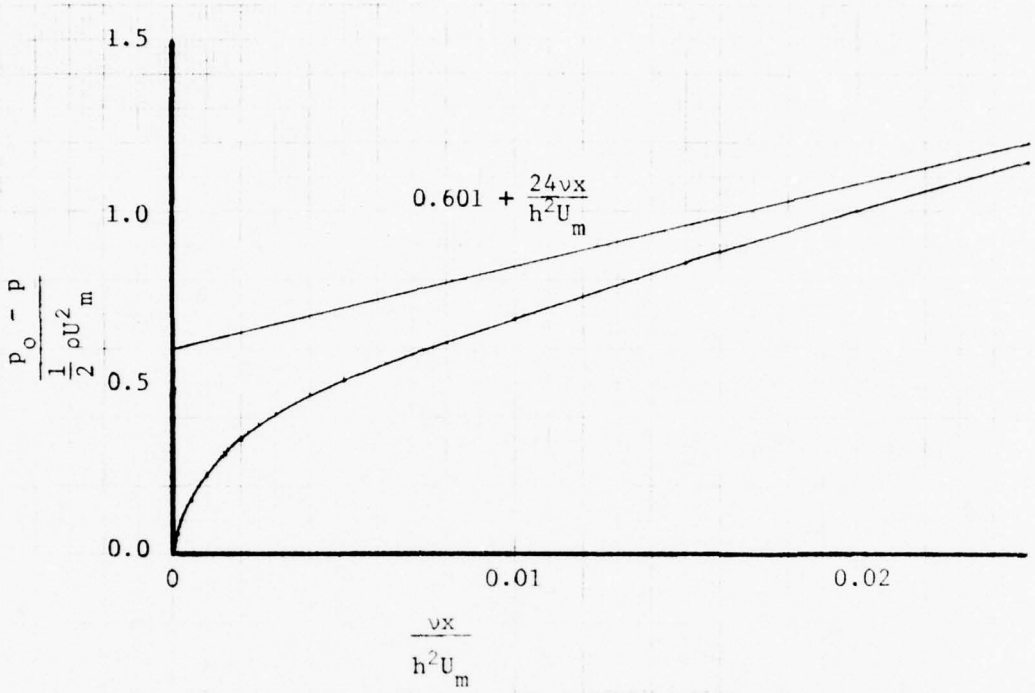

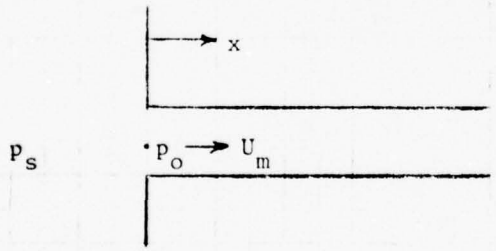

Fig. 5.1

Entrance Flow Development

The static pressure distribution has an asymptotic tangent which is in agreement with the lubrication theory (fully developed viscous channel flow). According to this result, if one replaces the curve in Figure 5.1 by its asymptotic tangent, the effective entry film pressure is lower than the upstream stagnation pressure by the amount

$$p_o - p_{eff} = 0.601 \left(\frac{\rho U_m^2}{2}\right) \tag{5.2}$$

If one wishes to account for the deviation between the asymptotic tangent and the actual curve, a "displacement" length can be calculated to be

$$\delta^+ = 0.00625 \frac{h^2 U_m}{\nu} \tag{5.3}$$

The integrated effect of this displacement length is a load deficiency of the amount

$$\delta W = 4.692 \times 10^{-3} \left(\frac{1}{2} \rho U_m^2\right)\left(\frac{h^2 U_m}{\nu}\right) \tag{5.4}$$

This is a second order effect which is much smaller than the terms which are neglected in the lubrication theory. Therefore, it is satisfactory to use Eq. (5.2) to account for a restrictor pressure drop without further concern regarding the details of pressure development in an entrance region of the fluid film.

The asymptotic law for inherent inlet pressure drop as given by Eq.(5.2) is mainly accountable by the nondissipative conversion of pressure to kinetic energy [20]. Therefore, one may extend this idea to compressible fluid dynamics as a basis for calculating the pressure drop through an inherent restrictor. The following conceptual steps are assumed in order to develop the applicable computational procedure (see Figure 5.2):

- The bearing wall is in thermal equilibrium with the reservoir gas.
- A throat section is recognized. Since the inlet edge in a practical construction would be more or less rounded, the throat section may be defined as the termination point of the edge round.

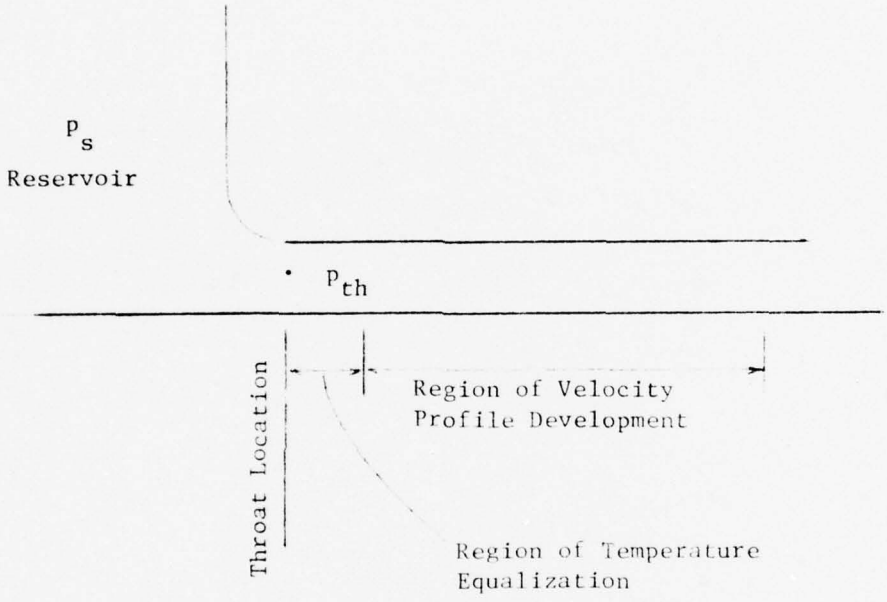

Fig. 5.2
Simplified Model of Compressible Film Entrance

- The flow process from the reservoir to the throat follow the isentropic law.
- Near the throat region, heat transfer between the walls and the gas flow takes place rapidly to equalize their temperatures with little pressure change.
- Further development of the velocity profile involves negligible compressibility effects.

Subscripts "s", "th", and "in" will be used to designate the respective states of supply stagnation, throat and effective film inlet.

Let the mass flux per unit inlet edge be

$$\Phi = \rho_{th} U_{th} h \tag{5.5}$$

According to the isentropic law,

$$\frac{\rho_{th}}{\rho_s} = \left(\frac{p_{th}}{p_s}\right)^{\frac{1}{\gamma}}; \qquad \frac{T_{th}}{T_s} = \left(\frac{p_{th}}{p_s}\right)^{\frac{\gamma-1}{\gamma}}$$

$$U_{th} = \left[\frac{2\gamma \mathcal{R} T_s}{(\gamma-1)}\left(1 - \left(\frac{p_{th}}{p_s}\right)^{\frac{\gamma-1}{\gamma}}\right)\right]^{\frac{1}{2}} \tag{5.6}$$

Thus, Equation (5.5) can be rewritten to express the mass flux in terms of the stagnation states of the reservoir and the pressure ratio (p_{th}/p_s):

$$\Phi = \sqrt{\frac{2\gamma}{(\gamma-1)\mathcal{R} T_s}}\; p_s \left(\frac{p_{th}}{p_s}\right)^{1/\gamma} \left[1 - \left(\frac{p_{th}}{p_s}\right)^{\frac{\gamma-1}{\gamma}}\right]^{1/2} h \tag{5.7}$$

With temperature equalization (the pressure being unchanged), the inlet velocity head becomes

$$\left(\frac{1}{2}\rho U_m^2\right)_{in} = \frac{1}{2}\frac{(\Phi/h)^2}{\rho_{th}\left(\frac{T_{th}}{T_s}\right)}$$

$$= \frac{1}{2}\frac{\mathcal{R}T_s\Phi^2}{p_{th}h^2} \tag{5.8}$$

Now, making use of Equation (5.2)

$$p_{th} = p_{in} + 0.601\left(\frac{1}{2}\rho U_m^2\right)_{in} \tag{5.9}$$

Combining Equations (5.7), (5.8), and (5.9), one obtains

$$\frac{p_{in}}{p_s} = \frac{p_{th}}{p_s} - 0.601\left(\frac{\gamma}{\gamma-1}\right)\left[\left(\frac{p_s}{p_{th}}\right) - \left(\frac{p_s}{p_{th}}\right)^{\frac{1}{\gamma}}\right]\left(\frac{p_{th}}{p_s}\right)^{\frac{2}{\gamma}} \tag{5.10}$$

For gas lubrication calculations, it is more convenient to use the pressure flux ψ instead of the mass flow Φ; that is

$$\psi = \mathcal{R}T_s\Phi$$

so that Equation (5.7) can be rewritten as

$$\Psi = \frac{\psi}{p_s\sqrt{\mathcal{R}T_s}\,h} = \left(\frac{p_{th}}{p_s}\right)^{\frac{1}{\gamma}}\left[\left(\frac{2\gamma}{\gamma-1}\right)\left(1 - \left(\frac{p_{th}}{p_s}\right)^{\frac{\gamma-1}{\gamma}}\right)\right]^{\frac{1}{2}} \tag{5.11}$$

Equations (5.10) and (5.11) allow one to calculate p_{in} upon given the stagnation state variables of the reservoir and the pressure flux.

Since the function of the restrictor is mainly in the preservation of an equilibrium condition, it is essential to know the differential perturbation characteristics of p_{in} with respect to ψ and h. This is obtained by differentiating Equations (5.11) and eliminating the differential of p_{th}/p_s:

$$\frac{\delta}{\delta \ell n \Psi} \left(\frac{P_{in}}{P_s}\right)$$

$$= \frac{\partial}{\partial \ell n \psi} \left(\frac{P_{in}}{P_s}\right)$$

$$= - \frac{\partial}{\partial \ell n h} \left(\frac{P_{in}}{P_s}\right)$$

$$= \left(\frac{\gamma}{\gamma-1}\right) \left(\frac{P_{th}}{P_s}\right) \left[1 - \left(\frac{\gamma+1}{2}\right) \left(\frac{P_{th}}{P_s}\right)^{\frac{\gamma-1}{\gamma}} \right]^{-1} \left[1 - \left(\frac{P_{th}}{P_s}\right)^{\frac{\gamma-1}{\gamma}} \right]$$

$$\cdot \left[\left(\frac{\gamma-1}{\gamma}\right) - 0.601 \left(\frac{P_s}{P_{th}}\right)^{\frac{\gamma-1}{\gamma}} \left(\frac{P_s}{P_{th}}\right)^{\frac{\gamma-1}{\gamma}} - \gamma \right] \qquad (5.12)$$

Graphical presentations of Equations (5.10), (5.11), and (5.12) are shown in Figure 5.3. Despite these rather complicated expressions, the following observations can be noted:

- Compressibility affects the restrictor pressure drop only modestly. Even if the flow should be sonic at the throat, the effect of inlet flow development is within 5% of the incompressible case. It is higher for a monatomic gas but lower by a similar fraction for a diatomic gas.
- The relationship between the dimensionless flow rate and the normalized supply-to-throat pressure drop is approximately an elliptical quadrant for both monatomic and diatomic gases.
- The pressure-flow perturbation relationship, when expressed in a dimensionless representation, is essentially same for both monatomic and diatomic gases.
- Perturbation of restrictor pressure drop by flow is relatively insignigicant unless the supply-to-throat pressure is at least 50% of the critical pressure drop.

Based on these observations, the following empirical formulae are proposed.

$$P_{th} - P_{in} = 0.601\sqrt{1 + C_o\left(\frac{P_s-P_{th}}{P_s-P_{cr}}\right)^2}\,(P_s - P_{th})$$

$$\Psi = \sqrt{\left(\frac{P_s-P_{th}}{P_s-P_{cr}}\right)\left(2 - \frac{P_s-P_{th}}{P_s-P_{cr}}\right)}\,\Psi_{cr} \qquad (5.13)$$

P_{cr} is the critical pressure for sonic flow, Ψ_{cr} is the corresponding flow function obtained by substituting P_{cr} for P_{th} in Eq.(5.11) and C_o is an empirical numerical constant. Their numerical values are

	Monatomic	Diatomic
P_{cr}/P_s	0.48714	0.52828
Ψ_{cr}	0.72618	0.68473
C_o	0.1139	-0.1150

These empirical formulae give "exact" results at either extremes of $P_{cr} \leq P_{th} \leq P_s$. At the midpoint, $P_{th} = 1/2\ (P_{cr} + P_s)$, the inaccuracies are

Error	Monatomic	Diatomic
% $(P_{th}-P_{in})$	1.244	0.742
% Ψ	0.496	-0.139

which are remarkably small.

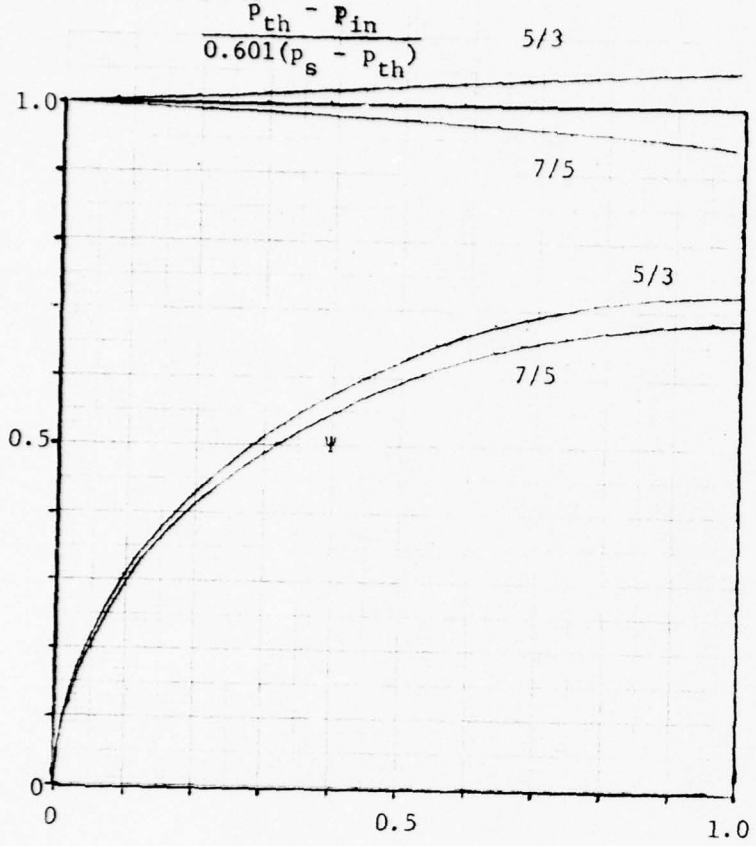

Fig. 5.3

"Exact" Inherent Restrictor Characteristics

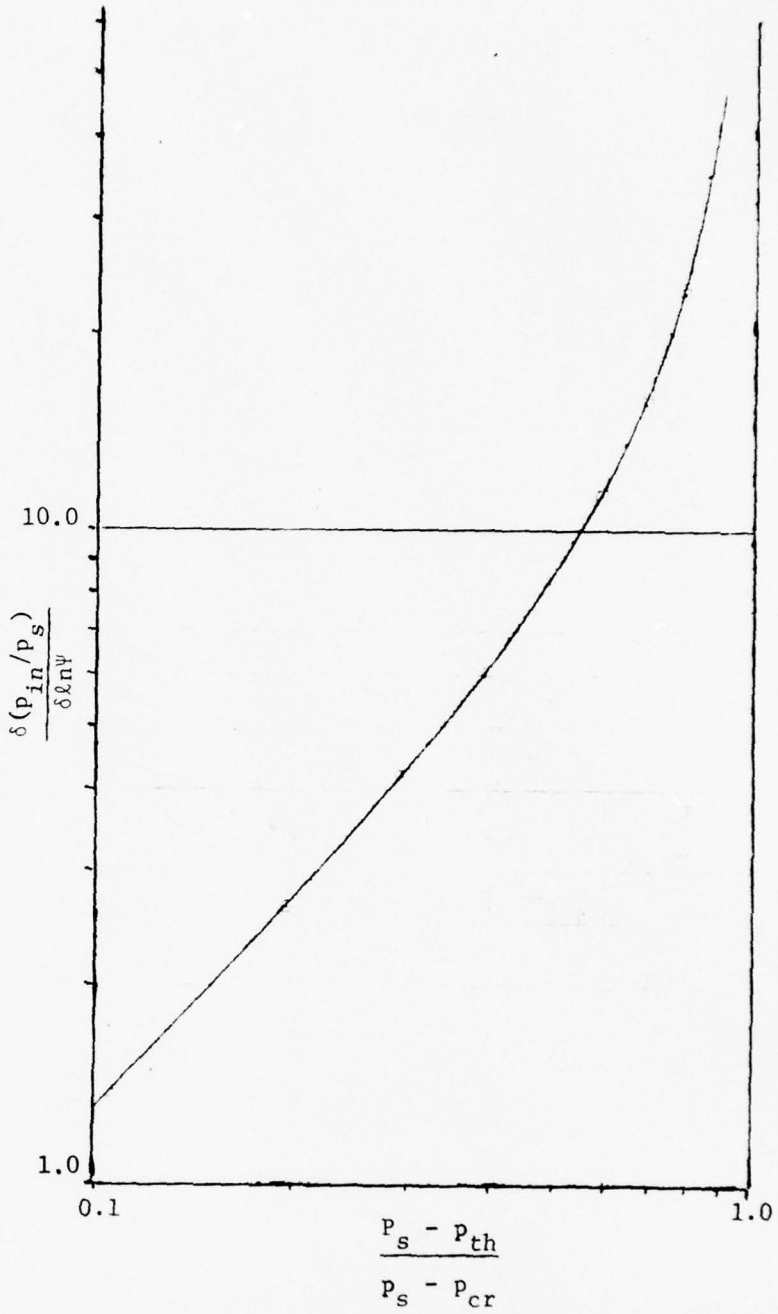

In Eqs.(5.13), $p_s - p_{th}$ can be eliminated to render

$$\frac{p_s - p_{in}}{p_s - p_{cr}} = \left[1 + 0.601\sqrt{1 + C_o X^2}\right] X$$

where (5.14)

$$X = \left(\frac{p_s - p_{th}}{p_s - p_{cr}}\right) = 1 - \sqrt{1 - \left(\frac{\Psi}{\Psi_{cr}}\right)^2}$$

Performing a variation operation on Eq.(5.14), it is found

$$\delta p_{in} = - (p_s - p_{cr})\left[1 + 0.601 \frac{(1 + 2C_o X^2)}{\sqrt{1 + C_o X^2}}\right] \frac{\Psi \, \delta\Psi}{\Psi_{cr}\sqrt{\Psi_{cr}^2 - \Psi^2}} \tag{5.15}$$

Since it has been shown in Figure 5.3 that restrictor pressure drop is most likely to be at least half of that for sonic flow, one may safely approximate $C_o X$ by C_o in these formulae. Thus one obtains

$$p_{in} = p_s - (p_s - p_{cr}) \left[1 + 0.601\sqrt{1 + C_o}\right]\left[1 - \sqrt{1 - \left(\frac{\Psi}{\Psi_{cr}}\right)^2}\right]$$

$$\frac{\delta p_{in}}{\delta \ell n \Psi} = \frac{\partial p_{in}}{\partial \ell n \psi} = - \frac{\partial p_{in}}{\partial \ell n h}$$

$$= - (p_s - p_{cr}) \left[1 + 0.601 \left(\frac{1 + 2C_o}{\sqrt{1 + C_o}}\right)\right] \frac{\Psi^2}{\Psi_{cr}\sqrt{\Psi_{cr}^2 - \Psi^2}} \tag{5.16}$$

The graphical relation between p_{in} and Ψ is shown in Figure 5.4. Eqs.(5.16) would be used in the analysis of externally pressurized gas bearings with inherent restrictors.

5.2 Centrally-Fed Strip (Figure 5.5)

With impermeable surfaces and a uniform gap, Equation (5.1) reduces to

$$h^3 \frac{d^2}{dx^2}\left(\frac{p^2}{2}\right) = 0$$

Integrating repeatedly, one finds

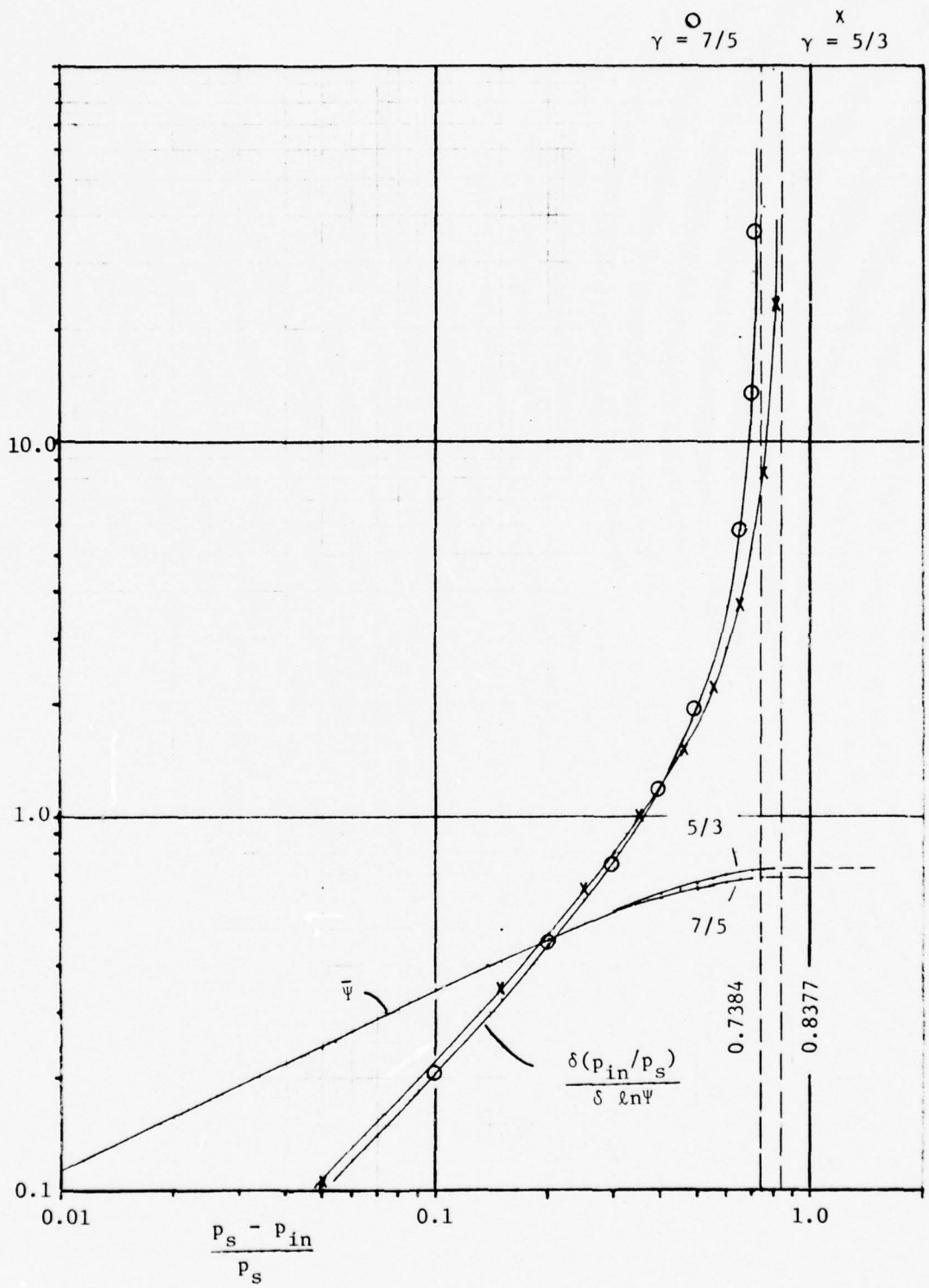

Fig. 5.4

Approximate Inherent Restrictor Characteristics

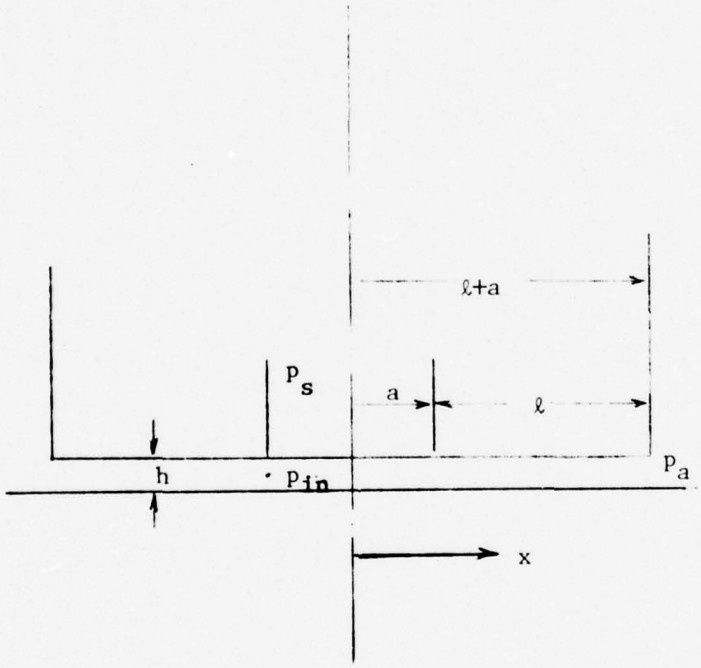

Fig. 5.5
Centrally Pressurized Strip

$$h^3 \frac{\partial}{\partial x}\left(\frac{p^2}{2}\right) = -12\mu\psi$$

$$\frac{1}{2}(p^2 - p_{in}^2) = \frac{12\mu\psi}{h^3}(a-x) \qquad \text{for } 0 < a-x < \ell \tag{5.17}$$

ψ is the pressure flux and is a constant of integration. The boundary condition $p(x=a) = p_a$ has been imposed in obtaining Equation (5.17). At the edge of the inherent restrictor

$$\frac{1}{2}(p_{in}^2 - p_a^2) = \frac{12\mu\psi\ell}{h^3} \tag{5.18}$$

Eliminating ψ between Eqs.(5.16) and (5.18), one obtains

$$h^2 = \frac{24\mu\ell\sqrt{RT_s}}{p_s} \frac{\Psi_{cr}\sqrt{K\left(1 - \frac{p_{in}}{p_s}\right)\left[2 - K\left(1 - \frac{p_{in}}{p_s}\right)\right]}}{\left[\left(\frac{p_{in}}{p_s}\right)^2 - \left(\frac{p_a}{p_s}\right)^2\right]} \tag{5.19}$$

where $K = \left[\left(1 - \frac{p_{cr}}{p_s}\right)\left[1 + 0.601\sqrt{1 + C_o}\right]\right]^{-1}$

Eq.(5.19) shows that for a given (p_a/p_s), how (p_{in}/p_s) varies with h as illustrated in Figure 5.6.

Sonic flow at the restrictor throat occurs at $p_{in} = p_{cr}$. For $p_{in} < p_{cr}$, flow is determined entirely by the sonic throat. Then, instead of Eq.(5.19), gap is related to p_{in} by setting ψ to ψ_{cr} in Eq.(5.18); that is

$$h^2 = \frac{24\mu\ell\sqrt{RT_s}}{p_s} \frac{\Psi_{cr}}{\left[\left(\frac{p_{in}}{p_s}\right)^2 - \left(\frac{p_a}{p_s}\right)^2\right]} \qquad \text{if } p_{in} < p_{cr} \tag{5.20}$$

Beyond the throat, prior to the full development of the viscous velocity profile, there would be an extended region of supersonic over expansion, then followed by a complicated "high Mach number viscous flow". A full account of the pressure field precisely by analytical means is not yet possible. For this reason, it is common engineering prudence to avoid restrictor choking.

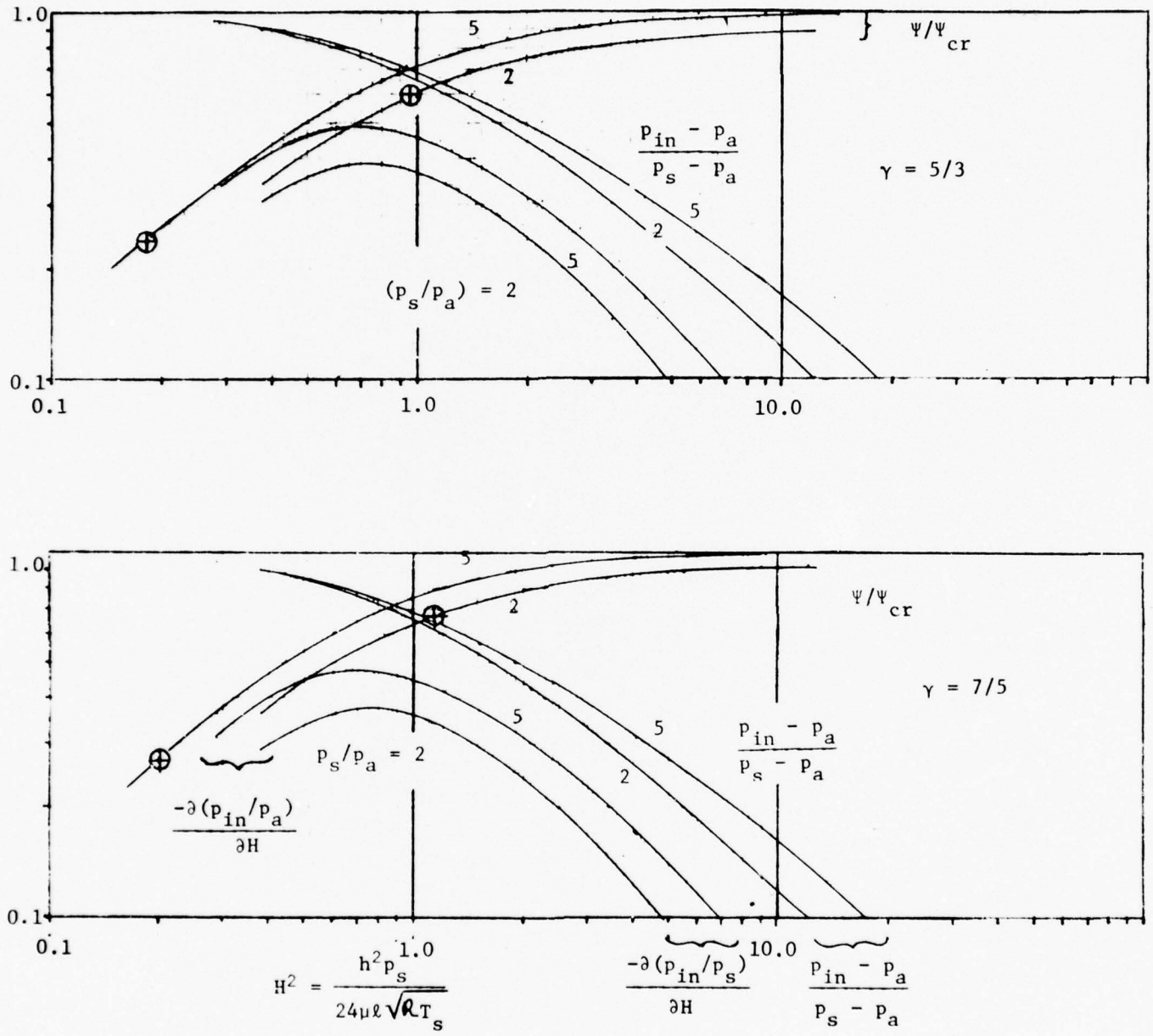

Fig. 5.6

Characteristics of Centrally Pressurized Strip

If one desires to compute the stiffness of the bearing, a variational perturbation with respect to h would be performed on Eq.(5.18):

$$p_{in}\ \delta p_{in} = \frac{12\mu\psi\ell}{h^3}\left[\delta\ell n\psi - 3\delta\ell nh\right] \tag{5.21}$$

With the aid of Eq.(5.16), $\delta\ell n\psi$ would be eliminated, yielding

$$\frac{\delta p_{in}}{\delta h} = \frac{-2}{\left[\dfrac{\Psi_{cr}\sqrt{\Psi_{cr}^2 - \Psi^2}}{(p_s - p_{cr})\left[1 + 0.601\left(\dfrac{1 + 2C_o}{\sqrt{1 + C_o}}\right)\Psi^2\right]} + \dfrac{2\ p_{in}}{(p_{in}^2 - p_a^2)}\right] h} \tag{5.22}$$

The numerical value of $\delta p_{in}/\delta h$ is approximately proportional to the bearing stiffness. As shown in Figure 5.6, it may be maximized for given (p_s, p_a) through a choice of h. This is generally regarded as the ideal design.

If p_s/p_a is large, then an "exit choking" condition can develop. This occurs when

$$\Psi\ (p_s/p_a) \simeq 1 \quad \text{or} \quad \frac{\Psi}{\Psi_{cr}} \simeq \begin{cases} 1.19\left(\dfrac{p_a}{p_s}\right) \\ 1.35\left(\dfrac{p_a}{ps}\right) \end{cases} \quad \text{for} \quad \gamma = \begin{cases} \dfrac{5}{3} \\ \dfrac{7}{5} \end{cases}$$

and are marked in Fig. 5.6 with the symbol "⊕". It is seen that the optimum design in the case $p_s/p_a = 5$ is not valid because "exit choking" would have taken place. "Exit choking" can be avoided by discrete feeding, this will be discussed in Section 5.4.

5.3 Various Axially-Symmetric Bearings

The above development can be readily generalized for various other bearing geometries so long as rotational symmetry exists with the centerline of the supply hole. With impermeable bearing walls, referring to Chapter 3, the governing equations for common bearing configurations are:

Journal Bearing

$$\frac{\partial}{\partial z}\left(h^3 p\ \frac{\partial p}{\partial z}\right) = 0 \tag{5.23a}$$

Thrust Bearing

$$r \frac{\partial}{\partial r} (rh\ p \frac{\partial p}{\partial r}) = 0 \tag{5.23b}$$

Conical Bearing

$$\sin\gamma r \frac{\partial}{\partial r} (\sin\ rh^3 p \frac{\partial p}{\partial r}) = 0 \tag{5.23c}$$

Spherical Bearing

$$\sin\phi \frac{\partial}{\partial \phi} (\sin\phi h^3 p \frac{\partial p}{\partial \phi}) = 0 \tag{5.23d}$$

If the film thickness is uniform, then with a suitable coordinate transformation each of these four equations can be reduced into Equation (5.17) so that the corresponding results--e.g., Figure 5.6--would be directly applicable, provided the term "ℓ" in the definition of the restriction parameters be accordingly identified. In the case of a journal bearing, there is no need to perform coordinate transformation; one may immediately recognize the axial coordinate "z" to be equivalent to "x" in Equation (5.15) and "ℓ" would simply be the axial distance from the feeding plane to the ambient end. For thrust and conical bearings Equation (3.27) provides the needed transformation, while Equation (3.28) furnishes the transformation for a spherical bearing. Thus, referring to Figure 5.6, the equivalent "ℓ" for these bearings are as follows:

Bearing Type	Equivalent "ℓ"
Journal	$L/2$
Thrust	$r_{in} \lvert \ell n(r_a/r_{in}) \rvert$
Conical	$\csc\gamma\ r_{in} \lvert \ell n(r_a/r_{in}) \rvert$
Spherical	$R \lvert \ell n\ (\frac{\tan\phi_a/2}{\tan\phi_{in}/2}) \rvert$

5.4 Feeding Through Discrete Holes

In the preceding sections, flow supply is assumed to enter the bearing gap through a line-feed. In order to achieve the desired degree of restriction without "exit choking" (see section 5.6), the "line-feed" is often replaced by a series of small feed-holes. Although qualitative aspects of the flow process through the discrete feed-holes are essentially unchanged, the following phenomena may substantially alter the restriction behavior quantitatively:

- The effective film pressure, p_{in}, at each feed-hole may be peaked substantially above that given by Equation (5.18).[21]
- Upon entering the bearing film, flow periphery may dilate significantly prior to full development of the viscous velocity profile.[22,23]
- Sonic condition is more likely to occur at the throat of each discrete restrictor. In the event of a sonic inlet condition, a supersonic overexpansion region may cover a large enough area to require correction to the pressure profile.[24]

If there are n feed-holes per unit length of feed line, then the restrictor flow area is $2\pi na$ times that of the film inlet area, "a" being the throat radius of each feed-hole. If n is chosen to be sufficiently large, pressure peaking at each feed-hole may be neglected. Then the analysis of Sections 5.2 and 5.3 can be directly used for the discretely fed bearing provided Ψ in eqs. (5.11), (5.13), (5.14), (5.15) and (5.16) are regarded as the flux through the discrete restrictors. Thus, in eqs. (5.17) and (5.18), ψ should be multiplied by the factor $(2\pi na)$. Consequently, eq. (5.19) can be adapted by adding a factor $(2\pi na)$ to its righthand side. The graphs of Fig. 5.6 would then be applicable if $(2\pi na)$ be divided into the abscissa and multiplied to (Ψ/Ψ_{cr}). The symbol "+" on each curve gives the upper bound of $(2\pi na)$ to avoid "exit choking". For example, for a diatomic gas with $p_s/p_a=5$, "exit choking" is avoided by requiring

$$2\pi na < 0.2921$$

When this is done, however, the restrictor would encounter sonic condition at the corresponding point so that eq. (5.19) should be replaced by eq. (5.20). Irrespective of the question of supersonic overexpansion downstreams of the restrictor throat, the portions for H^2 larger than that marked by " + " should be revised.

5.5 Non-uniform Bearing Gap

In the event of a non-uniform gap, the pressure profile would be altered in the film, even if the boundary pressures (p_{in}, p_a) are unchanged. This dependence of the pressure profile on the bearing gap distribution may have a significant influence on the bearing stiffness. An illustration of this issue will be given by a detailed analysis of a spherical bearing, which is fed through a port at the pole with an arbitrary axial eccentricity as shown in Figure 5.7. To focus our attention on the film pressure profile, restrictor behavior will be put aside; i.e. p_{in} (instead of p_s) is considered to be given.

The problem at hand is specified by the following set of equations:

$$\sin\phi h^3 p \frac{dp}{d\phi} = -12\mu R\psi$$

$$h = C\ (1 - \varepsilon\cos\phi) \tag{5.24}$$

$$p(\phi_{in}) = p_{in}; \quad p(\phi_a) = p_a$$

This problem can be simplified by the transformation

$$\eta = \left(\frac{C}{h}\right)^3 \frac{d\phi}{\sin\phi} \tag{5.25}$$

yielding

$$p \frac{dp}{d\eta} = -\frac{12\mu R\psi}{C^3}$$

$$\frac{1}{2}(p^2 - p_a^2) = -\frac{12\mu R\psi}{C^3}(\eta - \eta_a) \tag{5.26}$$

$$\left(\frac{p^2 - p_a^2}{p_{in}^2 - p_a^2}\right) = \left(\frac{\eta - \eta_a}{\eta_{in} - \eta_a}\right)$$

where

$$\eta(\phi) = (1 - \varepsilon^2)^{-3}\ 3\varepsilon^2\cos\chi + \frac{\varepsilon^3}{2}\cos^2\chi + \varepsilon(3 + \varepsilon^2)\ \ell n\ \sin\chi + (1 + 3\varepsilon^2)\ \ell n(\tan\tfrac{\chi}{2})$$

$$\chi(\phi) = 2\tan^{-1}\left(\frac{1 + \varepsilon}{1 - \varepsilon}\tan\frac{\phi}{2}\right) \tag{5.27}$$

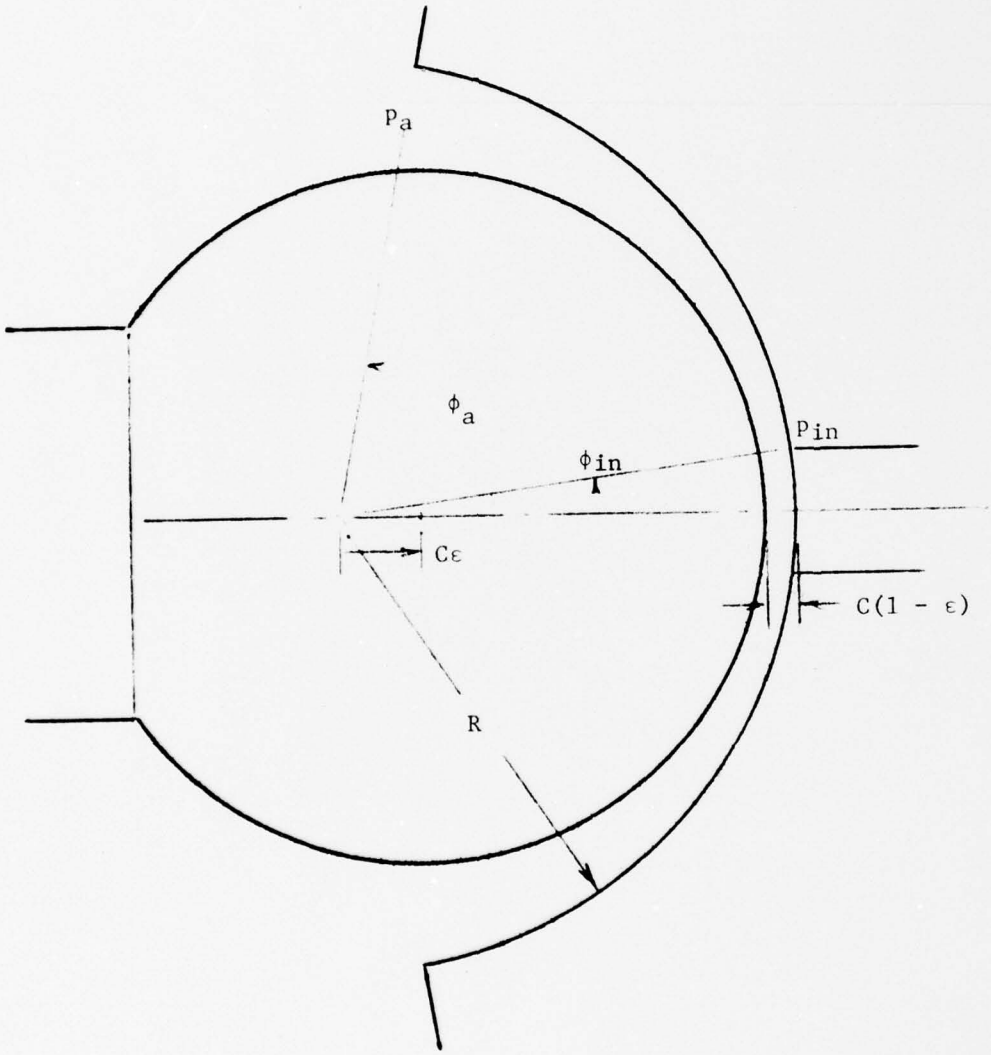

Fig. 5.7

Axially Displaced Spherical Bearing With Polar Feed Port

Graphical illustration of the above result is given in Figure 5.8. It is seen that, as ε increases (gap decreases), the area under the pressure profile decreases. This is the indication of a negative stiffness! Thus, unless there is a sufficient restrictor compensation of this effect, this type of bearing tends to "lock up".

The tendency for "lock up" to take place is aggravated by large eccentricity which causes significant gap non-uniformity. It is more serious in the case of a discretely-fed bearing than that of a line-fed bearing.

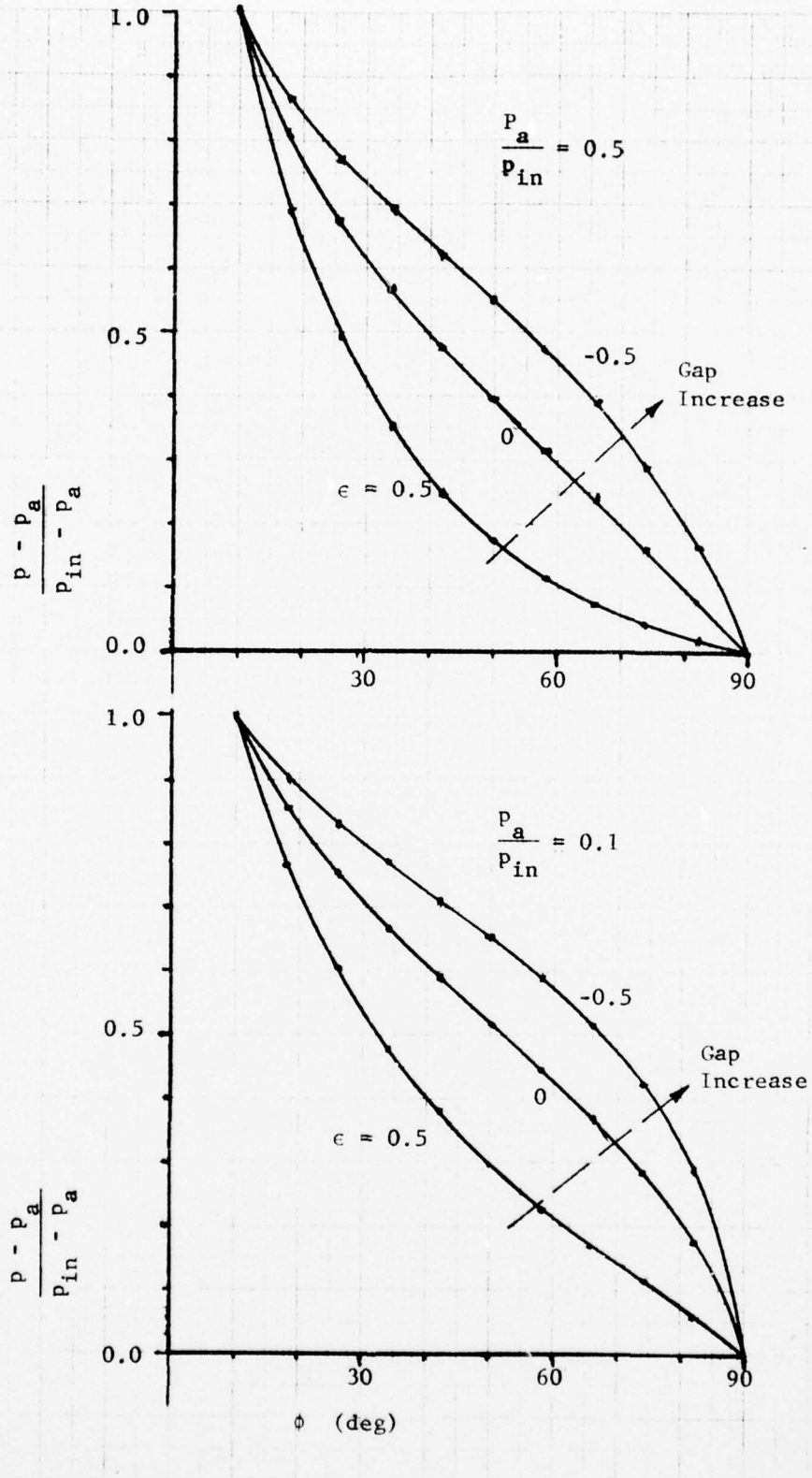

Fig. 5.8

Pressure Profile in Axially Displaced Spherical Gas Bearing

5.6 Exit Choking

For a line-fed strip bearing, sonic flow is most likely to occur at the exit because the film pressure is lowest so that flow speed is highest there. In a rigorous treatment of a high "Mach number" gas film, one should make allowance for inertia forces in the momentum balance and also include transverse viscosity variation due to temperature variation. In order to gain a first insight in the overall physical situation, the problem will first be examined with very rough approximations to minimize mathematical drudgery. Subsequently, the same problem will be reviewed with a more rigorous treatment and the basis for a more accurate theoretical treatment will be accordingly indicated.

5.6.1 An Approximate Treatment

For the present purpose, the isoviscous approximation will be adopted, and the convective inertia will be included with a presumed parabolic velocity profile. Such a treatment should be regarded as a first approximation (see Sections 2.2 and 2.4).

The assumed parabolic velocity profile is

$$u' = \frac{6y(h-y)}{h^2}\,\bar{u} \tag{5.28}$$

Furthermore, the continuity condition is approximated as

$$\frac{\partial}{\partial x}(\rho u') = 0 \qquad \text{or} \qquad \rho\frac{\partial u'}{\partial x} + u'\frac{\partial \rho}{\partial x} = 0 \tag{5.29}$$

Thus, using above approximations in estimating convective inertia, then, together with the perfect gas law $\rho = p/(\mathcal{R}T)$, one finds the momentum balance to yield

$$\frac{\partial^2 u}{\partial y^2} = \frac{1}{\mu}\left[\frac{\partial p}{\partial x} - u'^2\frac{\partial \rho}{\partial x}\right]$$

$$= \frac{1}{\mu}\frac{\partial p}{\partial x}\left[1 - \frac{36y^2(h-y)^2}{h^4}\frac{\bar{u}^2}{\mathcal{R}T}\right] \tag{5.30}$$

The second term on the right hand side is convective inertia effect peculiar to a compressible fluid since it originated from $u'^2\frac{\partial \rho}{\partial x}$.

Integrating twice with the boundary conditions $u(0) = u(h) = 0$, one obtains

$$u = \frac{y(y-h)}{2\mu}\frac{\partial p}{\partial x}\left[1 - \frac{6\bar{u}^2}{5\mathcal{R}T}\frac{(2y^4 - 4hy^3 + h^2y^2 + h^3y + h^4)}{h^4}\right] \tag{5.31}$$

Returning to the continuity condition, one can write

$$\int_0^h \rho u dy = \text{const} = \frac{\Psi}{\mathcal{R}T}$$

Or, from eq. (5.31),

$$\Psi = -\frac{h^3}{12\mu}\left(1 - \frac{54}{35}\frac{\bar{u}^2}{\mathcal{R}T}\right) p\frac{dp}{dx} = \bar{\rho u} h$$

$$p\frac{\partial p}{\partial x} - \frac{54}{35}\frac{\Psi^2}{h^2\mathcal{R}T}\frac{1}{p}\frac{dp}{dx} = -\frac{12\mu\Psi}{h^3} \tag{5.32}$$

This can be integrated with respect to x to yield

$$\frac{1}{2}(p^2 - p^{*2}) - p^{*2}\ell n\left(\frac{p}{p^*}\right) = -\frac{12\mu\Psi}{h^3}(x - x^*) \tag{5.33}$$

where the superscript "*" refers to the choking condition

$$p^* = \sqrt{\frac{54}{35}}\frac{\Psi}{h\sqrt{\mathcal{R}T}} = \frac{\bar{u}}{a^*h} = \left(\frac{\bar{u}}{a^*}\right) p \tag{5.34}$$

and

$$a^* = \sqrt{\frac{35}{54}\mathcal{R}T} \tag{5.35}$$

may be regarded as the effective sonic speed. Comparing with eq.(5.18), one reckons that the term $\ell n(p/p^*)$ in eq. (5.33) represents the approximate contribution of convective inertia.

Using symbols defined by eqs.(5.34 and (5.35), eq.(5.32) can be rewritten as

$$\left(\frac{p}{p^*} - \frac{p^*}{p}\right)\frac{d}{dx}\left(\frac{p}{p^*}\right) = -\frac{12\mu a^*}{p^* h^2} \tag{5.36}$$

For any $p(x=0) = p_{in}$, eq.(5.36) indicates that a monotonically decreasing pressure distribution cannot be continued below p^*. Thus, a correct solution of the film pressure must satisfy the inequality

$$p \geq p^* \tag{5.37}$$

Given the half-width of the bearing strip ℓ, along with (μ, a^*, p_{in}, p_a), eq.(5.36) can be integrated to yield

$$\frac{1}{2}\left(\frac{p_a}{p^*}\right)\left[\left(\frac{p_{in}}{p_a}\right)^2 - 1\right] - \left(\frac{p^*}{p_a}\right) \ell n \left(\frac{p_{in}}{p_a}\right) = \frac{12\, a^* \ell}{p_a h^2} \tag{5.38}$$

which may be solved to find the integration constant (p^*/p_a), which must not be larger than unity if the inequality (5.37) is to be satisfied. Violation of the latter condition can occur if ℓ is too small. The lower bound of ℓ is found by setting $p^* = p_a$ in eq.(5.38), i.e.

$$\ell^* = \frac{p_a h^2}{12\mu a^*}\left[\frac{1}{2}\left(\frac{p_{in}}{p_a}\right)^2 - 1 - \ell n \left(\frac{p_{in}}{p_a}\right)\right] \tag{5.39}$$

This relationship is graphically shown in Fig. 5.9. If $\ell < \ell^*$, the exit film pressure p^* satisfies the equation

$$\frac{12\mu a^*}{p_{in} h^2} = \frac{1}{2}\left(\frac{p_{in}}{p^*} - \frac{p^*}{p_{in}}\right) - \left(\frac{p^*}{p_{in}}\right) \ell n \left(\frac{p_{in}}{p^*}\right) \tag{5.40}$$

The apparent discontinuity between p^* and p_a is a necessary anomaly of the present analysis.

The exit choking phenomenon is seen to depend on two parameters which may be recognized as

$$\frac{12\mu a^* \ell}{p_a h^2} \quad \text{and} \quad \frac{p_{in}}{p_a}$$

The lower bound of the former parameter is fixed by eq.(5.39). Exit choking occurs if

- p_a/p_{in} is too small,
- ℓ is too narrow, or
- h is too large.

Representative pressure profiles, with and without exit choking, are illustrated in Fig. 5.10. In this example, exit choking takes place for $p_{in}/p_a > 10$. $(p^2-p_a)/(p_s^2-p_a^2)$ is plotted against x/ℓ. In the absence of convective inertia, such a plot would be a straight line. With $p_{in}/p_a = 6$, there is very little evidence of any significant convective inertia effect. As the condition of exit choking is approached, the pressure gradient steepens. Accordingly, the

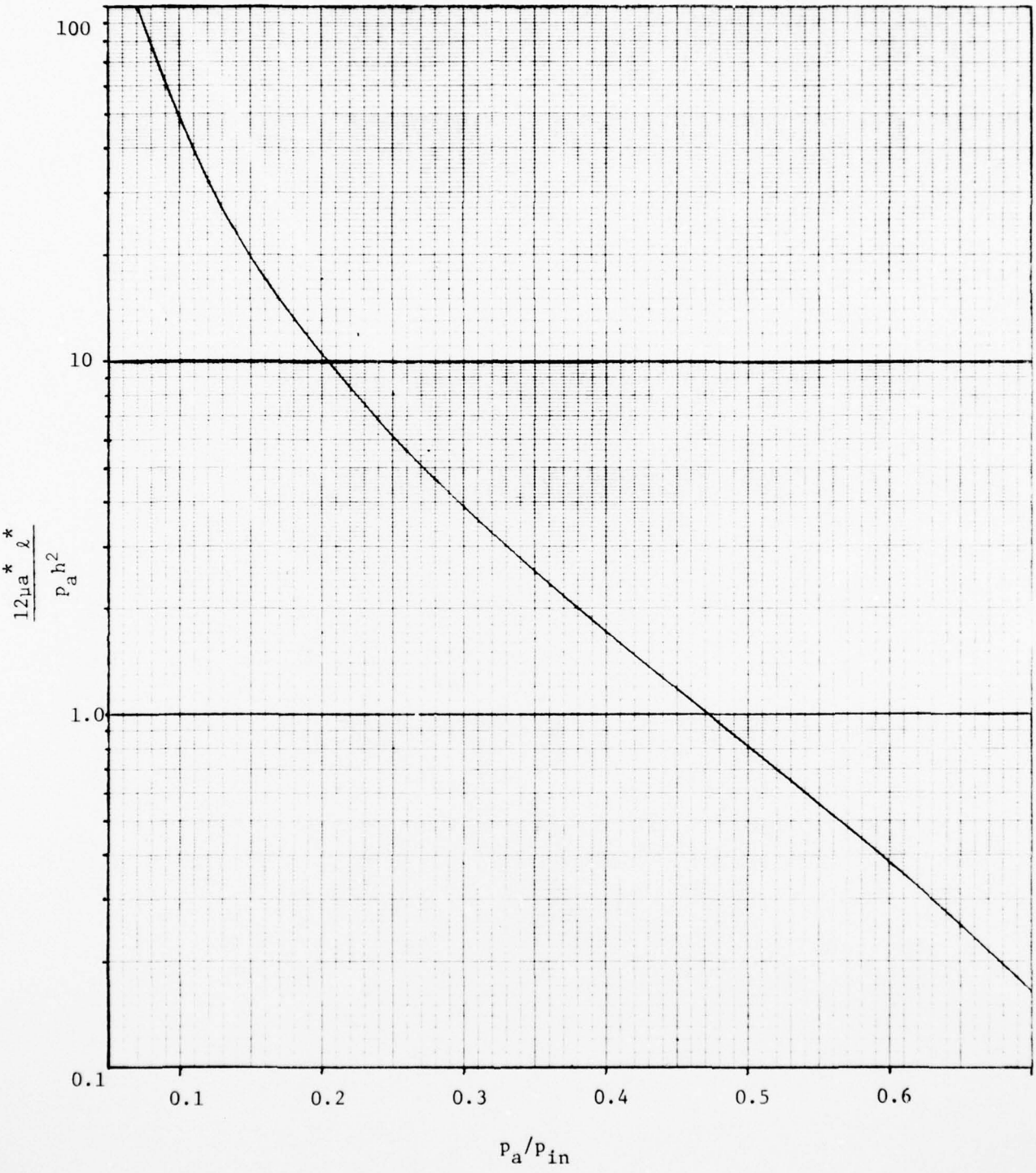

Fig. 5.9

Exit Choking Condition

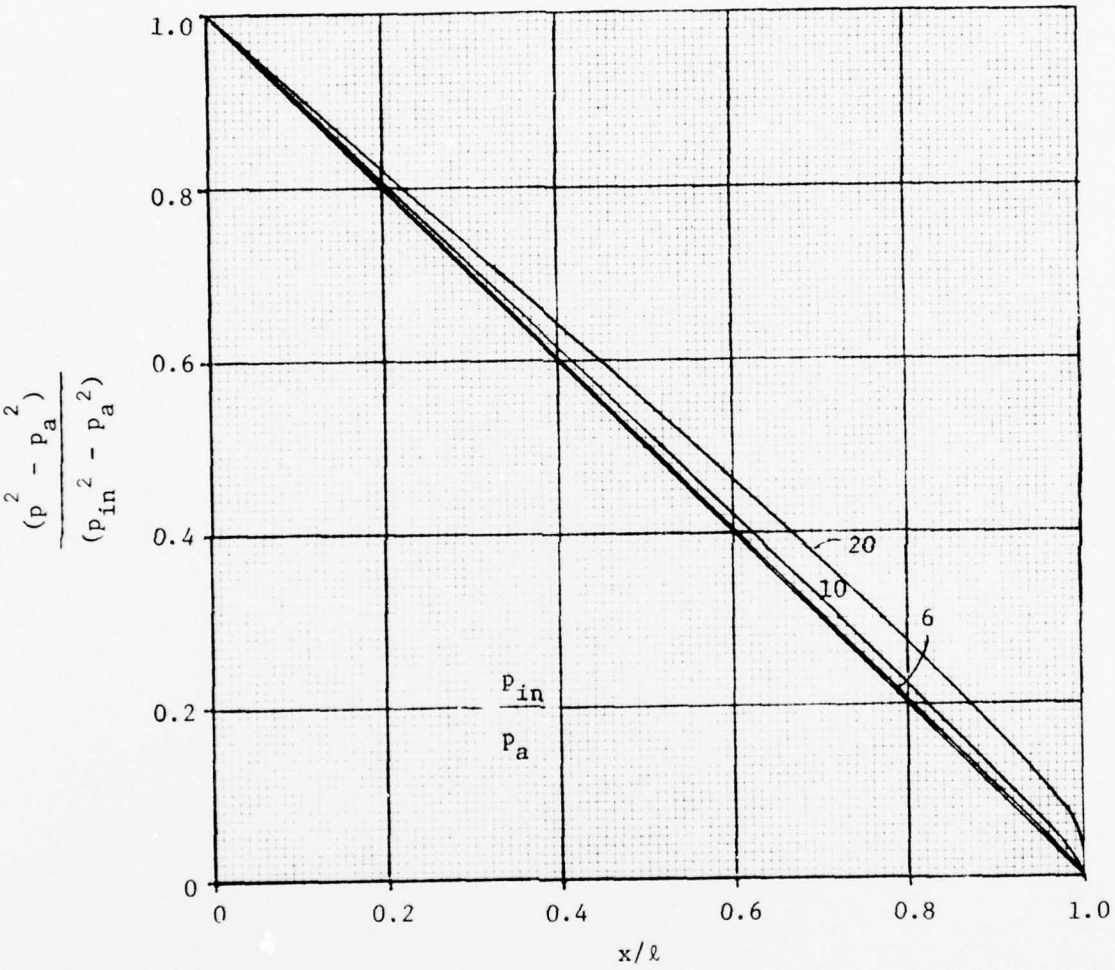

Fig. 5.10

Pressure Profiles Including Convective Inertia

$$\frac{12\mu a^* \ell}{p_a h^2} = 47.2$$

Exit Chokes for $p_{in}/p_a > 10$

pressure near the exit would increase with flow increase which would correspond to a larger gap. Thus, it is clear that "exit choking" causes a "negative stiffness" tendancy.

5.6.2. A Rigorous Re-examination

Credibility of the above analysis is a bit uncertain since the exit choking condition in fact contradicts the apriori assumption of an isothermal gas. Fortunately, a more satisfactory treatment is available [25], which is consistent with the compressible boundary layer theory and satisfies the energy equation by dint of the relatively inocuous assumption of a unity Prandtl number. This approach will be briefly outlined. It will be shown that the qualitative aspects of the approximate analysis presented above are not contradicted, albeit the accuracy of the quantitative results may be in doubt.

Adopting the boundary layer approximation and assuming a unity Prandtl number, the governing equations for the steady state flow of a gas between parallel plates are

$$\frac{\partial \rho u}{\partial x} + \frac{\partial \rho v}{\partial y} = 0$$

$$\rho \left(u\frac{\partial u}{\partial x} + v\frac{\partial u}{\partial y}\right) = -\frac{dp}{dx} + \frac{\partial}{\partial y}\left(\mu \frac{\partial u}{\partial y}\right) \tag{5.41}$$

$$p = \rho \mathcal{R} T$$

$$\frac{\gamma \mathcal{R} T}{\gamma - 1} + \frac{u^2}{2} = \text{const.} = \frac{\gamma \mathcal{R} T_w}{\gamma - 1}$$

where T_w is the wall temperature which is assumed to be a constant.

Now, making the substitutions

$$\hat{u} = \rho u, \quad \hat{v} = \rho v \tag{5.42}$$

one finds

$$\frac{\partial \hat{u}}{\partial x} + \frac{\partial \hat{v}}{\partial y} = 0 \tag{5.43}$$

$$\hat{u}\frac{\partial\hat{u}}{\partial x} + \hat{v}\frac{\partial\hat{u}}{\partial y} = -(1 - M^2)\rho\frac{dp}{dx} + \frac{\partial}{\partial y}\left(\frac{\partial\hat{u}}{\partial y}\right) - \theta$$

where

$$\theta = \frac{[3 + 2(\gamma - 1)M^2]}{[1 + (\gamma - 1)M^2]^2}\frac{(\gamma - 1)Ma}{\gamma p}\mu\left(\frac{\partial\hat{u}}{\partial y}\right)^2 \tag{5.44}$$

$$M^2 = \frac{u^2}{\gamma\mathcal{R}T}, \quad a^2 = \gamma\mathcal{R}T \tag{5.45}$$

In this form, compressibility effects show up in the coefficient of dp/dx and the term θ. Otherwise, the system of equations is exactly same as that of the incompressible entrance flow. Numerical solution reveals that, except in the entrance region, the velocity profile is approximately a parabola even when the Mach number is quite large.

Eqs. (5.43) can be integrated across the channel to yield

$$p\frac{dp}{dx}\int_0^h \left(\frac{1 - M^2}{\mathcal{R}T}\right) dy = \left[\mu\frac{\partial\hat{u}}{\partial y}\right]_{y=0}^{y=h} - \int_0^h \theta dy - \frac{d}{dx}\int_0^h \hat{u}^2 dy \tag{5.46}$$

It may be noted that the first two terms on the right hand side of eq.(5.46) are of the same sign. The second term represents the influence of transverse density variation on the wall shear stresses and is inversely proportional to the film pressure. The third term mainly accounts for change in the velocity profile. A detailed numerical study of eq.(5.43) revealed that, beyond the entrance region, the velocity profile is not too different from a parabola. One can thus devise a suitable approximate calculation method for eq.(5.46) by the assumption of a suitable distribution of $\hat{u}$. Write

$$\hat{u} = \hat{u}_o\, f\,(y/h) \tag{5.47}$$

f is the distribution function such that

$$\int_0^1 f\, d\left(\frac{y}{h}\right) = 1 \tag{5.48}$$

$\hat{u}_o$ is thus the mean value of $\hat{u}$. One can then define a "Mean Mach Number" to be

$$M_o = \sqrt{\frac{\mathcal{R} T_w}{\gamma}} \frac{\hat{u}_o}{p} \tag{5.49}$$

Accordingly, eq. (5.46) can be rewritten as

$$\frac{F(M_o)h^2}{12\mu_w \hat{u}_o \mathcal{R} T_w} p\frac{dp}{dx} = \frac{1}{12}\frac{df}{d(y/h)}\Bigg|_{y=0}^{y=h} - (\frac{\gamma-1}{\gamma})G(M_o) + H\frac{\hat{u}_o h}{\mu_w}\frac{dh}{dx} \tag{5.50}$$

where,

$$F(M_o) = \int_0^1 \frac{T_o}{T}(1 - M^2)d(y/h) \tag{5.51}$$

$$G(M_o) = \frac{M_o}{12}\int_0^1 \frac{\mu}{\mu_w}\sqrt{\frac{T}{T_w}\frac{[3 + 2(\gamma-1)M^2]}{[1 + (\gamma-1)M^2]^2}}\left[\frac{df}{d(y/h)}\right]^2 d(\frac{y}{h}) \tag{5.52}$$

$$H = \frac{1}{12}\int_0^1 f^2 d(y/h) \tag{5.53}$$

Upon given the distribution function f and the viscosity-temperature relationship $\mu(T)$, $F(M_o)$ and $G(M_o)$ can be calculated as universal functions of M_o. This is done for

$$f(\frac{y}{h}) = 6\frac{y}{h}(1 - \frac{y}{h}) \tag{5.54}$$

$$\frac{\mu}{\sqrt{T}} = \text{const.}$$

H is found to be a constant and is precisely 1/10. F and G are dependent on both γ and M_o as shown in Figure 5.11. F is seen to vanish at $M_o \simeq 1$ for either value of γ. In fact, $F \simeq 1 - M_o^2$ would be a very adequate approximation for the diatomic gas. In any case, the vanishing condition of F would establish exit choking. From this point of view, one might observe that, the "isothermal approximation" presented previously would somewhat prematurely predict choking at

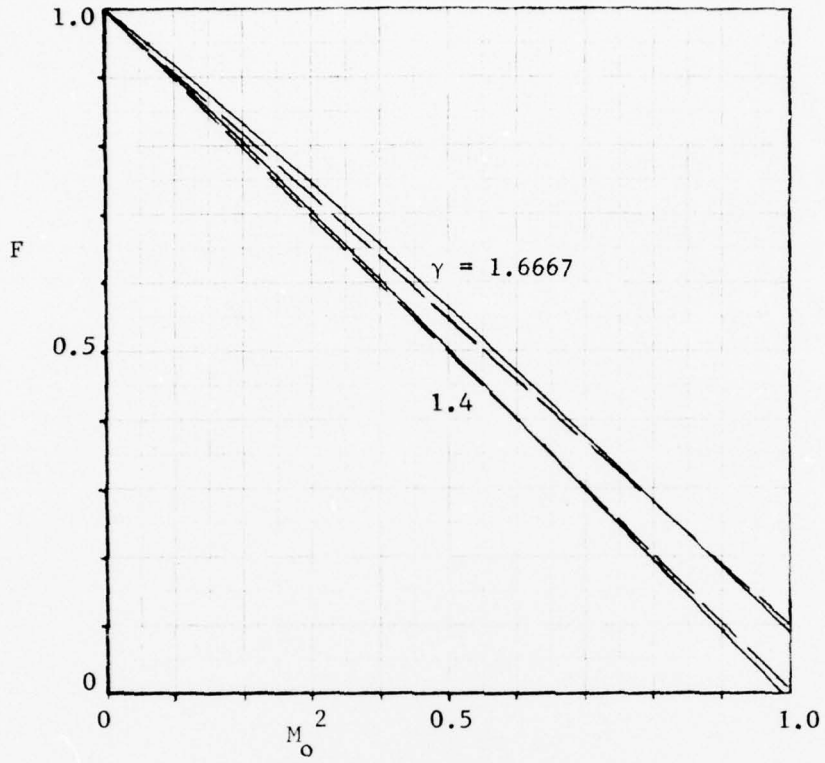

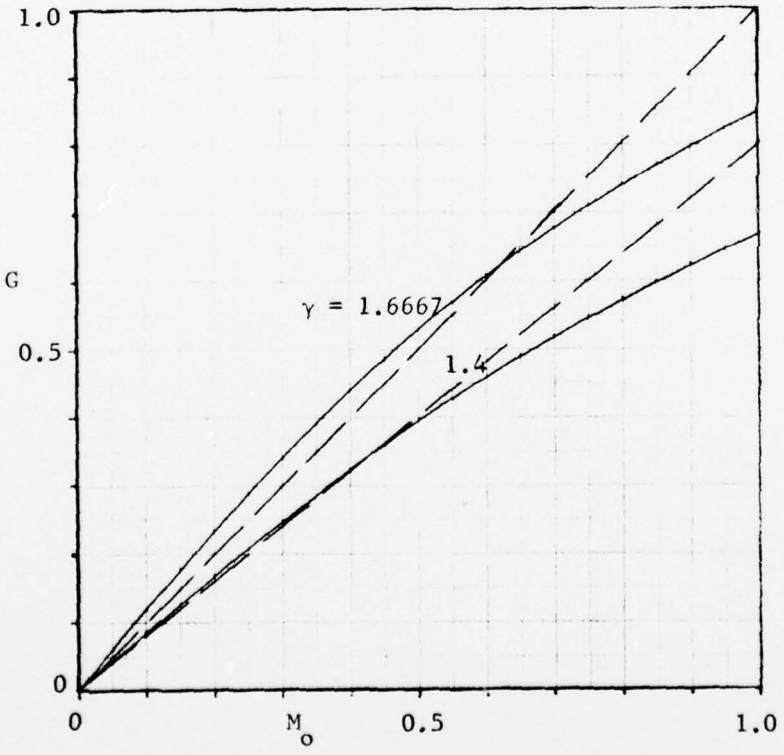

Fig. 5.11

Convective Inertia and Heat Transfer Effects

$$M_o = \sqrt{\frac{35}{54\gamma}}$$

which is 0.68 for $\gamma = 1.4$. On the other hand, G presents an additional effect here which tends to mask this discrepancy somewhat.

A reasonable approximation for F and G to permit closed form integration of eq. (5.50) is

$$F = 1 - \left(\frac{p_1^*}{p}\right)^2$$

$$G = \frac{p_2^*}{p} \tag{5.55}$$

where, p_1^* and p_2^* may take on the following numerical values, corresponding to the dashed lines shown in Figure 5.11:

γ	$\sqrt{\frac{\gamma}{\mathcal{R}T_w}}\,\frac{p_1^*}{\hat{u}_o}$	$\sqrt{\frac{\gamma}{\mathcal{R}T_w}}\,\frac{p_2^*}{\hat{u}_o}$
1.4	1.0	0.8
1.6667	0.95	1.0

where upon, eq.(5.50), for a constant h, can be integrated to become

$$(p_o - p)\left\{\frac{1}{2}(p_o + p) - p_2^*\right\} + (p_2^{*2} - p_1^{*2})\,\ell n\left(\frac{p_o + p_2^*}{p + p_2^*}\right)$$

$$= \frac{12\mu_w \hat{u}_o \ell T_w x}{h^2} \tag{5.56}$$

where p_o is the entrance fluid film pressure (neglecting inherent restriction) at x = 0. Choking takes place at ($p = p_1^*$, $x = \ell^*$); i. e.,

$$(p_o - p_1^*)\left\{\frac{1}{2}(p_o + p_1^* - p_2^*\right\} + (p_2^{*2} - p_1^{*2})\,\ell n\left(\frac{p_o + p_2^*}{p_1^* + p_2^*}\right)$$

$$= \frac{12\mu_w \hat{u}_o T_w \ell^*}{h^2} \tag{5.57}$$

($p = p_a$, $x = \ell$) would be an "unchoked" solution if the corresponding u_o, which satisfies eq.(5.56), would yield $\ell^* < \ell$ from eq.(5.57). For a choked exit condition, u_o is found from eq.(5.57) with $\ell^* = \ell$; and then $p(o \leq x \leq \ell) > p_a$. These features are qualitatively unaltered from the previous "isothermal approximation".

5.7 Nomenclature

Symbol	Definition	Chapter/ Section
a	Half-width of inlet slot	5.2
a	Feed-hole radius	5.4
a	Acoustic speed	5.6.2
a^*	Effective sonic speed	5.6.1
C_o	Empirical coefficient in eq. (5.13)	5.1
F	Function of M_o, eq. (5.51)	5.6.2
G	Function of M_o, eq. (5.52)	5.6.2
h	Bearing gap, $h_2 - h_1$	
K	A constant, eq. (5.19)	5.1
ℓ	Width of strip bearing gap	
ℓ^*	Lower bound of ℓ without exit choking	
M	Mach number	
M_o	Mean Mach number, eq. (5.49)	5.6.2
p	Fluid pressure	
p_a	Ambient pressure	
p_{cr}	Critical pressure for isentropic expansion	5.1
p_{eff}	Effective film inlet pressure of incompressible fluid	5.1
p_{in}	Compressible film inlet pressure	
p_o	Static pressure at film inlet	5.1
p_s	Stagnation pressure of supply	
p_{th}	"Throat" pressure at film inlet	5.1
p^*	Pressure at choking	5.6.1
$\mathcal{R}$	Gas constant	
T	Absolute temperature	

AD-A041 163 SHAKER RESEARCH CORP BALLSTON LAKE N Y F/G 13/9
FUNDAMENTALS OF GAS LUBRICATION.(U)
MAY 77 C H PAN N00014-74-C-0278
UNCLASSIFIED SRC-76-TR-22 NL

2 OF 2
ADA
041163

END

DATE
FILMED
7-77

Symbol	Definition	Chapter/ Section
T_s	Stagnation temperature of supply	5.1
T_{th}	"Throat" temperature at inlet	5.1
T_w	Temperature of bearing wall	
u	x-component of velocity	
u'	Velocity profile for calculation of convective inertia	5.6.1
$\bar{u}$	Mean velocity	5.6.1
$\hat{u}$	ρu	5.6.2
$\hat{u}_o$	Mean value of $\hat{u}$	5.6.2
U_m	Mean velocity	
U_{th}	Throat velocity at inlet	
v	y-component of velocity	
$\hat{v}$	ρv	
δW	Load deficiency due to entrance pressure drop	
x	Coordinate	
x	Distance from entry	5.1
X	Pressure drop ratio, eq. (5.14)	5.1
y	Normal coordinate measured from reference surface	
γ	Ratio of specific heats	
δ^+	"Displacement thickness" of entrance pressure profile	5.1
$\vec{\nabla}_2$	Two-dimensional surface spatial gradient operator	
ε	Axial eccentricity ratio of spherical bearing	
θ	Compressible dissipation function, eq. (5.44)	5.6.2
μ	Viscosity coefficient	
μ_w	Value of μ at wall	5.6.2
ν	Kinematic viscosity	

Symbol	Definition	Chapter/ Section
ρ	Density of gas	
ρ_{th}	"Throat" density at inlet	5.1
ϕ	Colattitudinal angle of spherical bearing	5.3,5.5
Φ	Inlet mass flux	
χ	"Sommerfeld angle"	5.5
ψ	Pressure flux	
Ψ	Dimensionless pressure flux, eq. (5.11)	5.1
Ψ_{cr}	Value of ψ for choking	5.1

6.0 TIME DEPENDENT EFFECTS

Transient variation in the gas bearing film pressure is a mass storage effect and may be considered as compressibility transient. It is exhibited both in terms of an initial transient and also in terms of a "steady-state" time-delay. Mathematically, as shown in Equation (2.24), a first order time-derivative appears simultaneously with second order space derivatives. The structure of this equation is similar to the diffusion equation which is commonly encountered in transient heat condition. In principle, the problem can always be solved by a "marching" process numerically. However, this type of calculating procedure is known to be vulnerable to numerical instability; therefore, special attention must be given to the algorithm in order to realize both spatial accuracy and temporal stability [26].

Step-by-step numerical integration, however, is not always a practically attractive approach. If one is content with perturbation solution and is not concerned with the initial transient, then the linearized time dependent problem can be treated in the frequency domain. In Section 6.1 the dynamically perturbed gas bearing problem will be rigorously examined in the context of operational calculus. In Section 6.2, the frequency domain solution will be examined in terms of its global characteristics.

Because compressibility transient is basically nonlinear, there is a nonlinear rectification effect when large amplitude time dependence is involved. Thus, a gas film with sustained finite amplitude oscillation is capable of supporting steady-state load. The theoretical description of such a phenomenon is treated in Section 6.3.

6.1 Time-Dependent Perturbation Problems

As a model problem, the time-dependent perturbation problem will be examined in some detail for a self-acting bearing with impermeable surfaces. For porous bearings, mass storage in the porous material must be also accounted for. Similarly, for externally-pressurized bearings, pressure transient in the supply line must be included if upstream flow restrictions are present.

The governing equations were previously given as Equations (2.27) through (2.30). To facilitate subsequent discussion, the following simplified notations are introduced for the perturbation problem:

$$\mathcal{P}\delta p \equiv \vec{\nabla}_2 \cdot \{\frac{1}{2}(\vec{U}_1 + \vec{U}_2) h_o \delta p - \frac{h_o^3}{12\mu} \vec{\nabla}_2 (p_o \delta p)\}$$

$$\mathcal{Q}\delta h \equiv \vec{\nabla}_2 \cdot \{\frac{1}{2}(\vec{U}_1 + \vec{U}_2) p_o - \frac{h_o^2}{4\mu} p_o \vec{\nabla}_2 p_o\}\delta h \tag{6.1}$$

Then Equation (2.30) can be rewritten as

$$(\mathcal{P} + h_o \frac{\partial}{\partial t})\delta p = -(\mathcal{Q} + p_o \frac{\partial}{\partial t})\delta h \tag{6.2}$$

Let the boundary conditions be

$$\delta p(\vec{r}_i, t) = 0 \tag{6.3}$$

The subscript "i" indicates the possibility of more than one bearing boundary. Let the initial conditions be

$$\delta p(\vec{r}, t=0) = \Pi(\vec{r}); \qquad \delta h(\vec{r}, t=0) = H(\vec{r}) \tag{6.4}$$

One can operate on Equation (6.2) with the Laplace transformation [27] so that

$$\delta\hat{p} = \int_o^\infty e^{-st}\, \delta p\, dt; \qquad \delta\hat{h} = \int_o^\infty e^{-st}\, \delta h\, dt \tag{6.5}$$

Then one obtains

$$(\mathcal{P} + sh_o)\delta\hat{p} = h_o \Pi + p_o H - (\mathcal{Q} + sp_o)\delta\hat{h} \tag{6.6}$$

and the boundary conditions become

$$\delta\hat{p}(\vec{r}_i) = 0 \tag{6.7}$$

In principle, one may regard the system of equations governing $\delta\hat{p}$ as

solvable by the Green's function method. Let $G(\vec{r}; \vec{u})$ be the Green's function; then by its definition,

$$(\mathcal{F} + h_o S)G = \mathcal{U}(\vec{r}, \vec{u}) \tag{6.8}$$

$\mathcal{U}(\vec{r}, \vec{u})$ is the two-dimensional Dirac delta function defined by

$$\iint_{A_u} \mathcal{U} dA = \begin{cases} 0 & \text{if } \vec{r} \text{ is excluded from } A_u \\ 1 & \text{if } \vec{r} \text{ is included in } A_u \end{cases} \tag{6.9}$$

A_u is any subdomain of the bearing surface. $\vec{u}$ is the dummy position vector of the area element dA. And

$$G(\vec{r}_i, \vec{u}) = 0 \tag{6.10}$$

Accordingly,

$$\delta\hat{p} = \iint G\{h_o \Pi + p_o H - (\mathcal{F} + sp_o)\delta\hat{h}\} dA \tag{6.11}$$

The above integral covers the entire bearing surface. All terms enclosed in brackets are regarded as functions of the dummy position vector $\vec{u}$. Finally, the inverse Laplace transform can be performed on Equation (6.11) so that

$$\delta p(\vec{r}, t) = \mathcal{L}^{-1}\{\delta\hat{p}(\vec{r}, s)\}$$

$$= \frac{1}{2\pi j} \cdot \int_{\beta-j\infty}^{\beta+j\infty} e^{st}\, \delta\hat{p}\, ds \tag{6.12}$$

β is a suitable constant which is larger than the real part of any pole of $\delta\hat{p}$. In general, Equation (6.12) indicates the sum of a number of exponentially time dependent term. The exponential coefficients are the poles of $\delta\hat{p}$. But according to Equation (6.11), the poles of $\delta\hat{p}$ must be also the poles of $G\delta\hat{h}$ since the spatial integration process weighted with either $h_o\Pi$ or $p_o H$ would

not cause any singular behavior. If the system is stable, then the initial conditions associated with Π and H would decay exponentially. At the same time, since the initial conditions do not affect the exponential coefficients, the question of perturbed dynamic stability is independent of the initial conditions.

For a stable system, Equation (6.12) can be evaluated with $\beta \to 0$. However, if δh contains a purely harmonic time dependence; i.e., $\delta h \sim e^{j\omega t}$, then $\delta\hat{h}$ would have poles at $s = \pm j\omega$. It would then be necessary to regard the limiting process $\beta \to 0$ to take place subsequent to the performance of the integral operation. Equation (6.12) can be rewritten as

$$\delta p(\vec{r}, t) = \frac{1}{\pi} \int_0^\infty \{f(\vec{r}, \omega)\cos\omega t - g(\vec{r}, \omega)\sin\omega t\}d\omega \qquad (6.13)$$

(f, g) are respectively the real and imaginary parts of $\delta\hat{p}(\vec{r}, \vec{s}\to j\omega)$. If $\delta\hat{p}$ is solved with both (Π, H) set to zero, then the above procedure would lead to a special solution with null initial conditions. The late time behavior of any solution with a different set of initial conditions is not distinguishable from this special solution.

6.2 Global Characteristics of Harmonically-Perturbed Gas Bearings

Again, the self-acting gas bearing with impermeable walls will be used as a model problem. Equations (6.1), (6.2), and (6.3) would be the system of governing equations. In the use of operational calculus to solve a linear time-dependent problem, the response to an impulse function together with the convolution theorem allows one to compute the response to any form of time dependent driving function [27]. The response to an impulse function can be expressed as a Fourier integral of harmonic response in the inversion formula. For this reason, the dynamic environment is often specified in the frequency domain. The harmonic perturbation solution is also a convenient tool in the evaluation of dynamic system stability in accordance with an energy flow criteria [28,29]. Margin of dynamic stability is one of the most important issues in the design of high-speed rotating equipment. Thus, the harmonic perturbation analysis of a gas bearing is a subject of considerable importance.

The harmonic perturbation solution can in principle be expressed in terms of a Green's function. For computation purposes, the Green's function formulation for gas bearings, however, cannot be conveniently implemented due to the complexity in the two-dimensional operator $\mathcal{P}$ as given by Equation (6.1). Therefore, the harmonic perturbation problem will be recast in a form which can be readily solved by relatively conventional numerical procedures.

To specify a harmonic perturbation problem, the perturbed bearing gap is specified by

$$\delta h(\vec{r}, t) = \delta g(\vec{r}) \cos\nu t \tag{6.14}$$

$\delta g(\vec{r})$ describes the spatial distribution of the perturbation, and ν is the particular frequency under consideration. The cosine function is chosen to indicate that time reference is fixed by the gap motion. With the omission of initial conditions, the dynamic perturbation problem is homogeneous in $(\delta p, \delta h)$. Consequently, δp must also have a harmonic time-dependence at the same frequency ν. Furthermore, one can write

$$\delta h = \delta g(\vec{r}) \, \mathrm{Re}\{e^{i\nu t}\} \tag{6.15}$$

and the unknown perturbed pressure may be expressed as

$$\delta p = \mathrm{Re}\{\delta q(\vec{r}) e^{i\nu t}\} \tag{6.16}$$

$\delta q(\vec{r})$ would generally be complex, indicating the possible presence of phase shift between δp and δh.

As both bearing surfaces are assumed to be fixed to rigid bodies, δg may represent the effect of either a translation or a rotation of one surface relative to the other. In the case of a translational perturbation, the relative motion between the two bodies is indicated by the perturbation vector $\delta\vec{e}\mathrm{Re}\{e^{i\nu t}\}$, then the perturbation of the bearing gap is

$$\delta h = \vec{n} \cdot \delta\vec{e} \, \mathrm{Re}\{e^{i\nu t}\} \tag{6.17}$$

Thus, by comparison with Equation (6.15),

$$\delta g = \vec{n} \cdot \delta\vec{e} \tag{6.18}$$

In the case of an angular or a rotational perturbation represented by the relative angular perturbation vector $\delta\vec{\gamma}\mathrm{Re}\{e^{i\nu t}\}$, bearing gap perturbation becomes

$$\delta h = -\vec{n} \cdot \vec{r} \times \delta\vec{\gamma}\ \mathrm{Re}\{e^{i\nu t}\} \tag{6.19}$$

Accordingly,

$$\delta g = -\vec{n} \cdot \vec{r} \times \delta\vec{\gamma} = \vec{r} \times \vec{n} \cdot \delta\vec{\gamma} \tag{6.20}$$

With δg represented by either Equation (6.18) or (6.20), substitution of Equation (6.15) and subsequent elimination of the common factors $e^{i\nu t}$ and $\mathrm{Re}\{\ \}$ from all terms, Equations (6.1) through (6.3) become

$$\vec{\nabla}_2 \cdot [\frac{1}{2}(\vec{U}_1 + \vec{U}_2)h_o\delta q - \frac{h_o^3}{12\mu}\vec{\nabla}_2(p_o\delta q)] + i\nu h_o\delta q$$

$$= -\vec{\nabla}_2 \cdot \{[\frac{1}{2}(\vec{U}_1 + \vec{U}_2)p_o - \frac{h_o^2}{4\mu}p_o(\vec{\nabla}_2 p_o)]\delta g\} - i\nu p_o\delta g \tag{6.21}$$

$$\delta q(\vec{r}_i) = 0 \tag{6.22}$$

Well-proven numerical methods for solving the above system of equations are available. Formally, one may write

$$\delta q = \mathcal{L}\,\delta g \tag{6.23}$$

with $\mathcal{L}$ indicating a linear operator. Then the corresponding perturbation of the force vector is, according to Equation (2.33)

$$\delta\vec{F} = \iint \vec{n}\,\delta q\,d\Lambda = \iint \vec{n}(\mathcal{L}\delta g)\,d\Lambda \tag{6.24}$$

For the translational perturbation problem, making use of Equation (6.18), one can write

$$\delta\vec{F} = \iint \vec{n}\,(\mathcal{L}\,\vec{n})\,dA \cdot \delta\vec{e} \tag{6.25}$$

Thus, staying with the vector notation, one can define the translational stiffness matrix to be

$$\overline{\overline{\mathcal{K}}}_{force} = -\iint \vec{n}\,(\quad\vec{n})\,dA \tag{6.26}$$

For the most general case, a perturbation force may also be induced by an angular perturbation. However, for most commonly used bearings, there is a sufficient degree of symmetry so that it is usually possible to locate the origin of the coordinate system to eliminate induction of force by angular perturbation as well as induction of moment by translational perturbation. Therefore, perturbation of the moment vector will next be examined with Equation (6.20), yielding

$$\delta\vec{M}_p = \iint \vec{r}\times\vec{n}\,(\mathcal{L}\,\vec{r}\times\vec{n})\,dA \cdot \delta\vec{Y} \tag{6.27}$$

Again, the angular stiffness matrix can be defined as

$$\overline{\overline{\mathcal{K}}}_{moment} = -\iint \vec{r}\times\vec{n}\,(\mathcal{L}\,\vec{r}\times\vec{n})\,dA \tag{6.28}$$

As presented in Equations (6.26) and (6.28), there are no apparent formal distinction between a gas bearing and an incompressible fluid-film bearing. There is actually a very important difference which is implicit in the structure of the operator $\mathcal{L}$, which reflects the lefthand side of Equation (6.21). For an incompressible fluid-film bearing, they are all related to the spatial differential operators and are all real. The righthand side contains a frequency independent real part and an imaginary part which is directly proportional to the frequency. For this reason, the "dynamic stiffness" matrix of an incompressible fluid-film bearing is usually

represented by a set of "stiffness matrix coefficients" and a set of "damping matrix coefficients." For a gas bearing, because of the presence of $i\nu h_o \delta q$ on the lefthand side of Equation (6.21), both real and imaginary parts of [illegible] are frequency dependent. Consequently, one can regard both "stiffness and damping matrix coefficients" of a gas bearing to be frequency dependent.

6.3 Rectification Effects of High-Frequency Oscillations

A gas film undergoing sustained oscillation develops a mean pressure above ambient. Historically, this phenomenon was reported as evidence of an anomalous rheological property of air [30]. Nevertheless, a correct theoretical analysis as well as the recognition of the true mechanism actually predated the intense gas lubrication efforts of the 60's [31].

By sustaining the high-frequency oscillation with an electrical or a magnetic means, load support capability can be developed by a thin gas film. A gas bearing operating on this principle is called a squeeze-film gas bearing. Squeeze-film gas bearings of various geometrical shapes are illustrated in Figure 6.1. The asymptotic theory for squeeze-film gas bearings is briefly outlined below.

Consider the most general equation of the isothermal gas bearing equation for impermeable walls:

$$\frac{\partial}{\partial t}(ph) + \vec{\nabla}_2 \cdot \left\{ \frac{1}{2}(\vec{U}_1 + \vec{U}_2)\, ph - \frac{h^3}{12\mu} p \vec{\nabla}_2 p \right\} = 0 \tag{6.29}$$

If a sustained fluctuation at a sufficiently high frequency is present, the leading term of Equation (6.29) dominates; thus

$$\frac{\partial}{\partial t}(ph) \simeq 0 \tag{6.30}$$

Time independence of (ph), however, is obviously not valid at bearing edges; therefore, Equation (6.30) is a legitimate approximation only in the internal region. Suppose

$$\vec{U}_1 = \vec{U}_2 = \vec{\nabla}_2 h = 0 \tag{6.31}$$

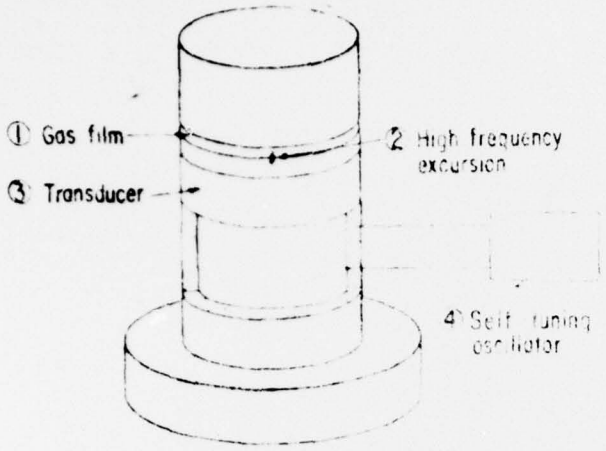

Elements of Squeeze-Film Bearing

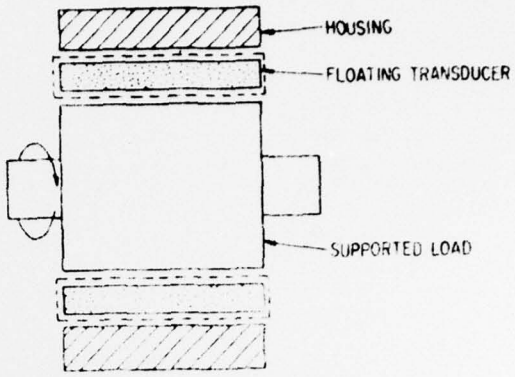

Schematic of Floating-Transducer Journal-Thrust Bearing

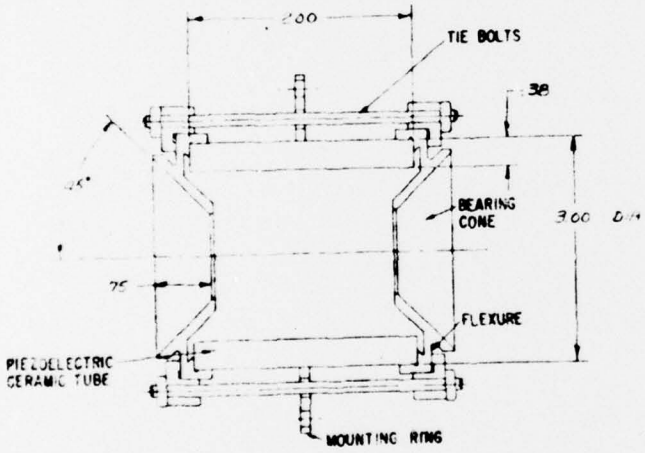

Experimental Axial-Excursion Conical Squeeze-Film Bearing With Wave Extender Type Transducer

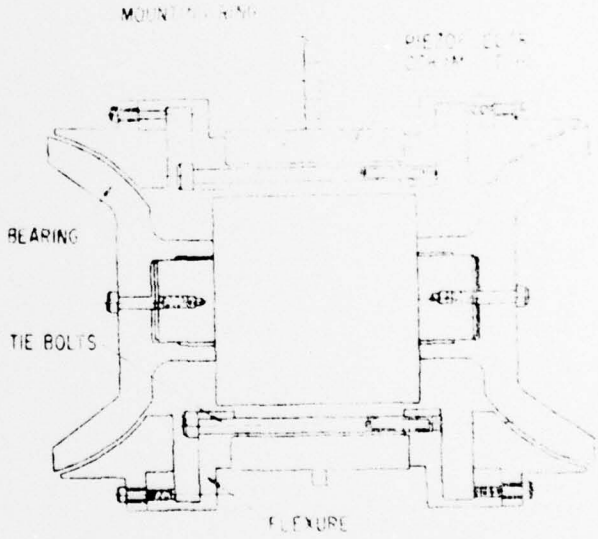

Experimental Spherical Squeeze-Film Bearing with Wave Extender Type Transducer

Fig. 6.1

Various Squeeze-Film Gas Bearings

Then Equation (6.29) is reduced to

$$\frac{\partial}{\partial t}(ph) - \frac{1}{24\mu}\vec{\nabla}_2 \cdot \vec{\nabla}_2 (p^2h^3) = 0 \tag{6.32}$$

If one performs a "time-series average" on Equation (6.32), one obtains

$$\vec{\nabla}_2 \cdot \vec{\nabla}_2 \langle p^2h^3 \rangle = 0 \tag{6.33}$$

The symbol $\langle\ \rangle$ designates the averaged result of the enclosed quantity. Since p and h are both uniform along the bearing edges,

$$\langle p^2h^3 \rangle = p_a^2 \langle h^3 \rangle \tag{6.34}$$

is a solution of Equation (6.33). This result may be regarded as an analogy of the "mass content rule" discussed in Section 4.4.2. In the internal region, then

$$\langle p^2h^3 \rangle = (ph)^2 \langle h \rangle = p_a^2 \langle h^3 \rangle$$

or

$$ph = p_a \sqrt{\frac{\langle h^3 \rangle}{\langle h \rangle}} \tag{6.35}$$

If h is a simple harmonic function; e.g., $h = C(1 - \varepsilon\cos\nu t)$, then

$$ph = \sqrt{1 + \frac{3}{2}\varepsilon^2}\ p_a C \tag{6.36}$$

The temporally averaged pressure is then

$$\langle p \rangle = \sqrt{1 + \frac{3}{2}\varepsilon^2}\ p_a \left\langle \frac{1}{1+\varepsilon\cos\nu t} \right\rangle = \sqrt{\frac{1 + \frac{3}{2}\varepsilon^2}{1-\varepsilon^2}}\ p_a \tag{6.37}$$

If $\varepsilon \to 1$, a significant amount of pressure elevation above p_a is seen possible. The question remains, how high should the frequency be to justify Equation (6.30)? The answer lies in rewriting Equation (6.29)

in a dimensionless form, scaling $\vec{\nabla}_2$ with 1/R, h with C, and p with p_a; one would then establish

$$\sigma = \frac{12\mu\nu R^2}{p_a C^2} >> 1 \tag{6.38}$$

to be the required condition. To be thoroughly rigorous, one must be cautious that Equation (6.38) does not violate the prerequisite for an isothermal analysis; namely,

$$(\frac{\mu C}{\kappa})(\gamma-1)M^2 << 1 \tag{6.39}$$

Above results have been generalized to relax the assumptions of Equations (6.31) and (6.38) [32,33], and to consider "long time scale" dynamics [34] as well as "hybrid squeeze-slide" gas films [35].

6.4 Nomenclature

Symbol	Definition	Chapter/ Section
C_p	Specific heat at constant pressure	
$\delta\vec{e}$	Translational perturbation vector	
f	Real part of $\delta\hat{p}$ for $s \to j\omega$	
$\delta\vec{F}$	Perturbation force vector	
g	Imaginary part of $\delta\hat{p}$ for $s \to j\omega$	
δg	Spatial distribution of harmonic gap perturbation	
G	Green's function of $\delta\hat{p}$	
h_o	Steady-state film thickness	
δh	Gap perturbation	
$\delta\hat{h}$	Laplace transform of δh	
H	Initial condition of δh	
$\underset{\sim}{K}$ = force	Force-stiffness matrix	
$\underset{\sim}{K}$ = moment	Moment-stiffness matrix	
$\mathcal{L}$	Linear operator	
M	Mach number	
$\delta\vec{M}_p$	Perturbation moment vector due to δp	
$\vec{n}$	Outward unit normal vector of bearing surface	
p_a	Ambient pressure	
p_o	Steady-state pressure	
δp	Pressure perturbation	
$\delta\hat{p}$	Laplace transform of δp	
$\mathcal{P}$	Linear operator for δp, eq. (6.1)	
δq	Spatial distribution of harmonic pressure	
$\mathcal{Q}$	Linear operator for δp, eq. (6.1)	
$\vec{r}$	Surface position vector	
$\vec{r}_i$	Position vector of ith boundary	

Symbol	Definition	Chapter/ Section
s	Laplace parameter	
t	time	
$\vec{u}$	Dummy variable of $\vec{r}$	
[illegible]	Two-dimensional Dirac delta function	
$\delta\vec{\gamma}$	Angular perturbation vector	
$\vec{\nabla}_2$	Two-dimensional surface spatial gradient operator	
ε	Excursion ratio of harmonic motion	
κ	Thermal conductivity	
μ	Viscosity coefficient	
ν	Frequency of harmonic motion	
Π_o	Initial condition of δp	
σ	Squeeze number, $\dfrac{12\mu\nu R^2}{p_a C^2}$	

Subscripts

1	referring to lower bearing surface
2	referring to upper bearing surface
< >	Time-series average

REFERENCES

1. Murray, S.F, "Material Combinations for Hydrodynamic Inert Gas-Lubricated Bearings", ASME Trans., JOLT, Vol. 90, Series F, No.1, January 1968, p.49.

2. Rabinowicz, Ernest, Friction and Wear of Materials, John Wiley and Sons, Inc., New York

3. Reynolds, Osborne, "On the Theory of Lubrication and Its Application to Mr. Beauchamp Tower's Experiments", Phil. Trans, Roy, Soc., London, Vol. 177, part 1, 1886.

4. Elrod, H.G., Jr. and Burgdorfer, A., "Refinement of the Theory of Gas Lubricated Journal Bearing of Infinite Length", Proc. of the First International Symposium on Gas Lubricated Bearings, Washington, 1959, pp. 93-118.

5. Cole, J.A. and Hughes, C.J., "Oil Flow and Film Extent in Complete Journal Bearings", Proc. Inst. Mech. Engr. (London), Vol. 170, No. 17, 1956.

6. "Cavitation and Related Phenomena in Lubrication", Proc. of the First Leeds-Lyon Symposium on Tribology, The University of Leeds Symposium, 1974, Edited by: D. Dawson, M. Godet and C.M. Taylor, Published by: Mechanical Engineering Publications for the Institute of Triboloty, Leeds University and the Institut National des Sciences Appliquées de Lyon, London; New York.

7. Burgdorfer, A., "The Influence of the Molecular Mean Free Path on the Performance of Hydrodynamic Gas-Lubricated Bearings", Journal of Basic Engineering, Trans. ASME, Series D, Vol. 80, No. 1, March 1959, pp 94-100.

8. Bevers, G S. and Joseph, D.D., "Boundary Conditions at a Naturally Permeable Wall", J. of Fluid Mech., Vol. 30, 1967, pp 197-207.

9. Grinnell, S.K., "Flow of a Compressible Fluid in a Thin Passage", Trans. ASME, 78, 765-771, May 1956.

10. Constantinescu, V.N., "On Turbulent Lubrication", Proc. of the Institute of Mechanical Engineers, Vol. 173, pp. 881-900, 1959.

11. Pan, C.H.T., and Vohr, J.H., "Super Luminar Flow in Bearings and Seals", Bearing and Seal Design in Nuclear Power Machinery, ASME, New York, pp. 219-250, 1967.

12. Harrison, W.I., "The Hydrodynamic Theory of Lubrication with Special Reference to Air as a Lubricant", Trans, Cambridge, Phil. Soc., XXII, pp. 37-54, (1913).

References (Continued)

13. Raimondi, A.A., "A Numerical Solution for the Gas-Lubricated, Full Journal Bearing of Finite Length", Trans. ASME, April, 1961, Vol. IV, pp. 131-155.

14. Elrod, H.G., Jr. and Malanoski, S.B., "Theory and Design Data for Continuous-Film, Self-Acting Journal Bearings of Finite Length", Report I-A 2049-13, Nov. 1960 and Report I-A 2049-17, The Franklin Institute Laboratories for Research and Development.

15. Ausman, J.S., "Finite Gas Lubricated Journal Bearings", The Institution of Mechanical Engineers, Conference on Lubrication and Wear, October 1957, Paper 22.

16. Ausman, J.S., "Theroy and Design of Self-Acting Gas-Lubricated Journal Bearings Including Misalignment Effects", First International Symposium on Gas-Lubricated Bearings, October 26-28, 1959, Office of Naval Research, Department of the Navy ACR-49, pp. 161-192.

17. Ausman, J.S., "An Improved Analytical Solution for Self-Acting, Gas Lubricated Journal Bearings of Finite Length", Journal of Basic Engineering, Trans. ASME, Series D, Vol. 83, No. 2, June 1961, pp. 188-194.

18. Van Dyck, Milton, Pertubation Methods in Fluid Mechanics, Academic Press, New York, NY 1964.

19. Schlichting, H., "Laminare Katnaleinlaufströmung", Zeitschr. f. angew, Math. U. Mech. 14, 1934, pp. 368-373.

20. Pan, C.H.T., "Calculation of Pressure, Shear, and Flow in Lubricating Films for High Speed Bearings", JOLT, Trans. ASME, Series F, Vol. 96, No. 1, January 1974, pp. 80-94.

21. Lund, J.W., Wernick, R.J., and Malanoski, S.B., "Analysis of the Hydrostatic Journal and Thrust Bearing for the NASA AB-5 Gyro Gimbal Bearing", Mechanical Technology, Inc., Report No. MTI-62-TR-26, 1962.

22. Vohr, J.H., "A Study of Inherent Restrictor Characteristics for Hydro-Static Gas Bearings", Proceedings of Gas Bearing Symposium, U. of Southampton, England, April 1969.

23. McCabe, J.T., Elrod, H.G., Carfagno, S., and Colsher, R., "Summary of Investigations of Entrance Effects of Circular Thrust Bearings", Proc. of Gas Bearing Symposium, U. of Southampton, England, April, 1969.

24. Mori, H., "A Theoretical Investigation of Pressure Depression in Externally Pressurized Gas-Lubricated Circular Thrust Bearings", J. of Basic Engineering, Trans. ASME, Series D, Vol. 83, No. 2, June, 1961, pp. 201-208.

References (Continued)

25. Elrod, H.G. and Chu, T.Y., "Inertia and Energy Effects in the Developing Gas Film Between Two Parallel Flat Plates", Journal of Lubrication Technology, Trans. ASME, Presented at ASME-ASLE Lubrication Conference, New York, N.Y., October 9-12, 1972.

26. Castelli, V. and Pirvics, J., "Review of Numerical Methods in Gas Bearing Film Analysis", JOLT, Trans. ASME, Series F, Vol. 90, No. 4, October 1968, pp. 777-792.

27. Churchill, R.V., Modern Operational Mathematics in Engineering, First Edition, Seventh Impression, McGraw-Hill, New York, NY. 1944.

28. Lund, J.W., "Calculation of Stiffness and Damping Properties of Gas Bearings", JOLT, Trans. ASME, Series F, Vol. 90, No. 4, October 1968, pp. 793-803.

29. Pan, C.H.T., "Spectral Analysis of Gas Bearing Systems for Stability Studies", Proc. of the 9th Midwestern Mechanics Conference, Part 2, Dynamics and Fluid Mechanics, Wiley, New York, NY.

30. Reiner, M., "The Centripetal-Pump Effect in a Vacuum Pump", Proc. Roy. Sec. A, Vol. 247, September 16, 1958, pp. 152-167.

31. Taylor, G.I, and Saffman, "Effects of Compressibility at Low Reynolds Numbers", Journal Aero Sci, Vo. 24, 1957, p. 553.

32. Pan, C.H.T. and Broussard, P.H., Jr., "Squeeze-Film Gas Lubrications", Paper No. 12, Gas Bearing Symposium on Design Methods and Applications, University of Southampton, Dept. of Mechanical Engineering, April 1967.

33. Pan, C.H.T., "The Gaseous Squeeze-Film at Moderately Large Squeeze Numbers", Journal of Basic Engineering, Trans. ASME, Series D, Vol. 91, No. 4, December 1970, pp. 766-781.

34. Pan, C.H.T. and Chiang, T., "Dynamic Behavior of the Spherical Squeeze-Film Hybrid Bearing", JOLT, Trans. ASME, Series F, Vol. 91, No. 1, January 1969, pp. 149-160.

35. Chiang, T., Malanoski, S.B., and Pan, C.H.T., "Spherical Squeeze-Film Hybrid Bearing with Small Steady-State Radial Displacement", JOLT, Trans. ASME, Series F, Vol. 89, No. 3, July 1967, pp. 254-262.

GENERAL REFERENCES

36. Grassam, N.S. and Powell, J.W., Gas Lubricated Bearings, 1964. London; Buttersworth.

37. Proceedings of the First International Symposium on Gas Lubricated Bearings, 1959. Washington.

38. Gross, W.A., Gas Film Lubrication, 1962, New York; Wiley.

39. Constantinescu, V.N., Gas Lubrication, 1969, New York; ASME.

40. Proceedings of the Second International Symposium on Gas Lubricated Bearings, 1968, Las Vegas, Printed as JOLT, Trans. ASME, Series F., Vol. 90, No. 4, October 1968 and Vol. 91, No. 1, January 1969.